

FV0 3006

netow svp
aan secw. CRT-PI

Technische Universiteit Delft
Faculteit STM
Proces- en Regeltechniek
Julland
262212

THE DESIGN OF THE INTERCONNECTED FLUIDIZED BED PILOT PLANT

FINAL REPORT

April 1993

Harry Bronk
Adrie de Putter

 **TU Delft**

Technische Universiteit Delft

Faculteit der Scheikundige Technologie en der Materiaalkunde
Laboratory for Process Equipment

THE DESIGN OF
THE INTERCONNECTED FLUIDIZED BED
PILOT PLANT

FINAL REPORT

Harry Bronk
Adrie de Putter

Laboratory for Process Equipment
Delft University of Technology

April 1993

Summary

This final report is the result of the collective design project which is part of the post-MSc study of chemical design engineering at the Delft University of Technology. In this report the design of the Interconnected Fluidized Bed pilot plant is presented. This pilot plant is designed for the regenerative desulphurization of simulation gases containing SO_2 with the sorbent SGC-500. In the pilot plant it is also possible to burn small quantities of coal. The modifications to the pilot plant to use the plant for H_2S removal with a sorbent of MnO on $\gamma\text{Al}_2\text{O}_3$, are indicated.

Very large amounts of nitrogen are needed in the pilot plant, as it is used as the main fluidization gas. Therefore N_2 will be supplied from a large storage vessel. Air will be supplied by the local pressurized air system while all other gases (SO_2 , H_2 , CO) are supplied from gas cylinders. A wide range of gas flows and compositions are possible. The fluidization gas flows (nitrogen, air) will be heated up electrically by elements directly placed in these flows. The solids supply system can feed small quantities of coal or sand (which is used for segregation experiments) to the reactor.

The dimensions of the reactor have been chosen based on model calculations. Sizes have been given for the bed areas and bed heights and for the orifice diameter and orifice heights. It is possible to dismantle the reactor so that the weir heights and the orifice diameters can be changed. The reactor and the downstream equipment will be constructed of a material which is resistant to the different environments (sulphurous, reducing, oxidizing) and high temperatures. The gas distributors ensure uniformly fluidized beds. The reactor will be provided with a electrical heating jacket for extra heat input. There are sampling points for both gases and solids in the reactor. A freeboard is used to allow return of entrained particles to the fluidized bed.

In the off-gas treatment section both dust and hazardous and environmental harmful components are removed. In this section first dust will be removed with a cyclone. The combustible components (H_2S , S_2 , H_2 , CO) will be converted at high temperature which is reached by burning of natural gas. In a CaO -bed the SO_2 will be removed. After cooling of the gases removal of fine dust is possible with a bag filter.

The process control mechanisms will ensure a safe and stable operation of the pilot plant. The safety measures needed for the operation of the pilot plant are presented. The investment costs of the pilot plant are estimated at Dfl. 180,000.-. The operating costs are Dfl. 34.- per hour experiment.

light lag

stabilities?

Outline

Summary

Outline

1 Introduction	1
2 Basis of the design of the pilot plant	4
2.1 Purposes of the design	4
2.2 Requirements on the design	4
2.3 Desired range of operating conditions	5
3 Preliminary design of a 100 MW power plant and downscaling	8
4 Set-up of the pilot plant	10
4.1 Flowsheet of the pilot plant	10
5 Design of the reactor section	12
5.1 Choice of the dimensions of the reactor	12
5.2 Construction of the reactor	14
5.3 Reactor heating and insulation	15
5.4 Gas distributor	16
5.5 Freeboard	17
6 Supply section	19
6.1 Gas supply	19
6.2 Solids supply	21
7 Sampling section	24
7.1 Place of the sampling points	24
7.2 Gas sampling	24
7.3 Solids sampling	24
8 Off-gas treatment section	27
8.1 The cyclone	27
8.2 Conversion of the combustible components	28
8.3 Removal of SO ₂ in a CaO-bed	29
8.4 Cooling of the gas flow and dust removal with a bag filter	30
9 Process control	31
9.1 Control strategies	31
9.2 Process control mechanisms	32
9.3 Global procedures for the pilot plant operation	35
10 Safety	36
10.1 Safety study	36
10.2 Safety measures	36

11 Cost estimation	38
11.1 Estimation of the investment costs	38
11.2 Operating costs of the pilot plant	39
12 Conclusions	41
List of symbols	43
List of references	46

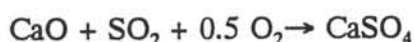
Appendices:

1	Modelling of regenerative desulphurization in an Interconnected Fluidized Bed (SO ₂ removal)
2	Modelling of a regenerative H ₂ S removal process with alumina supported MnO
3	Equations for calculating the terminal and minimum fluidization velocities and the bed voidage
4	Segregation of ash and sorbent
5	Modelling of the solids flow and the gas leaks through the orifices
6	Estimation of the capacity of the reactor heater
7	Design procedure for the gas distributor
8	Solids feed systems
9	Measurement methods, valves and pipe sizing
10	Safety study
11	Safety aspects of the gases
12	Safety report
13	Modifications to the designed pilot plant for the H ₂ S removal process

Chapter One: Introduction

The use of coal as an energy source has become more attractive again, as the available sources of natural gas and oil are diminishing fast. The remaining resources of coal are sufficient for at least the next three hundred years at the present level of consumption, while the sources of natural gas and oil will be exhausted within 60 and 40 years respectively. However the use of coal as an energy source causes more environmental problems than gas or oil. Relative more CO_2 is produced than with natural gas or oil. CO_2 is the main component contributing to the greenhouse effect. Also the sulphur content of coal and consequently the emission of SO_2 during the combustion of coal is high.

Two relative new ways to use coal as a source for electricity production are fluidized bed coal combustion and coal gasification. Fluidized Bed Combustion (FBC) has several advantages compared to other coal combustion techniques. The combustion temperature is low, 850°C , so less NO_x is formed due to oxidation of N_2 from the air. This reduces the total NO_x emission with about 50 %. Also the SO_x emissions can be reduced by adding a sorbent in situ in the combustor. At present limestone is used as a sorbent. It is cheap, but difficult to regenerate, so a lot of solid waste is produced. A new regenerative sorbent, CaO on a carrier of $\gamma\text{-Al}_2\text{O}_3$ has been developed at Delft University of Technology. This sorbent can capture SO_2 at the conditions of coal combustion in a fluidized bed, according to the reaction:



The sulphur loaded sorbent is regenerated at the same temperature in a separate bed with H_2 or CO :



At this temperature also CaS can be produced in the regeneration:



The production of CaS is undesired as it reduces the regeneration efficiency. When the regeneration yields an off-gas with over 4 v% SO_x , the off-gas can be used to produce sulphur or sulphuric acid.

In a coal gasifier coal is gasified with oxygen and steam to produce a fuel gas with CO and H_2 as the main components. The sulphur from the coal is present as H_2S . The fuel gas can be combusted at a high temperature. Because of the higher combustion temperature the efficiency of a coal gasifier is higher than of a modern coal combustion plant. Before the fuel gas is combusted, the H_2S in the gas has to be removed. The reasons for removing H_2S before the combustion are:

- the volume of the fuel gases is lower. The sulphur can be removed easier and more concentrated.
- protection of the downstream equipment.

Several methods are available for desulphurization at low temperature. However these

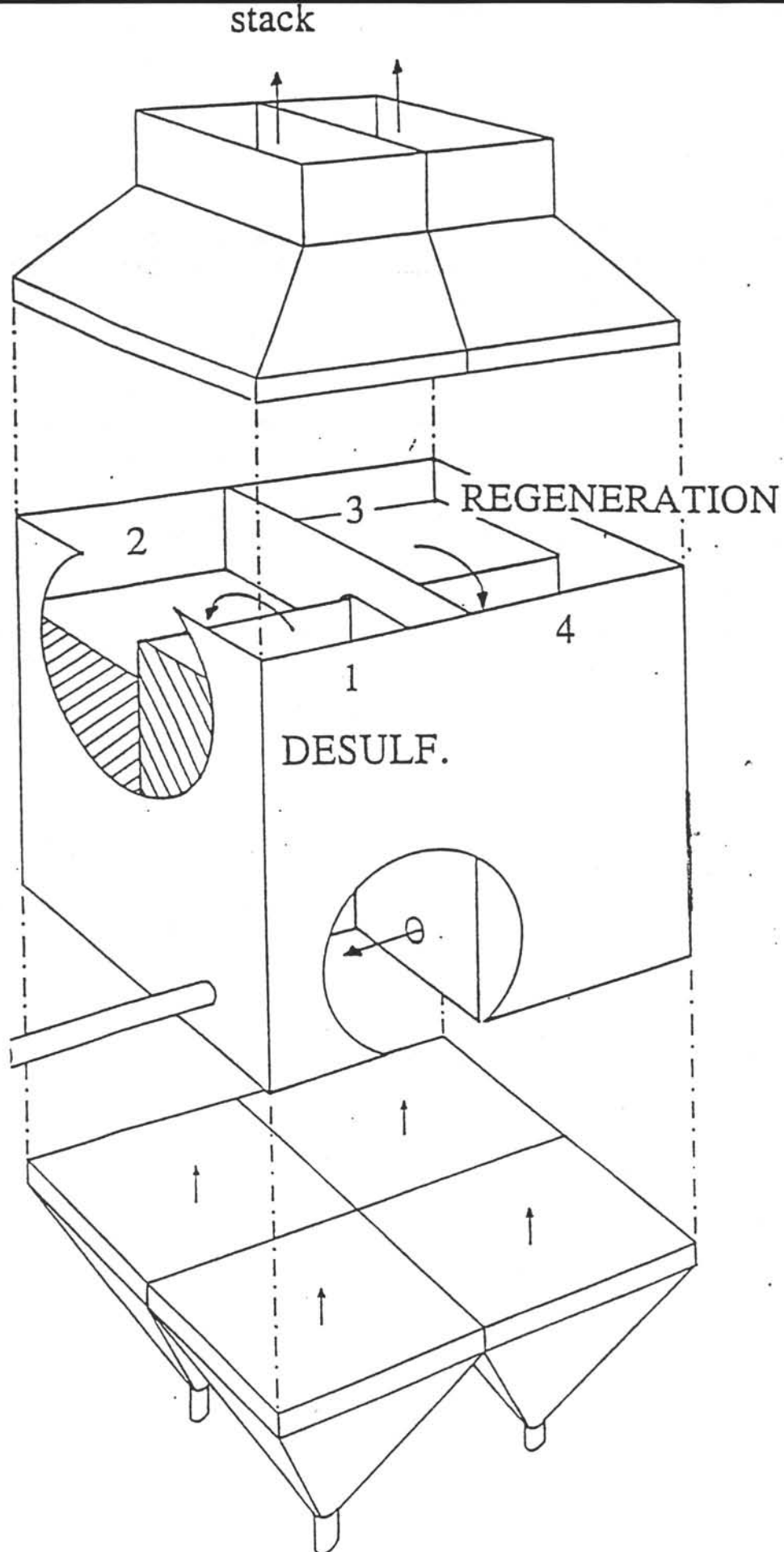
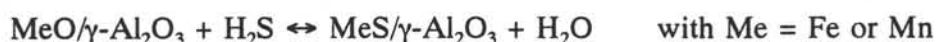


Figure 1.1: Principle of an Interconnected Fluidized Bed (IFB)

methods make the process complicated. Many steps are necessary and the temperature changes are high. H₂S removal at high temperature is advantageous because the equipment is simpler and the overall efficiency of the coal gasifier is improved.

Two types of fuel gases are distinguished, 'wet' and 'dry' fuel gas. For 'dry' fuel gases the oxides MnO and FeO on γ -Al₂O₃ can be used as sorbent. The sulphation rates are high but the capacity is rather low. These sorbents were investigated at the TU Delft. It was shown that the following reaction is reversible:



This means that these sorbents can be regenerated with steam. As regeneration product H₂S is formed what can be used to produce elemental sulphur. The experimental work with these sorbents was done in a fixed bed reactor, but this process can also be done in a fluidized bed. Advantage of a fluidized bed is that continuous operation is possible, disadvantage is that a fluidized bed is better mixed and therefore the H₂S retention is lower.

For both processes, the fluidized bed combustor and the desulphurization step in a coal gasifier two fluidized beds are necessary: a combustion or desulphurization bed and a regeneration bed. The sorbent particles have to be transported from the combustion or desulphurization bed to the regeneration bed and back. In pneumatic conveyance through tubes particles will have a high velocity (10-20 m/s). Collisions with the walls will lead to particle breakage, what should be avoided. An elegant solution is the Interconnected Fluidized Bed (IFB) system. The basis of the IFB is shown in figure 1.1. The system consists of four different beds, which can be operated independently with four different gases and gas velocities. When two beds are separated by a weir and have different gas velocities, particles of the bed with the higher gas velocity will fall over the weir into the bed with the lower gas velocity. When there is an orifice at the bottom of a separating wall between two beds, solids and gas will flow through this orifice from the bed with the lower gas velocity and higher bed density (dense bed) to the bed with the higher gas velocity and lower bed density (lean bed). In the system of figure 1.1 there are weirs between bed 1 and 2 and between bed 3 and 4, and there are orifices between bed 2 and 3 and between bed 4 and 1. The gas flows from bed 1 and 2 come together above the weir, just as the gas flows from bed 3 and 4. When bed 1 and 3 are fluidized with a high velocity and bed 2 and 4 with a low gas velocity, solids will flow from bed 1 over the weir to bed 2, from bed 2 through the orifice to bed 3, from bed 3 over the weir to bed 4 and from bed 4 through the orifice to bed 1. Bed 1 is used as combustion or desulphurization bed, while bed 3 is used as regeneration bed. The oxidizing environment of bed 1 is thus separated from the reducing environment of bed 3. Pneumatic conveyance is avoided and only fluidized bed attrition and some attrition in the orifices will occur. In case of coal combustion bed 2 can be used to separate the ash, which remains after coal combustion, from the sorbent particles by segregation. Bed 4 is used to control the solids flow through the system. In this bed the gas velocity is below the minimum fluidization velocity, so the bed is defluidized. The downward solids flow in this bed is determined by the friction forces between particles and the wall. When the gas velocity is increased the friction forces are reduced and the solids flow will increase.

Research has already been done with a cold flow IFB. A new IFB pilot plant will be built in which both described processes will be investigated at the appropriate temperatures. The SO_2 retention in fluidized bed combustion will be simulated by using a feed gas containing SO_2 and O_2 . The fuel gases from a coal gasifier will be simulated by a feed gas containing H_2S , CO and H_2 . This report discusses the design of the new pilot plant. In Chapter Two first the purposes for which the pilot plant will be built, the requirements the pilot plant must meet and the operating conditions will be discussed. In Chapter Three a summary is given of the results of the preliminary design of a commercial 100 MW power plant, using fluidized bed combustion of coal and IFB technology. In Chapter Four the set-up of the pilot plant is introduced. The pilot plant set-up is divided in a reactor section, a supply section, a sampling section and an off-gas treatment section. Each section is discussed in a separate chapter. In Chapter Nine the control aspects of the plant are discussed and in Chapter Ten some of the safety aspects. In Chapter Eleven an estimation of the investment and the operating costs of the pilot plant is given.

Chapter Two: Basis of design of the pilot plant

2.1 Purposes of the design

A pilot plant can be built for several reasons. In the case of research of new processes in new installations the purposes are:

- research on the process itself, determination of the regime and obtaining rules for scale-up
- research on suitable construction materials
- research on accumulation characteristics
- research on the dynamic behaviour of the process
- process demonstration
- making a process description

The specific research goals for this pilot plant are:

- research on the retention of SO_2 by a regenerative sorbent of CaO on $\gamma\text{-Al}_2\text{O}_3$.
- research on the retention of H_2S by a regenerative sorbent of MnO on $\gamma\text{-Al}_2\text{O}_3$.
- research on the influence of coal combustion on the retention of SO_2 by a regenerative sorbent of CaO on $\gamma\text{-Al}_2\text{O}_3$.
- research on the segregation of coal ash or sand and the sorbent.
- research on attrition of both sorbents.
- research on the operation of an IFB system (control of the sorbent flow through the IFB).

2.2 Requirements on the pilot plant

To be able to satisfy the purposes, the pilot plant should meet a number of requirements. The following were selected:

- The pilot plant should be suitable for the regenerative desulphurization of simulation gases containing SO_2 and H_2S . Also it must be possible to burn small quantities of coal in bed 1.
- Variation of the operation conditions (temperature, pressure, gas flows and gas compositions) in a wide range must be possible.
- An undisturbed and variable supply of feed materials (gases and solids) and a suitable discharge of the products must be possible.
- Sampling of the gas phase and the solid phase in the reactor must be possible, without disturbing the process.
- There must be pressure and temperature measuring points in the reactor.
- The pilot plant should be made of suitable materials.
- The reactor should be as flexible as possible. For example the weirs and the orifices should be adjustable.
- The hold-up of the equipment should be low, so that the stationary state is quickly reached.

- The process must be carried out in a safe and stable way.
- The off-gases should be cleaned, the dust from the fluidized bed and the hazardous or environmental harmful components should be removed.

2.3 Desired range of operating conditions

One of the most important requirements is a wide range of operating conditions in the pilot plant. The range of operating conditions are quite different for the two different processes, so they will be discussed separately.

SO₂ retention

The operating temperature in fluidized bed coal combustion is about 850 °C. The temperature in the reactor must be variable around this temperature, up to about 1000 °C. The pressure in the reactor should be somewhat higher than atmospheric, to supply the pressure drop over the off-gas treatment equipment. The pressure in the reactor will therefore range from 1.1 to 1.5 bar.

The gas velocities in the reactor depend on the minimal fluidization velocity of the sorbent. The sorbent for SO₂ retention has a minimal fluidization velocity of 0.65 m/s at 850 °C. The fluidization velocity in bed 1 and 3 should be considerably higher than the minimal fluidization velocity, while the gas velocity in bed 2 and 4 should be under or just above the minimum fluidization velocity. The ranges in which the gas velocities will be varied in the different beds, are shown in table 2.1.

Table 2.1: Ranges of the gas velocities for the SO₂ process.

Bed	Range of the gas velocities (m/s)
#1	1-2
#2	0.4-1
#3	1-2
#4	0.2-1

The concentration of SO₂ in the feed gas should be about the same as the concentration in the bed during the combustion of coal. When coal with a low sulphur content is chosen, for example Polish-5 (0.75 weight % S), the concentration of SO₂ in the off-gas at stoichiometric combustion is about 700 ppm. The feed gas should also contain some O₂, as in a real combustor also O₂ is present and it is needed for the sulphation of the sorbent. The concentration of H₂ or CO in the feed gas to bed 3 should be high enough for complete regeneration of the sorbent. The range of the gas compositions of the feed gases is shown in table 2.2.

Table 2.2: Ranges of the gas compositions of the feed gases for the SO₂ process.

gas	bed #1	bed #2	bed #3	bed #4
SO ₂ (ppm)	300-1300	-	-	-
O ₂ (v%)	1-5	-	-	-
H ₂ (v%)	-	-	0.5-5	-
CO (v%)	-	-	0.5-5	-
N ₂ (v%)	balance	100	balance	100

H₂S process

The optimal working temperature of the sorbent for the H₂S process is 600 °C, so the temperature in the reactor must be variable around this temperature. The pressure variation in the reactor is the same as for the SO₂ process. The size of the sorbent particles can be chosen freely. Here is chosen for the same size as used in the experiments done until now (0.4 mm). The minimum fluidization velocity of the sorbent is 5.1 cm/s. The range of the gas velocities are shown in table 2.3.

Table 2.3: Range of gas velocities for the H₂S process.

bed	range of gas velocities (m/s)
#1	0.10-0.50
#2	0.02-0.10
#3	0.10-0.50
#4	0.01-0.10

The gas composition of the feed gas to bed 1 should be around the gas composition of the fuel gas of a Shell coal gasifier. The gas composition of a Shell coal gasifier and the range for the feed gases chosen for the pilot plant are shown in table 2.4.

Table 2.4: Range of the gas composition of the feed gases for the H₂S process.

gas	Shell process	bed #1	bed #2	bed #3	bed #4
H ₂ S (v%)	0.3	0-1	-	-	-
CO (v%)	64	0-70	-	-	-
H ₂ (v%)	32	0-40	-	-	-
CO ₂ (v%)	1	0-5	-	-	-
H ₂ O (v%)	1.5	0-5	-	10-90	-
N ₂ (v%)	0.7	balance	100	balance	100



Chapter Three: Preliminary design of a 100 MW power plant and downscaling

The scale-up of a new process from laboratory to commercial scale can be done in several ways. One is to work in small steps from small to large scale: laboratory scale, bench scale, pilot plant, test plant, commercial plant. This way of working is expensive and time consuming. The progress in chemical engineering has made it possible to make models with sufficient predicting value to design commercial plants on paper in one step from laboratory scale to commercial scale. This preliminary design can then be studied to see which details of the design need further investigation on a smaller scale in a pilot plant. This is called downscaling.

In scale-up and downscaling techniques like dimension and regime analysis can be useful. In dimension analysis process quantities are joined together to form dimensionless groups like Reynolds, Froude and Fourier. These groups should have about the same value for the small and large scale plant. Often it is impossible to keep all dimensionless groups constant on small and large scale. Therefore it is necessary to analyze which dimensionless groups are really important. This is called regime analysis. A problem is that the regimes on small and large scale can be different. This is especially true for fluidized beds, in which mixing and mass and heat transfer strongly depends on the rising gas bubbles or slugs. A not unusual approach in the scale-up of fluidized beds is to investigate the hydrodynamics first in a cold model.

Van Hout and van Keep (1992) made a preliminary design of a 100 MW power plant, based on coal combustion with regenerative SO_2 removal in an IFB. Their work was continued by Dekker and Eyssen (1992), who also did some work on downscaling. Their results will be summarized here.

For the design of the coal combustor the following assumptions were made:

- the fuel is Polish-5 coal
- the coal is combusted with air
- the coal is completely combusted in bed 1
- the thermal yield of the plant is 39 %.
- the bed temperature is 850 °C
- the maximum bed height is 4 m
- the sorbent for SO_2 removal is SGC-500
- the maximum SO_x emission is 700 mg/m³
- the maximum NO_x emission is 100 mg/m³
- the maximum dust emission is 20 mg/m³

The necessary amount of coal was calculated from the desired power and the thermal yield. When the coal flow is known, the product of the area of bed 1 and the superficial gas velocity in bed 1 is fixed by the amount of oxygen needed for the combustion. The product of the area of bed 3 and the superficial gas velocity in bed 3 is fixed by the amount of hydrogen needed for the regeneration. When values for the superficial gas velocities are chosen the areas of bed 1 and 3 can be calculated. The area of bed 2 is fixed by assuming that a certain solids residence time is needed to allow segregation of ash and

sorbent. The area of bed 4 should be chosen as small as possible. The following results for the dimensions of the reactor were obtained:

Table 3.1: Dimensions of the reactor of a 100 MW power plant

	bed 1	bed 2	bed 3	bed 4
H (m)	4	3.9	4	3.5
A (m ²)	96	2	2.6	2
u (m/s)	3	0.8	1.56	0.63
τ_{sb} (s)	26809	780	849	700

For the calculation of the SO₂ retention the model described in Appendix 1 was used. The SO₂ and NO_x emissions were found to be far below the allowed values with the chosen bed height. A regeneration gas with 4 mol % SO₂ was obtained. However this gas is mixed with the gases from bed 4 so the final obtained SO₂ concentration will be lower.

Downscaling

By dimension analysis Dekker and Eyssen (1992) found dimensionless numbers. However they found it impossible to keep all these numbers constant for the large scale plant and the pilot plant. As they choose to keep the ratio of the areas of bed 1 and 3 and the height/diameter ratio constant no reasonable dimensions for the pilot plant were found. However some conclusions can be drawn from their design. It is clear that a regeneration gas with a high SO₂ concentration can only be obtained by a high ratio of the flows through bed 1 and bed 3. This ratio is about 70 in their design. The area of bed 1 is much larger than the area of bed 3. For the pilot plant can be concluded that the ratio of the areas should be as high as possible. Other important parameters are the height/diameter ratio and the gas residence time, which preferably should be the same. In Chapter Five these parameters are discussed in the section about the choice of the dimensions of the reactor of the pilot plant.

Chapter Four: Set-up of the pilot plant

The pilot plant will be used for both the H_2S and the SO_2 process. In the past most research has been done on the retention and regeneration of SO_2 in fluidized beds, whereas the H_2S process hasn't been tested before in fluidized beds. The pilot plant will first be used for research on the SO_2 process. For this process the sorbent SGC-500 will be used. A storage of 500 kg of this sorbent is already available. The average particle size of this sorbent is 2.5-3 mm, its measured minimum fluidization velocity 0.65 m. High gas flows are therefore necessary to operate the IFB.

When the same gas flows would be used for the H_2S process, the costs for these gases will be very high. The fuel gas obtained from a coal gasifier contains a lot of CO and H_2 , compared to N_2 expensive gases. Adding even a small amount of CO to the simulation gas, will increase the costs of the gases enormously. When a lower particle size is chosen smaller gas flows are needed. Using smaller gas flows will involve a number of changes to the pilot plant.

The pilot plant discussed in the next chapters is designed for the SO_2 process. The changes which are necessary to adjust the pilot plant to the H_2S process when smaller gas flows are used, will be discussed in Appendix 13.

4.2 Flowsheet of the pilot plant

In figure 4.1 the flowsheet of the pilot plant is shown. The pilot plant can be divided in four sections: supply section, reactor section, sampling and analyzing section (not shown in the flowsheet) and off-gas treatment section.

Large amounts of N_2 and air are needed. N_2 is supplied from a large tank, while air is supplied from the local pressurized air system. All the other gases are supplied from gas bottles. The pressure of the gases is reduced to the desired value by pressure reducers. The nitrogen and air flows are preheated. The flow of each gas is separately adjusted by mass flow controllers. To each bed in the reactor a separate gas flow is supplied. To bed 1 N_2 , SO_2 , and air can be supplied, to bed 2 only N_2 , to bed 3 N_2 , H_2 or CO and to bed 4 N_2 . For measurements of the gas leaks through the orifices in the gases, there is the possibility to supply a tracer gas to each bed.

The reactor section consists of the gas distributor, the reactor part itself and a freeboard. The reactor is heated electrically. The sampling points for the gas and the solids, the temperature and pressure measuring points and the solids feed system for feeding sand or coal to the reactor are not shown in this flowsheet. Only the sampling section is discussed in this report. The design of the analyzing section itself and the choice of the tracer gas depends on the analyzing equipment chosen, and is not included in this design.

In most fluidized bed set-ups built in the 'Proeffabriek' until now, only dust was removed from the off-gases. In this design it has been chosen to remove also the hazardous components, like H_2S , SO_2 and CO from the gases. Behind the reactor a cyclone is placed

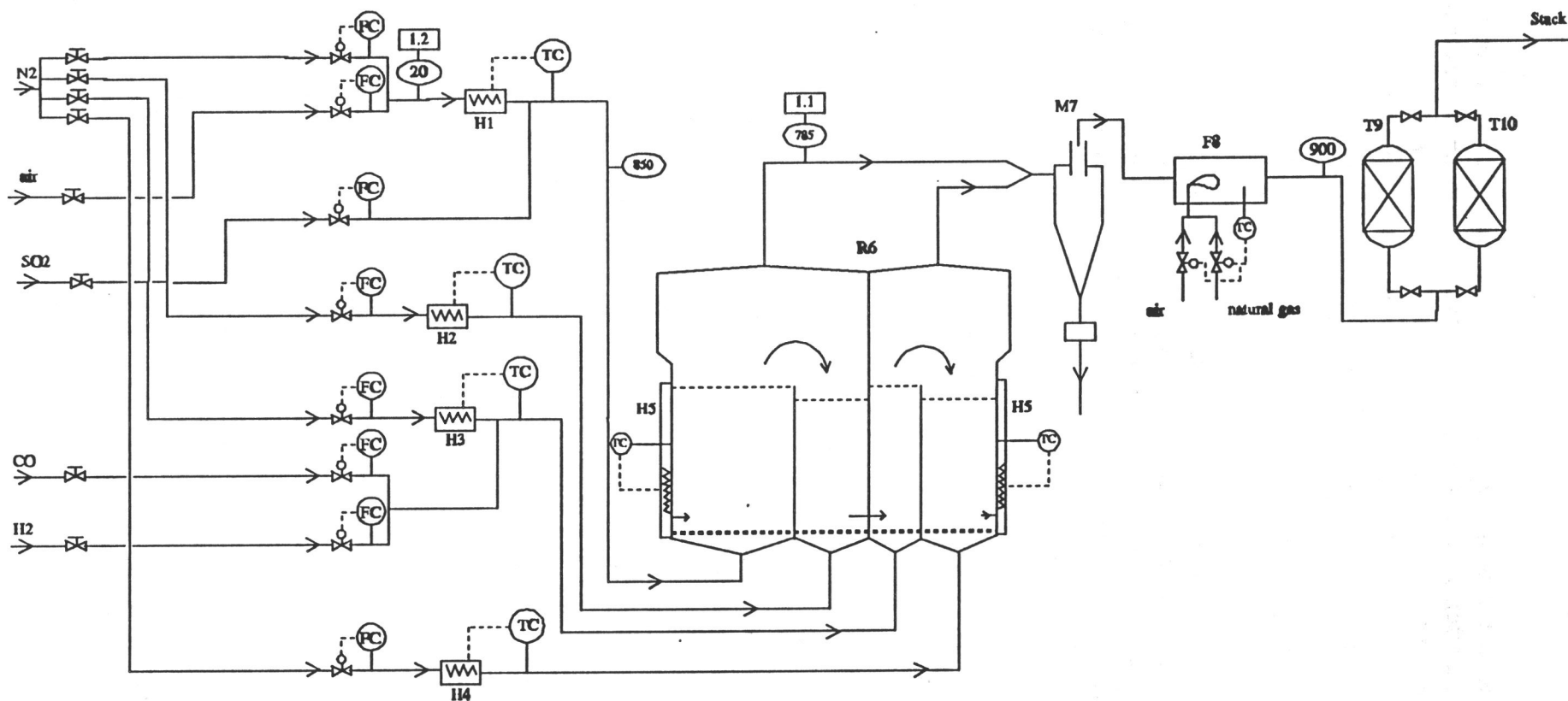


Figure 4.1 Flowsheet Pilot Plant IFB

EQUIPMENT

H1 Electrical preheater, bed 1
 H2 Electrical preheater, bed 2
 H3 Electrical preheater, bed 3
 H4 Electrical preheater, bed 4
 H5 Electrical reactor heater
 R6 IFB reactor

M7 Cyclone
 F8 Waste gas converter
 T9 CaO packed bed
 T10 CaO packed bed

FLWSHEET PILOT PLANT IFB

P

pressure (bar)

T

temperature (°C)

to remove most of the dust from the fluidized bed. Blockage of the off-gas treatment equipment by dust is thus prevented. All combustible components (CO , H_2 , S_2 and H_2S) will then be converted to CO_2 , H_2O and SO_2 . Natural gas is burned with air to provide a temperature high enough to ensure conversion of all combustible components. The gases are then led through a bed of limestone or spent sorbent to remove the SO_2 from the gas flow. The temperature drop of the gas flow through the freeboard and the cyclone will be about 100°C . The temperature will then increase again due to the burning of natural gas to 900°C . Because of the high temperatures, the part of the set-up from the gas preheating to the CaO -bed should be well insulated. The gases leaving the CaO -bed are blown off through the roof. If required the gases should be cooled down after the CaO -bed and fine dust be removed by a bag filter.

In the next Chapters these sections will be discussed in detail.

Chapter Five: Design of the reactor section.

5.1 Choice of the reactor dimensions.

Bed areas

As discussed in Chapter 3 in a commercial plant the ratio of the areas of bed 1 and 3 was chosen high to obtain a regeneration off-gas with a high concentration of SO_2 . Also for the pilot plant a high ratio is desired. To make the ratio of the areas of bed 1 and 3 as high as possible, bed 3 should be small. The minimal dimensions of bed 3 are given by the particle size of the used sorbent material. Wall effects play an important role when the ratio bed diameter/particle diameter is small. To make the effect of the wall sufficiently small, this ratio must have a minimum value of 20 (Sie, 1992). The sorbent that will be used in the IFB (SGC-500) has a mean particle size of 2.5 mm. Therefore the minimal dimensions of bed 3 must be 50*50 mm. The dimensions of bed 3 were chosen to be 60*60 mm, to leave some more space for the orifice construction. The choice of the dimensions of bed 1 were determined by two considerations, the ratio of the areas of bed 1 and 3 should be as high as possible, but the costs of the gases should be reasonable. A bed size of 140*140 mm was chosen. At this size the costs of the gases were found to be reasonable. The ratio however is considerable lower than in the design of the large scale plant. This means that in the pilot plant a lower H_2 concentration in the feed gas of bed 3 has to be used and a lower SO_2 concentration will be obtained in the off-gas. For the total configuration a square of 200*200 mm was chosen. The dimensions of all beds are given in table 5.1.

Table 5.1: Dimensions of the four beds in the reactor

bed	dimensions (mm)	area (m^2)
1	140*140	0.0196
2	60*140	0.0084
3	60*60	0.0036
4	60*140	0.0084
totaal	200*200	0.0400

Bed height

When we look at the choice of the height of the reactor we should consider several points: the height/diameter ratio, the gas residence time, the solids circulation time and the solids and gas flows through the orifices.

When the height/diameter ratio in the pilot plant and in the large scale plant differ substantially, the fluidization regime be different. Because a very small diameter is chosen for bed 3, the fluidization regime will not longer be slugging when a very high bed is

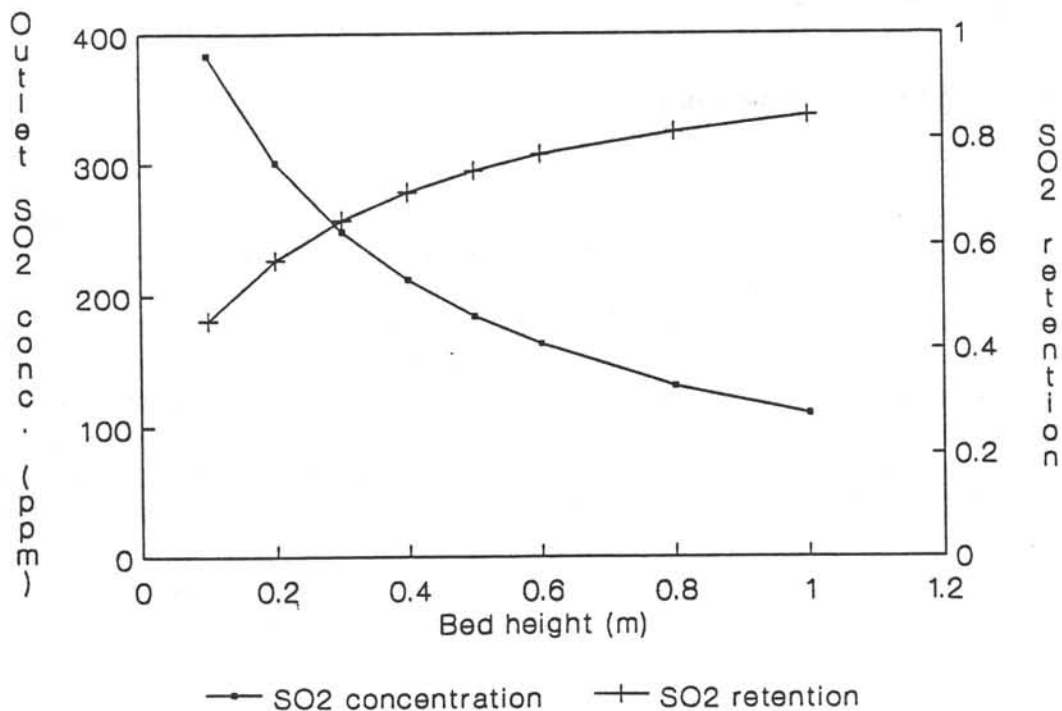


Figure 5.1: Influence of the bed height on the outlet SO₂ concentration and the SO₂ retention in bed 1 ($u_1 = 1.5$ m/s, $C_{\text{SO}_2,1}^0 = 700$ ppm)

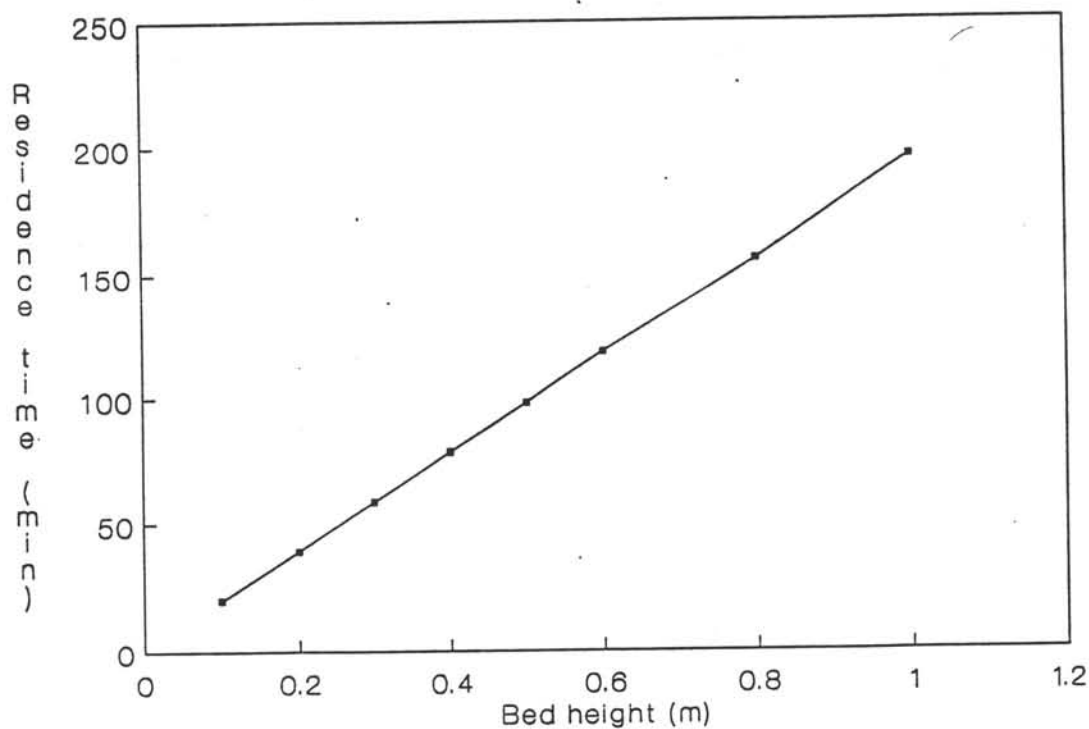


Figure 5.2: Influence of the bed height on the solids circulation time in the IFB ($\phi_{\text{sb}} = 2$ g/s)

chosen. In the design of a large scale plant the height/diameter ratio for bed 3 is about 2.5. When the same ratio is applied in the pilot plant, the height should be 0.15 m.

The fluidization velocities in the pilot plant are the same as in the large scale plant as the same sorbent is used. When the height of the bed is lower than in the design of the large scale plant, the gas residence time will be lower. In figure 5.1 the influence of the bed height on the outlet SO_2 concentration in bed 1 and the SO_2 retention is shown. The calculations were done with a MathCad 2.5 computer program based on the models discussed in Appendix 1. The norm laid down by legal regulations for coal combustion plants is an outlet SO_2 concentration of 215 ppm. For the pilot plant however it is not necessary to meet this norm, it is sufficient to obtain a considerable conversion so that the outlet concentrations can be measured accurately. We see that even at low bed heights a considerable retention is obtained.

As it takes 3 to 5 times the solids circulation time before the IFB can be assumed to be stable, the circulation time may not be too high. The circulation time depends on the solids flow through the IFB and the bed height. The circulation time increases linearly with the bed height, if all other input variables are kept constant. Figure 5.2 shows the influence of the bed height on the circulation time at a solids flow of 2 g/s. At a bed height of 0.3 m the circulation time is about 60 minutes, so it would take about 3 to 5 hours for the IFB to become stable.

In figure 5.3 the solids flow and relative gas leak through the orifice between bed 2 and bed 3 are shown as a function of the bed height and the orifice diameter. The simulation was done with a program based on the model for calculating the solids flow and the gas leak through an orifice, which is given in Appendix 5. The relative gas leak is defined as the gas flow through the orifice divided by the gas flow through bed 2. The solids flow increases with the square root of the bed height. The relative gas leak increases linearly with the bed height. We can conclude from this picture that the bed height should be as low as possible, because when the diameter of the orifice is 15 mm the solids flow is high enough, while the relative gas leak should be kept as low as possible. The bed height should not be higher than 0.6 m.

Based on these considerations a bed height of 0.3 m was chosen. In the reactor there will be space for extending the bed height to maximal 0.6 m.

Orifice diameter

Model calculations showed that the needed sorbent flow through the reactor will be between 0.5 and 5 g/s for the SO_2 process. From figure 5.3 it can be concluded that an orifice diameter of 15 mm is large enough to allow these solids flows, although the gas leaks can, depending upon the bed height, be considerable. Orifices with a different shape may be used to reduce the gas leaks. These kinds of orifices can first be investigated in the cold model IFB.

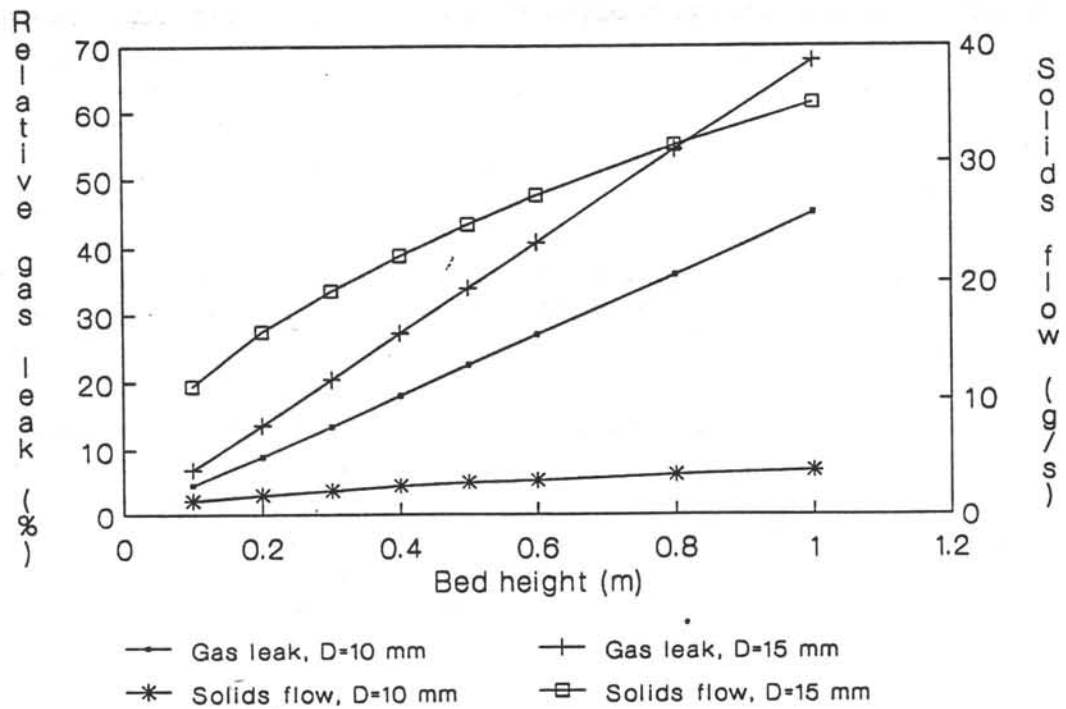


Figure 5.3: Influence of the bed height on the solids flow and the relative gas leak through the orifice between bed 2 and bed 3 with different orifice diameters ($u_2 = 0.8 \text{ m/s}$, $u_3 = 1.5 \text{ m/s}$)

Orifice height

The centre of the orifice between bed 1 and 4 is located at 0.03 m above the gas distributor to leave some space for changing the orifice. The orifice between bed 2 and bed 3 should be located higher. Bed 2 is used for the segregation of ash and sorbent or of sand and sorbent (when sand is used to simulate ash), so the bottom layer of the bed will consist of ash or sand. The ash should be removed at the bottom while only sorbent should go through the orifice. When the maximum flow of sand is 0.1 g/s the maximum height of the sand layer as calculated with the models in Appendix 4 is about 0.02 m. The height of this orifice is chosen to be twice the maximum height of the sand layer higher than the other orifice. The centre of this orifice is then located at 0.07 m above the gas distributor plate.

5.2 Construction of the reactor.

The reactor material must meet a lot of requirements. The material should be resistant to oxidizing, reducing and sulphurous environments at a high temperature. The material should also be suitable for welding and screwing. A material that can meet all these requirements is the alloy Haynes HR-120. This material has been chosen.

The minimum wall thickness of the reactor can be calculated with:

$$t_w = \frac{P.D}{2.\sigma_t.E} + c \quad 5.1$$

with:

- t_w = wall thickness (m)
- P = design pressure = 3.10^5 Pa
- D = diameter reactor = 0.2 m
- σ_t = yield strength of the material at 870 °C = 185 MPa
- E = welding factor = 0.7
- c = corrosion factor = 0.002 m

The calculated minimum wall thickness is 2.3 mm. However the wall thickness should be much thicker to allow welding and screwing of the reactor parts. A wall thickness of 6 mm has therefore been chosen.

A drawing of the reactor is shown in figure 5.4. The separating wall between bed 1 and 2 on one side and bed 3 and 4 on the other side is the basis of the reactor. This wall should be made of one piece from the bottom to the top of the reactor to separate the oxidizing environment of bed 1 and the reducing environment of bed 3. At the bottom of this wall the orifices are made. The weir between bed 1 and 2 and the weir between bed 3 and 4 are welded to this wall. These weirs should have a height of 0.3 m. The side walls of the reactor should be removable as to be able to change the orifice diameter. Four different parts are made and connected to the separating wall and the weirs with screws. These parts are 0.6 m high as to allow a maximum bed height of 0.6 m. At the top they are connected to the freeboard. A graphite seal (Grafoil) can be used. At the top of the

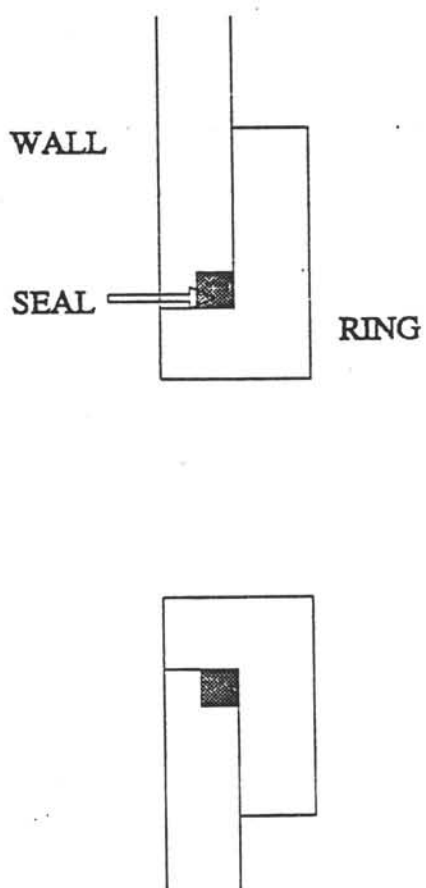


Figure 5.5: Construction of the orifice

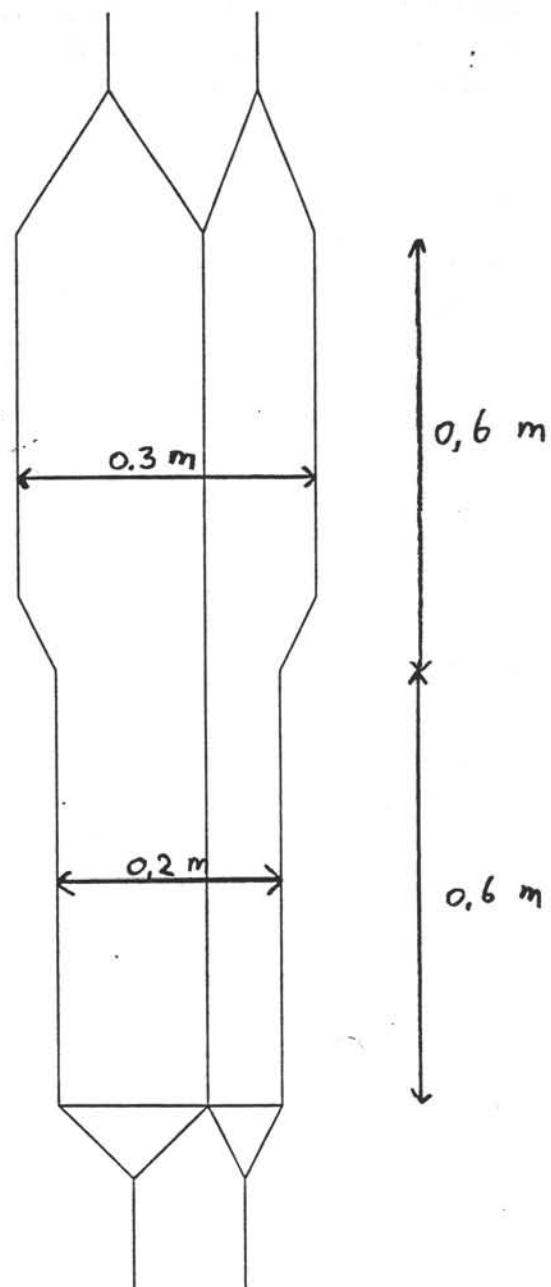


Figure 5.4: The reactor

freeboard the gas outlets are connected. In the freeboard there are also holes to be able to supply fresh sorbent at the beginning of an experiment.

The size of the orifices should be easily variable. The orifice diameter should range from 10 to 40 mm. The following construction is suggested. In the separating wall a hole is made of 46 mm. In this hole rings with different innerside holes can be connected. The rings can be connected in two different ways:

- with a high temperature glue (Gluecon 1000). The glue holds the ring in the hole at high temperatures, but the ring can be removed at low temperatures.
- with a grafit seal (Grafoil) or a metallic seal (Inconel) (see figure 5.5).

The first solution is preferred, as it is the easiest one.

5.3 Reactor heating and insulation

The gas flow will be preheated up to the desired temperature. In the stationary state this is sufficient to keep the temperature in the reactor at the desired value. At the start-up however the reactor should be heated up. This is not possible only by the gas flow. Additional reactor heating is needed. In Appendix 6 calculations are done concerning the heating up of the reactor. These calculations show that a reactor heater capacity of 4 kW should be sufficient. The reactor heater consists of 4 Moduthal panels, placed on each side of the reactor. The elements are made of Kanthal A1 (FeCrAl), imbedded in Al_2O_3 . It is possible to make holes in these elements for sampling and measuring points.

When experiments are done with coal combustion in the reactor, heat is produced in bed 1. For stable operation it is necessary to remove this heat. As the reactor is well insulated and it is difficult to provide the reactor with cooling elements, the heat must be removed by the gas flow through bed 1. The maximum amount of coal that can be combusted depends on the heat that can be removed. The heat removed by the gas flow is maximal when the gas flow is heated up from 298 to 1123 K in the bed. This requires 12 kW. When Polish-5 coal is used (heat of combustion: 29370 kJ/kg) maximal 0.4 g/s of coal can be combusted.

At the start-up of a coal combustion experiment the reactor should first be heated up to the desired temperature (1123 K). The coal combustion can then be started with a small amount of coal. The amount of coal combusted is gradually increased and the temperature of the inlet gas flow gradually decreased, keeping the temperature in the reactor constant.

The reactor should of course be well insulated. A choice has been made for Fiberfrax Durablanket, a ceramic fibre made of alumina and silica. It is light, strong, and has a low thermal conductivity. It can also easily be processed. It is available with different densities and layer thicknesses. The choice of the layer thickness depends on the temperature at the outside of the insulation. The temperature at the outside of the insulation material is 102 °C with a layer thickness of 76 mm, while it is 87 °C with a layer thickness of 102 mm (data from the supplier). Increasing the layer thickness even further will have little effect. A layer thickness of 102 mm has therefore been chosen. This means that there should be warnings in the neighbourhood of the reactor, to make people aware of the danger of the hot surface of the reactor insulation.

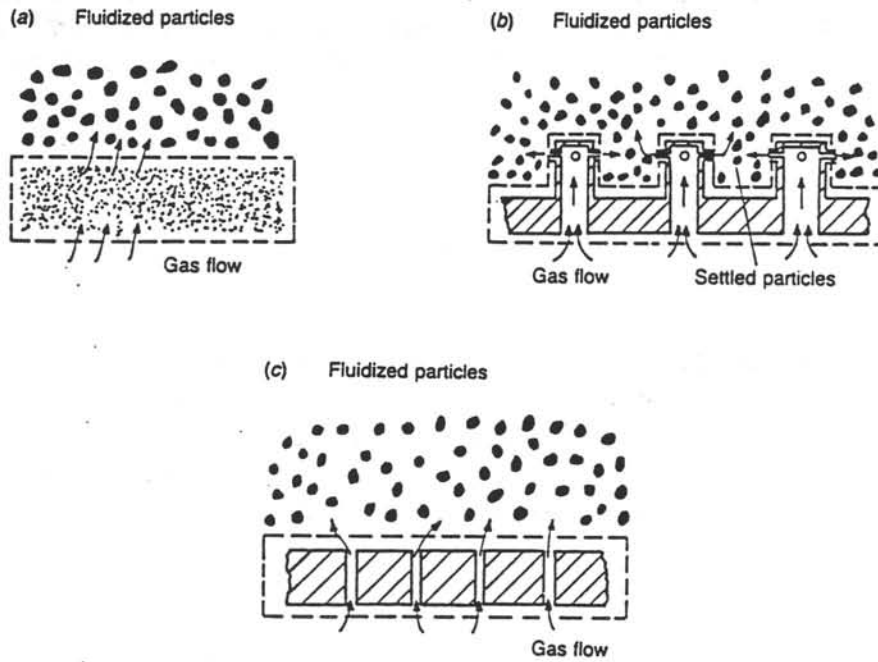


Figure 5.6 Alternative types of distributor: (A) porous plate, (B) tuyère distributor, (C) perforated plates

5.4 Gas distributor

Three different types of gas distributors can be distinguished for use in fluidized beds: perforated plates, porous plates and tuyère distributors. In figure 5.6 these three distributors are shown. Perforated plates have been chosen as gas distributors in the IFB.

Disadvantages of porous plates are the uncertainties of the performance caused by differences in thickness and permeability, the fragility and the possibility of blockage of the holes by dust. In tuyère distributors the gas is blown into the bed through nozzles in horizontal position. In this type of distributor excessive high gas velocities at the nozzles may be required to satisfy a high enough pressure drop over the distributor. This may result in erosion and breakage of the sorbent particles which is undesirable. An advantage of both the porous plates and the tuyère distributors is that particles cannot drain into the windbox when defluidized. In case of using perforated plates drainage of particles is indeed possible. Geldart and Baeyens (1985) suggested that if the holes in perforated plates are larger than about 5 times the average d_p , the bed will drain into the windbox. However, this limitation can be avoided by the use of mesh under the perforated plate.

To design the perforated plates a procedure has been set up based on design rules suggested by Geldart (1986), Sathiyamoorthy and Rao (1981) and Kunii and Levenspiel (1991). In appendix 7 this procedure will be explained and will be applied for the design of the gas distributors in the IFB. Before this procedure is used for design calculations, the characteristics of the gas distributors will be discussed. In the design procedure the maximum allowable velocity through the orifices has been chosen to be equal to 80 - 90 m/s. At higher gas velocities through the orifices, the pressure drop over the distributor will become out of proportion. The high gas velocities may cause channeling of the bed because of possible breakthrough of jets to the bed surface. Another problem with high gas velocities that will occur, is the increasing attrition of the sorbent particles. Geldart and Baeyens (1985) reported that gas velocities through the orifices higher than 90 m/s are generally causing a high degree of attrition.

Choice of the characteristics of the distributor

The distributor consists of a perforated plate that is made of the same construction material as the reactor. The orifices in the distribution plate have a diameter $d_{or} = 0.002$ m. The thickness of the plate $t_d = 4$ mm. With the choice for the orifice diameter the ease of perforating the plate has been taken into account. Distributors with orifice diameters which are smaller than 1 mm are very difficult to make. The sorbent particles are large so that drainage through these orifices is prevented. The thickness of the plate will depend on the loadings by the bed mass under high temperature conditions. Calculations of strength has shown that the plate is thick enough. The four necessary distributors will all be made using one plate.

To ensure an uniformly fluidized bed not only the design of the gas distributor but also the arrangements of the windbox are important. In figure 5.7 a few examples of these arrangements are shown. In this figure the preferred and less preferred options have been indicated for both horizontal and vertical gas flow into the windbox. In the preferred arrangements the gas flow will enhance the gas distribution over the perforated plate. The horizontal flow entrance has been chosen.

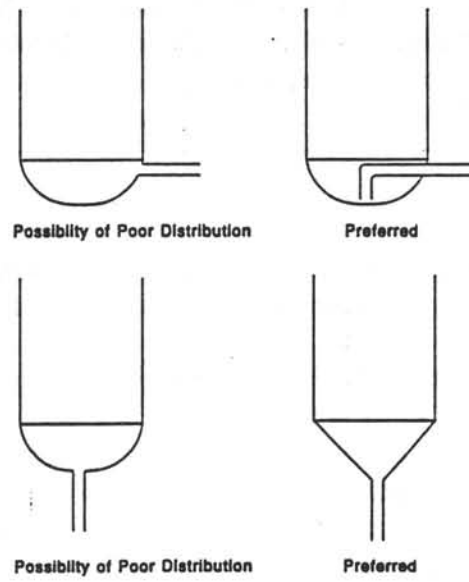


Figure 5.7 Some possible arrangements for the windbox of the fluidized bed

5.5 Freeboard

Entrainment is the ejection of particles from the surface of a fluidized bed by bursting of bubbles. Depending on their terminal velocity and the gas velocity, particles are carried up to various heights. The larger particles fall back, while particles with a terminal velocity smaller than the gas velocity, will be dragged along with the gas. Because particles with a terminal velocity higher than the gas velocity will fall back, the solids loading of the gas will decline with height. The Transport Disengagement Height (TDH) is the height at which the solids loading of the gas reaches a constant value. To allow maximum return of the solids to the bed, the height of the freeboard should be higher than the TDH. The TDH is a function of the column diameter, the gas velocity and the bubble size.

Two freeboard configurations will be considered here, a freeboard with a diameter which is the same as the reactor diameter (20 cm) and a freeboard with a larger diameter of 30 cm. Bed 1 is the bed with the largest surface and the highest gas velocity, so we will consider this bed. The diameter of this bed is 14 cm, therefore it is assumed that the maximum bubble diameter will also be about 14 cm. In the freeboard the gases of bed 1 and 2 come together so the maximum gas velocity will be lower than the maximum gas velocity in bed 1, and is assumed to be 1.7 m/s. The TDH is estimated from a plot of Zenz and Weil (1958) who give the TDH as a function of bubble size and the gas velocity.

The terminal velocity is given by with equation A3.2 (Appendix 3), which is valid for $0.4 < Re_p < 500$. For particles with a diameter larger than about $50 \mu\text{m}$, Re_p is within this range. With this equation the diameter of the particles d_p , which will be dragged along with the gas, can be calculated. Table 5.2 shows the gas velocity in the freeboard, the TDH and the diameter of the particles that will be dragged along, for both freeboard configurations.

Table 5.2: u_{fb} , TDH and critical particle diameter

D_{fb} (m)	u_{fb} (m/s)	TDH (m)	d_p (μm)
0.2	1.7	1.73	273
0.3	0.84	0.48	135

Based on these figures a diameter of the freeboard of 0.3 m and a height of 0.6 m are chosen. The angle of the connection part between the freeboard and reactor is 60° to allow falling particles to roll back into the bed. The freeboard should be made of the same material as the reactor.

The temperature of the off-gases should stay high to allow conversion of the combustible components in the gas and the SO_2 removal in the CaO-bed. Although the freeboard, the cyclone and connecting pipes will be insulated the gases will cool down. As the freeboard has the largest outer area, the temperature drop of the gas flow will be the highest in the freeboard. Therefore the cooling of the gas flow in the freeboard was calculated. A heat

balance is considered over an element dz of the freeboard:

$$\phi_g \cdot C_{p,g} \cdot \frac{dT_g}{dz} = O \cdot \frac{1}{\frac{d_{ins}}{\lambda_{ins}} + \frac{1}{\alpha_L}} \cdot (T_g - T_{env}) \quad 5.2$$

The left hand term describes the cooling of the gas flow, while the right hand term is the heat loss through the insulation of the freeboard. It is assumed that the heat transfer of the gas flow to the steel wall of the freeboard is not rate limiting so that the steel wall has the same temperature as the gas. Integration of equation 5.2 over the height of the freeboard yields depending on the gas flow a temperature drop of 30 to 90 °C.

Chapter Six: Supply section

In the description of the gas supply section attention will be paid to the sources of the gases and the gas preheating section. The supply system for coal and sand particles will be discussed in the second part of this chapter.

6.1 Gas supply

Sources of the gases

In the gas supply section two types of gas flows are distinguished: the fluidization gas flow and the reactive gas flow. The fluidization gas flow is the main gas flow which is used to fluidize the beds. The reactive gas flows are much smaller than the fluidization gas flows as the gas concentrations of the reactive components are small in the reactor. In appendix 9 an estimation of the diameters is given for each of the lines in the feed section.

Nitrogen

The amount of nitrogen (maximum total flow is about $67 \text{ Nm}^3/\text{h}$) needed for experiments with the pilot plant is too large to use nitrogen from cylinders. A storage vessel with liquid nitrogen will be used for the nitrogen supply. The liquid nitrogen will be evaporated and led to the pilot plant at a pressure of 10 bar.

Only for safety purposes a cylinder with nitrogen will be available.

Air

The maximum flow expected for oxygen is about $1.8 \text{ Nm}^3/\text{h}$ (5 v% in total flow). Using maximum oxygen flowrates, only a few experiments are possible with one cylinder. Because of this, it has been chosen to use pressurized air instead of cylinders. The pressurized air flow will be delivered by the main compressor of the faculty. The maximum air flow from this compressor is $400 \text{ Nm}^3/\text{h}$ at a pressure of 6-7 bar. This air flow is large enough since the maximum air flow to bed 1 is expected to be about $40 \text{ Nm}^3/\text{h}$. The compressor has been provided with a dry column device so that no extra dry column is needed in the air supply line to the reactor. The pressurized air flow will contain the amount of oxygen needed for both coal combustion experiments and experiments with simulation gases. A mixture of air and nitrogen will flow to bed 1.

Reactive gases: sulphur dioxide, hydrogen and carbon monoxide

Carbon monoxide, hydrogen and sulphur dioxide can be delivered from cylinders at a maximum pressure of 200 bar. The maximum flows for carbon monoxide and hydrogen are expected to be about $0.4 \text{ Nm}^3/\text{h}$ (5 v% in total flow to bed 3). The cylinders have a content of 10 Nm^3 and are capable to supply gas during a number of experiments.

An optional sulphur dioxide supplier is a cylinder which contains nitrogen with 5% sulphur dioxide. This option is only interesting when experiments are done under higher pressures. The dilution with nitrogen is intended to lower the vapour pressure of sulphur dioxide. At a temperature of 20°C , the vapour pressure of pure sulphur dioxide is 3.3 bar. Since only experiments at (nearly) atmospheric conditions are done, no problems are expected with the supply from cylinders with pure sulphur dioxide.



Natural gas

A connection with the local network of natural gas is needed for the supply to the converter.

Heating of the gases

The different strategies for the heating of the gases will be discussed. The calculation of the amount of heat will be included. In the set-up of these strategies mass flow controlling and the sequence of mixing and heating will be considered.

To heat up the gases electrical heating is preferred. It is possible to use porous ceramic elements which contain electrical wires with a large contact area with the gas. These elements are relatively small and can easily be placed in the gas flow lines.

In the set-up of the heating of the gas flows it has been chosen to heat up the fluidization gas flows only. The cold reactive gas flows will be mixed with the hot fluidization gas flows. The temperature of the mixed gas flows will be measured and controlled by changing the heat input to the fluidization gas flow. In this set-up extra heat input for the fluidization gas flow is needed to heat up the cold reactive gas flows. Some heat will be lost by the connections of the cold lines with the reactive gas flows. The advantage of this set-up is that only inert gas (nitrogen) will come in contact with the heating elements. This means that the material of these elements does not need to be resistant to a oxidizing, a reducing or a sulphurous environment.

The mass flow controllers for the fluidization gases are placed at the cold side of the gas supply section where it is very easy to measure and to control the gas flows. Under hot conditions some difficulties regarding mass flow controlling may arise; accurate mass flow measurement at high temperature is not possible with the normal methods. Mass flow controllers for the fluidization gases at the hot side would have the advantage that in one preheater the gases could be heated up and then the mass flows could be controlled. The use of one preheater would have simplified the set-up but the temperature of the gas flows (after mixing with the reactive gases) would have been difficult to control.

Calculations

The basis of the calculations of the amount of heat input is that the gases have to be heated up to maximum 1000 °C. The total heat input for each of the four gas flows can be calculated with:

$$Q_j = \sum_i \left(\phi m_{i,j} \cdot \int_{T_0}^{T_{des}} C p_i(T) \cdot dT \right) \quad 6.1$$

where Q_j is the heat input to gas flow j (W)

$\phi m_{i,j}$ is the molar flow of component i in gas flow j (mol/s)

$C p_i$ is the heat capacity component i (J/(mol*K))

T_0 is the inlet temperature (K)

T_{des} is the desired temperature (K)

In equation 6.1 the heat capacities are a function of temperature T:

$$Cp_i(T) = a_i + b_i \left(\frac{c_i}{T} \right)^2 + d_i \left(\frac{e_i}{T} \right)^2 \quad 6.2$$

For each component in the gas flows the five parameters in this equation: a_i , b_i , c_i , d_i and e_i are taken from data collected by Daubert and Danner (1989).

In the calculations it has been assumed that heat losses due to the cold line connections are negligible. Preliminary calculations have been carried out for a number of different compositions of the gas flows. From these calculations it has been concluded that the heat input to gas flows containing different components only slightly differs from the input to flows containing only nitrogen. Therefore the heat input to the gas flows will be calculated here for gas flows containing only nitrogen. For each bed the maximum amount of heat input to the feed gas flow for that bed has been calculated using the maximum values for ϕm_{ij} and T_{des} (1273 K). The values for the amount of heat input are presented in table 6.1.

Table 6.1: Heat input to the gas flows

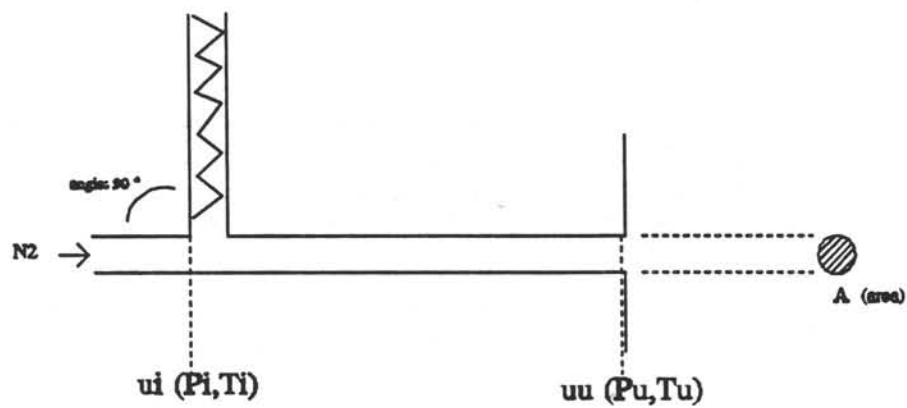
gas flow	ϕm_{ij} (mol/s)	Q_j (kW)
bed 1	0.3972	12.21
bed 2	0.0851	2.62
bed 3	0.0730	2.24
bed 4	0.0851	2.62

6.2 Solids supply

Three different solids supplies can be distinguished: sorbent, coal and sand. The sorbent particles are only fed to the reactor before starting experiments. At the top of the reactor two holes are available through which sorbent particles can be fed using a funnel device. The coal and sand particles will be fed semi-continuously to the reactor. Some experiments with the IFB will be done with real combustion of coal instead of using a simulation gas containing SO_2 . The sand flow is used for segregation experiments in bed 2. From this bed sand particles which simulate the bottom ash particles, will be taken out of the reactor through a hole in the reactor wall.

During coal combustion the bed will be fluidized with air. The coal feed has a maximum value of about 0.4 g/s (see 5.3). The maximum sand feed flow is taken to be 0.1 g/s. A solids feed system will be designed for the semi-continuous supply of coal and sand.

In principle there are two possible mechanisms for the solids feed system: a mechanical valve and a hydraulic valve. The mechanical valve consists of a mechanical device which controls the solids feed flow directly to the reactor or using a pneumatic system which will blow the



view from above: the screw line and the pneumatic conveying line
have been connected in a perpendicular position

Figure 6.1 Schematic drawing of the pneumatic conveying line

particles in the reactor. In a hydraulic valve a fluidized bed is used to control the solids feed flow. The solids may be transported from a hopper device to the fluidized bed and from this bed the solids may flow over a weir to the reactor. With this type of valve it is more difficult to control accurately the small solids flows than with a mechanical valve. Therefore it has been chosen to use a mechanical valve.

The solids feed system will be connected to the reactor near the bottom of the bed to avoid that solids will leave bed 1 immediately. Three possible mechanical devices are: the rotary valve, the screw conveyor and the vibrating conveyor. With the first two devices more accurate solids feed flow control is possible than with a vibrating conveyor. Both these systems have the disadvantage that attrition may occur. Despite of possible attrition, the final choice for the solids feed mechanism will be made between the rotary valve and the screw conveyor. These two mechanisms will be compared in Appendix 8. In this appendix calculations have been set up for both the mechanisms and the most suitable one have been chosen. Based on the estimations of the dimensions of these mechanisms a screw conveyor has been chosen.

The screw conveyor systems can be supplied by contractors as complete units including a hopper device and a driver gear system. The hopper device is closed during experiments. Before starting experiments the hopper can be filled by opening the top. To maintain the same pressure above the solids in the hopper as the inlet pressure of the conveying gas flow, a line will connect these two points. This line ensures that no gas from the reactor can flow into the hopper. Especially when the hopper has been filled with coal, a hot gas (air) from the reactor would be extremely dangerous.

At the end of the screw, the solids will be blown by a nitrogen flow through a horizontal line into the reactor. Direct solids feeding from the screw into the reactor is not possible. Problems with direct feeding are that hot gas from the reactor can flow into the screw. When coal is feeded to the reactor, combustion of coal will already take place in the screw itself. Other problems are that the material of the screw system become too hot; special material is needed that is resistant to the conditions in bed 1.

Nitrogen will be used to transport the solids from the screw to the reactor. The screw line and the pneumatic conveying line can be connected in a perpendicular position or in a -Y-position in which the angle between the lines is smaller than 90°. In figure 6.1 a schematic drawing of the conveying line is presented. Cold nitrogen will be blown into the reactor. If this nitrogen flow is small enough, the influence on the bed temperature can be assumed to be negligible. To check whether this influence is negligible or not, a calculation example of the pneumatic conveying system is given.

In this calculation example the minimum transport velocity (u_i) in the pneumatic conveying line is about 15 - 20 m/s. A value of 20 m/s is chosen, while the pipe diameter is chosen to be: $D = 0.005$ m. The gas mass flow through the conveying line can be calculated with:

$$\phi_g = \frac{\pi}{4} \cdot D^2 \cdot \rho_g \cdot u_i \quad 6.3$$

The calculated gas flow is: 0.585 g/s or 0.02088 mol/s. This flow is compared with the total flow through bed 1, 0.0115 kg/s or 0.4093 mol/s. The gas flow used in the conveying line is thus about 5% of the total flow. The temperature of the reactor will be lowered to 810 °C by the conveying gas flow. This change of temperature can be compensated with the reactor heating elements.

The range of values of the solids loading ratio in the conveying line is 0.02 - 0.68 kg/kg_g.

($\phi_{so} = 0.01 - 0.4$ g/s). These values show that a very dilute gas will flow into the reactor. Possible disturbance of the bed by the gas conveying jet can be determined by calculating the penetration length of the horizontal gas jet produced by the conveying gas into the fluidized bed. As it can be seen from the solids loading ratio the dilute phase system in the conveying line may well be considered as a pure gas flow. Merry (1971) suggested that the penetration length l_j for pure horizontal gas jets may be calculated using the equation:

$$\frac{l_j}{D} + 4.5 = 5.25 \left(\frac{\rho_g u_u^2}{(1-\epsilon) \rho_g g d_p} \right)^{0.4} \left(\frac{\rho_g}{\rho_{so}} \right)^{0.2} \left(\frac{d_p}{D} \right)^{0.2} \quad 6.4$$

where d_p is the diameter of the solids in the bed = 0.0025 m

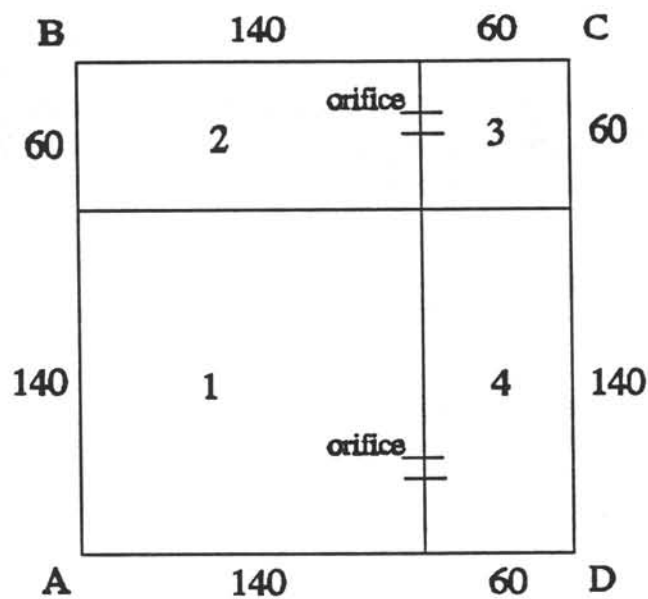
ρ_{so} is the density of the solids in the bed = 1400 kg/m³

ϵ is the bed voidage = 0.55

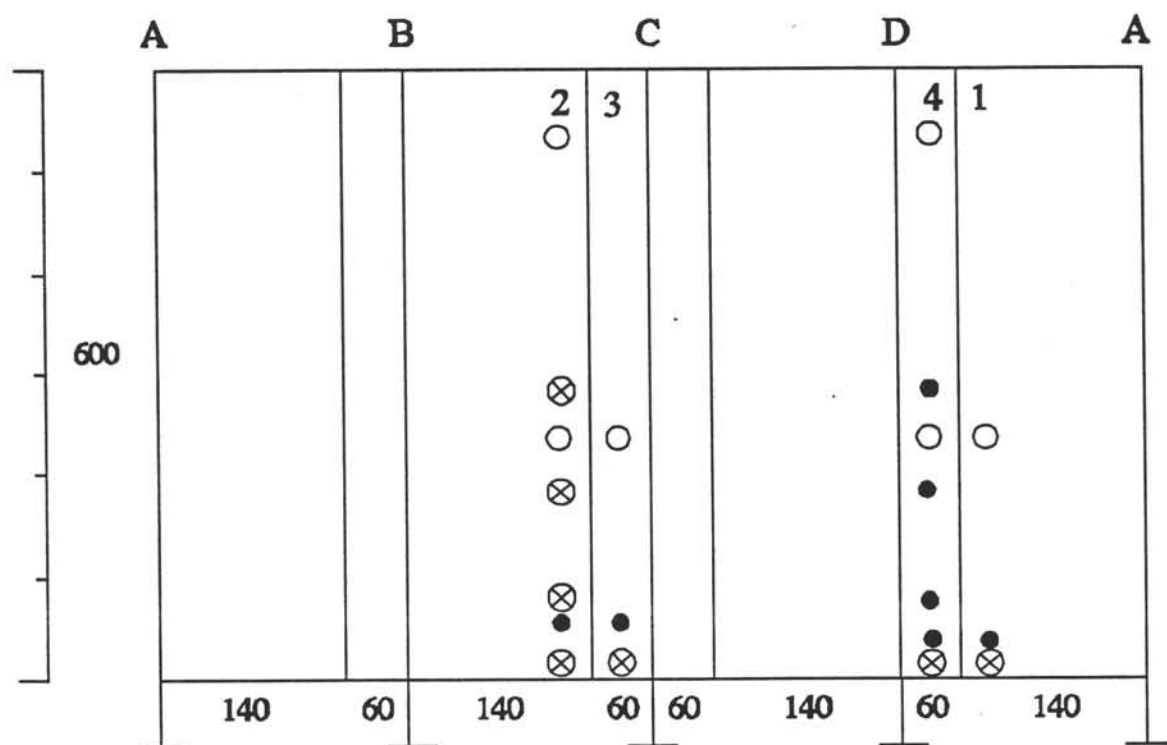
u_u is the velocity at the inlet of the reactor which can be calculated using the ideal gas law:

$$u_u = u_i \cdot \frac{T_u}{T_i} \cdot \frac{P_i}{P_u} \quad 6.5$$

It has been found for the above suggested parameters that the penetration length is 0.0056 m. If the minimum transport velocity is smaller, say 15 m/s and keeping the other parameters constant the value for l_j becomes negative. Merry (1971) suggested that if the penetration length is zero or negative the theory of jets may no longer be applied for such conditions, because jetting has been replaced by bubbling at the nozzle. From these calculations it can be concluded that there are no problems concerning the disturbance of the bed.



Cross-sectional view of the reactor



View of the side walls with positions of measuring points

- gas sampling point
- ⊗ solids sampling point
- pressure measuring point

Figure 7.1 Indication of the measuring points in the reactor

Chapter Seven: Sampling section

In this chapter the methods will be described for sampling of the gases and the solids. For both sampling methods a system will be described with which it is possible to take samples from the reactor. In the description of the solids sampling system also attention will be paid to the removal of all solids from the reactor. This chapter will start with a description of the position of the sampling points in the reactor.

7.1 Place of the sampling points

In figure 7.1 the suggested position of the sampling and measuring points are indicated. It has been chosen that all points are on one row in each bed. The position of these rows has been chosen such that the pressure measuring points on either side of the orifice are at the same distance from the orifice. Pressure measuring points are suggested at 0.03 m in bed 1 and 4 and at 0.07 m in bed 2 and 3 (these values are the heights of the orifices between the beds). Other pressure measuring points are at 0.1 m, 0.2 m and 0.3 m, only in bed 4.

Solids sampling points are suggested in bed 2 to be able to measure the amount of segregation in bed 2 at 0.02 m, 0.1 m, 0.2 m and 0.3 m. In the other beds one solids sampling point annex solids removal point is suggested at 0.02 m. Gas sampling points are suggested in each bed at 0.25 m. Two gas sampling points are suggested at 0.55 m to measure the mixed gas streams of bed 1 and 2 and of bed 3 and 4.

7.2 Gas sampling

In figure 7.2 a schematic drawing of the gas sampling method is presented. A thin pipe with an internal diameter of about 2 to 3 mm is connected to the reactor wall. The gas flow through such a thin pipe will not disturb the bed. At the end of this pipe a fine mesh can be placed to prevent incoming dust. In this pipe a ball valve and, in case the analyzing unit is very sensitive to dust, a filter can be installed. The valve will be opened for a short period when taking a gas sample. The gas will flow by the pressure gradient to the sampling unit because of the higher pressure in the reactor. The gas samples have to be cooled down to the temperature in the analyzing unit. Using long lines will be enough to cool down the gas samples.

7.3 Solids sampling

In figure 7.3 a schematic drawing of the solids sampling method is shown. A pipeline with an internal diameter of about 10 to 12 mm is connected to the reactor wall. Sampling is possible by opening a ball valve for a short time. The gas with the solids will flow to a gravity settling chamber in which the solids are separated from the gas. A gravity settling chamber is the most simple collecting device for large particles like the sorbent particles (Maas (1979)). In this chamber the gas flow rate will be reduced to a value at which the solids fall out the gas flow. The solids settle due to gravitational forces and will be collected at the bottom of this chamber. After the solids have been cooled down, they may be drawn

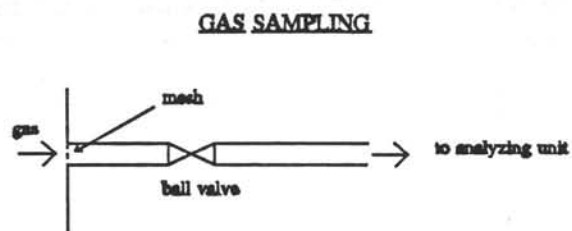


Figure 7.2 Schematic drawing of the gas sampling method

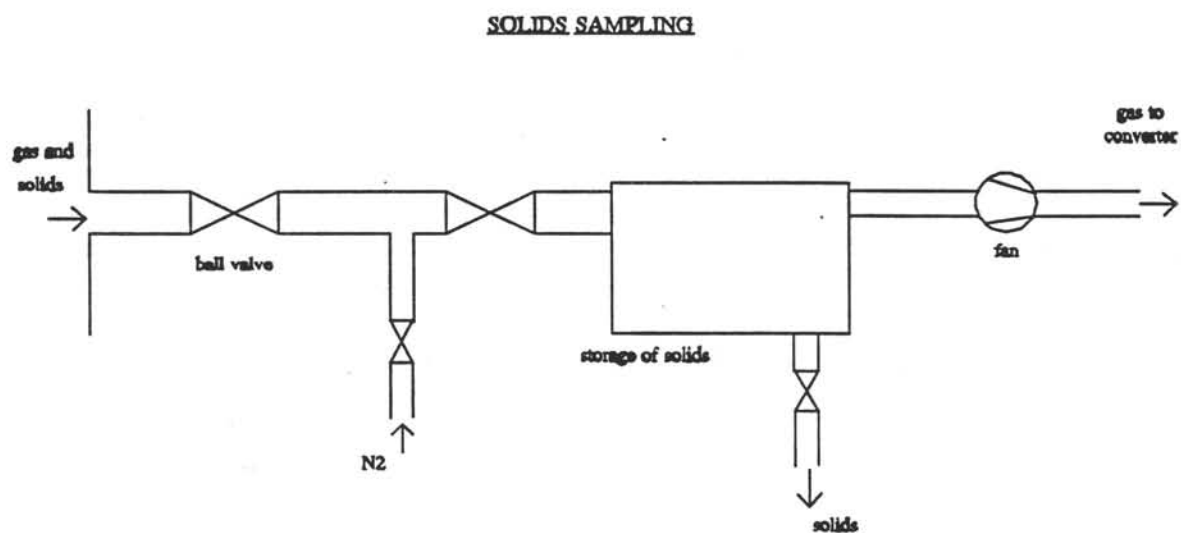


Figure 7.3 Schematic drawing of the solids sampling method

off from this chamber for analyzing purposes. After sampling, solids may settle in the pipeline. These solids can be blown back to the reactor by a nitrogen injection while the valve just ahead the chamber has been closed. The gas flow from the settling chamber passes a fine mesh to prevent incoming dust and will be transported to the converter section. A fan is used to enhance the pressure gradient needed for the gas and solids flow through the pipeline.

For the estimation of the size of the settling chamber in which the solids will be collected two things are important: the settling and the storage of the solids. A box of rectangular shape will be used as settling chamber. To allow settling, the flow area of the box has to be enlarged compared to the flow area of the pipeline through which the solids will be drawn off from the reactor. In a calculation example the design of the settling chamber will be illustrated.

In this calculation it is assumed that the diameter of the pipeline is 0.01 m and the gas velocity in it is 20 m/s. This line diameter is sufficient for free flowing of sorbent particles with a diameter of 2.5 mm. The assumption for the gas velocity has been related to the settling velocity. The settling or terminal velocity of the sorbent particles under reactor conditions can be calculated with equation A3.2 (appendix 3): $u_t = 15.7$ m/s.

In the chamber the gas velocity will be lowered to a value of u_u [m/s]. For stationary gas flow, the flow area of the chamber can be calculated: $A_u = (u_t/u_u) * A_i$ [m²] (u_i : gas velocity in the line to the chamber = 20 m/s and A_i : area of the line = $7.85 \cdot 10^{-5}$ m²). The flow area A_u is equal to $H_{ch} * B_{ch}$ (H_{ch} : height of the chamber, B_{ch} : width of the chamber). The performance of gravity settling chambers, η is equal to (Maas (1979)):

$$\eta = \frac{u_t \cdot L_{ch}}{H_{ch} \cdot u_u} \quad 7.1$$

The length of the chamber L_{ch} depends on the desired value of the particle size which should be settled and on the storage capacity.

The settling efficiency is calculated for the following configuration: $u_u = 0.5$ m/s, $H_{ch} = 0.056$ m and $L_{ch} = 0.015$ m. The settling efficiency can be characterized by the minimum particle size for 100% settling ($\eta = 1$) dp_{100} and the particle size for 50% settling ($\eta = 0.5$) dp_{50} . With equation 7.1 a terminal velocity can be calculated and a particle size follows from the appropriate equation for u_t (appendix 3). The settling efficiency is then: $dp_{100} = 105 \mu\text{m}$ and $dp_{50} = 81 \mu\text{m}$.

To ensure solids settling in the chamber a restriction may be installed in the chamber. An example of such a restriction is a plate connected to the top of the chamber halfway in the chamber and covers half the flow area. This may cause an extra pressure drop across the chamber but is like the pressure drops caused by contraction and enlargement of the gas flow in the chamber, negligible compared to the pressure drop enhanced by the fan.

For small capacities and pressures a propeller fan can be used. It has been assumed that the gas flow is compressed adiabatically to a gauge pressure of 0.05 bar. The molar flow which will be compressed can be calculated with the assumption that the gas flow contains only nitrogen, and with the ideal gas law for the conditions at the outlet of the reactor ($P = 1.1$ bar, $T = 1123$ K). The molar gas flow ϕ_m is then 0.0185 mol/s.

The theoretical work W_t expended on the gas during adiabatic compression is equal to:

$$W_t = \phi m \left(\frac{\gamma}{\gamma - 1} \right) \cdot R \cdot T_i \left[\left(\frac{P_u}{P_i} \right)^{\left(\frac{\gamma - 1}{\gamma} \right)} - 1 \right] \quad 7.2$$

where γ is the specific heat ratio = 1.4

P_i, T_i is the condition in the suction line ($P_i = 1.1$ bar, $T_i = 293 - 1123$ K)

P_u is the downstream pressure = 1.15 bar

With the assumption that the efficiency of the fan is 0.6, the actual work W can be calculated. The results of these calculations are for the different conditions in the suction line: $T_i = 293 - 1123$ K ; $W = 3.3 - 12.8$ W.

Solids removal

After experiments with the IFB the sorbent particles might be taken out of the reactor. For this purpose the same points as for the solids sampling can be used. The size of the pipes therefore has to be large enough to get a smooth flow of particles out of the reactor. Some arrangements of the solids sampling system have to be changed. The chamber and other lines have to be disconnected so that a short line with the ball valve is left. Through this line the solids can easily be removed from the reactor and may be collected with a bucket. The last solids left in the reactor may be taken out the reactor using a dust aspirator device. This device can be put through the short line in the reactor to remove these solids.

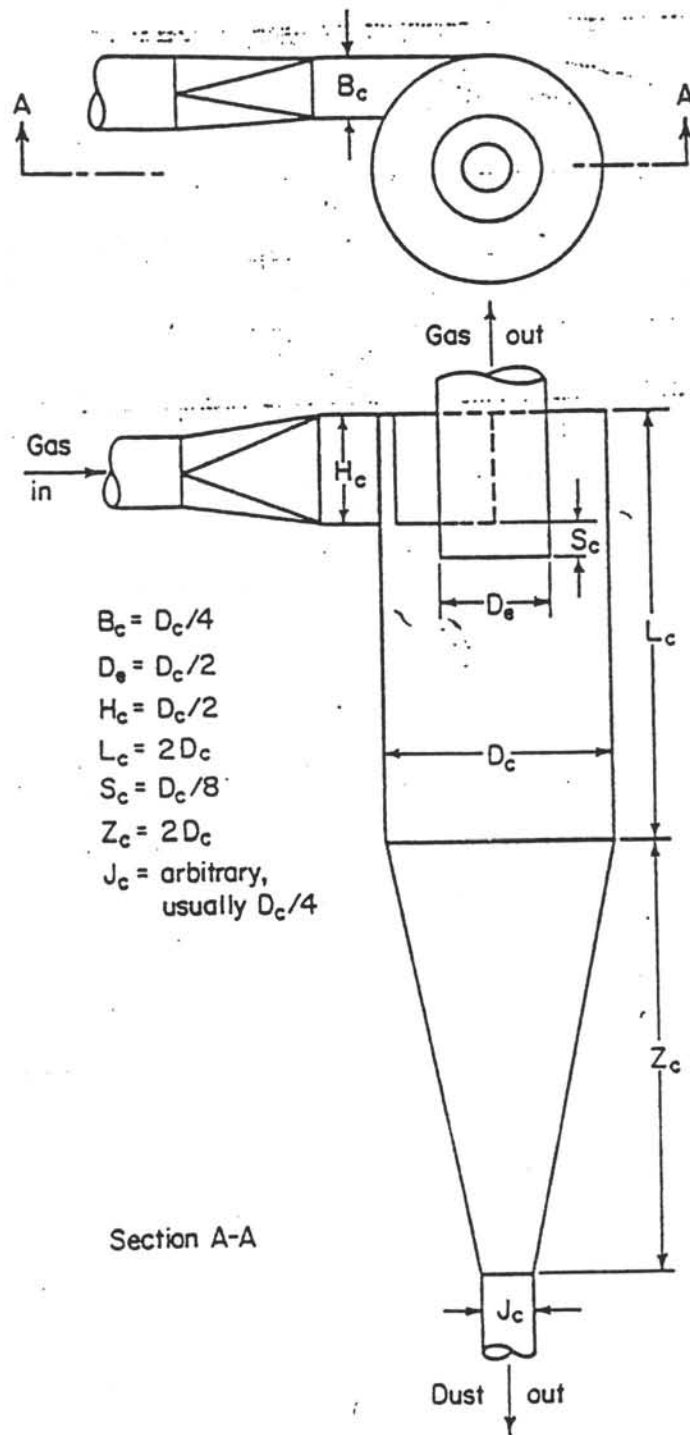


Figure 8.1: Standard gas cyclone

Chapter Eight: Off-gas treatment section

8.1 The cyclone

The gas flow leaving the reactor section will first flow into a cyclone. The cyclone is chosen first to prevent that dust particles are accumulated in the off-gas treatment equipment and cause blockage.

In a cyclone a dust-laden gas enters a cylindrical chamber tangentially and leaves through a central opening (see figure 8.1). Because of the tangential inlet a rotating flow will exist and the dust particles will tend to move toward the outside separator wall. The removed particles will flow along the cyclone wall through a conical outlet into a receiver, in this case a closed vessel. Cyclones can be used for temperatures up to 1000 °C, provided that they are made of suitable materials. As the temperature in the cyclone is not much lower than in the reactor, the cyclone should be made of the same material as the reactor.

The dimensions of gas cyclones are standardized (figure 8.1). All dimensions are related to the cyclone diameter D_c . Common inlet velocities for cyclones vary between 6 and 21 m/s according to Perry (1984). The minimum gas flow through the cyclone will be 0.03 m³/s, the maximum gas flow 0.0632 m³/s. The diameter of the cyclone is chosen in such a way that in both cases the inlet velocities are in the range given by Perry (1984). The inlet velocity u_i is calculated with:

$$u_i = \frac{\phi v_g}{A_i} = \frac{\phi v_g}{0.5 \cdot D_c \cdot 0.25 \cdot D_c} \quad 8.1$$

When we choose a cyclone diameter of 0.17 m, the inlet velocity in case of minimum gas flow is 8.3 m/s, the inlet velocity in case of maximum flow is 17.5 m/s.

Several models exist for calculating the efficiency of a cyclone and the pressure drop over the cyclone (Perry (1984), Hoffmann (1989)). A simple model is chosen here. According to de Graauw en Bruinsma (1992) d_{p50} , the particle size at which 50 % of the particles are collected by the cyclone can be calculated with:

$$d_{p50} = \left[\frac{0.14 \cdot \mu_g \cdot D_c}{\Delta \rho \cdot u_i} \right]^{0.5} \quad 8.2$$

The pressure drop over the cyclone is then:

$$\Delta P_C = 4 \cdot \rho_g \cdot u_i^2 \quad 8.3$$

d_{p50} and ΔP_C are calculated for the minimum and maximum values of the gas flow and shown in table 8.1.

Table 8.1 : d_{p50} and ΔP_c

gas flow (m^3/s)	d_{p50} (μm)	ΔP_c (Pa)
0.03	9.7	83
0.0632	6.7	368

8.2 Conversion of the combustible components

In general three ways can be distinguished to dispose of combustible components in waste gases. Gases with a high heating value can be flared, i.e. directly be combusted without adding a gas with a high heating value (natural gas). The gas flows from the IFB will contain only low percentages of combustible components, so flaring of the gases is not possible.

Two other options are thermal and catalytic incineration. Thermal incinerators can be used over a fairly wide but low range of concentrations of combustible components. The concentrations of these components in air must be below the lower explosive limit. Along with the off-gases, air and fuel are continuously delivered to the incinerator, where the fuel (natural gas) is combusted with air in a burner. The products of combustion and the off-gases are mixed and the combustible components are converted. Thermal incinerators require operating temperatures in the range of 650 to 820 °C. The residence time of the gas in the incinerator should be 0.3 to 0.5 s to ensure complete combustion of the combustible components. The thermal incinerator has the disadvantages of high operating costs, fire hazards and flashback possibilities.

Catalytic incinerators operate at lower temperatures (350 to 425 °C). The off-gases pass through a catalyst bed, where the combustion reaction occurs. The catalyst can be platinum or various oxides of copper, chromium, vanadium, nickel or cobalt. The catalyst is easily poisoned by sulphur compounds. The catalyst should be regenerated regularly.

Initially a choice was made for a thermal incinerator as the temperature of the gas flow coming from the reactor was high enough. Contact with a supplier of incinerators showed however that the gas flow is too low for standard available incinerators. Another option however would be the conversion of the combustible components without ignition source at high temperature with a surplus of oxygen. According to information from the supplier this isn't possible at 800 °C, but at 900 °C the combustible components will be converted nearly completely. Chosen is therefore to heat up the off-gases to 900 °C. This is done by direct heating by combustion of natural gas in the gas flow. Heating elements which are placed in the gas flow, such as those used in the gas preheating might get easily damaged by the reactive components. Electrical heating elements as used for the reactor require a large heat transfer area. The needed amount of natural gas to heat up the maximum gas flow from 750 to 900 °C is 0.36 Nm^3/hour . This is low, so direct heating is also a cheap solution. The conversion is done in a long cylindrical tube, where the burner is placed at the beginning of the tube. The diameter of the tube is 0.20 m, the length 0.5 m, so that the residence time in the tube will range from 0.25 to 0.5 s, which should be long enough for the conversion.

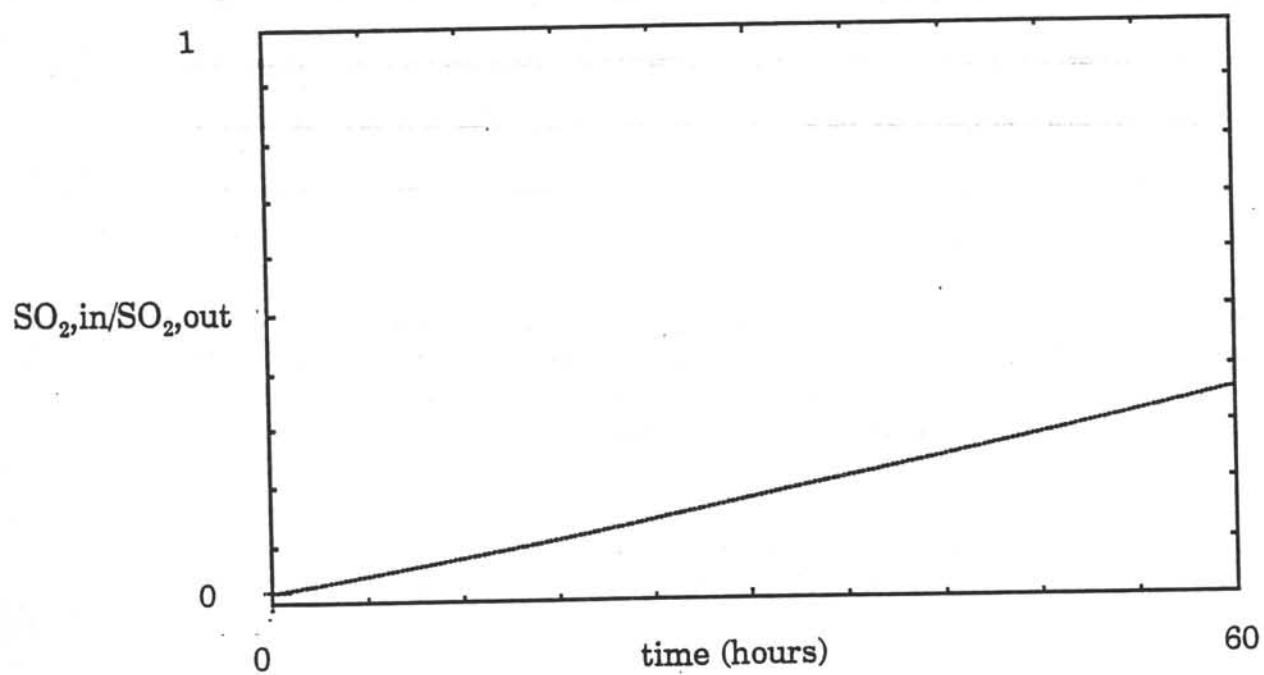


Figure 8.2: SO_2 capture in a fluidized bed with sorbent material

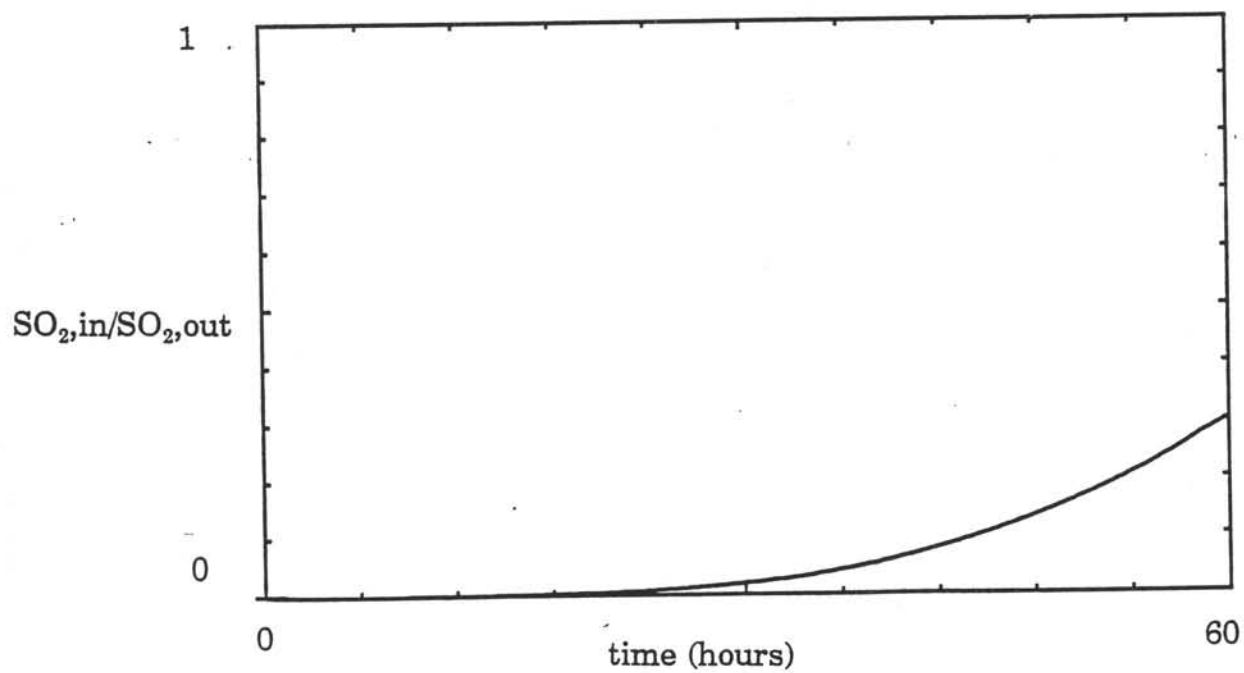


Figure 8.3: SO_2 capture in a fixed bed with sorbent material

8.3 SO₂ removal in a CaO-bed

After all sulphur compounds in the gas flow have been converted to SO₂, this SO₂ can be removed with a bed containing CaO. A choice should be made between a fluidized bed and a fixed bed. In a fluidized bed continuous supply of fresh CaO and removal of used CaO is possible. In a fixed bed however the retention of SO₂ and the CaO conversion that can be achieved are higher. The difference is shown in figure 8.2 and 8.3. The simulations shown in this figures were done with the SURE2 model (Appendix 1), and show the SO₂ retention in a fixed and fluidized bed, with in each bed an equal amount of sorbent. The inlet molar flow of SO₂ is for an average experiment ($u_1 = 1.5$ m/s, $C_{SO_2,1}^0 = 1000$ ppm). As goal is set that the SO₂ retention should be at least 70 %. In figure 8.2 we see for the fluidized bed that the retention becomes lower than 70 % after 50 hours. The average CaO conversion in the bed is than 60 %. The retention in the fixed bed becomes lower than 70 % only after 56 hours, while the average CaO conversion is then 90 %. A fixed bed is chosen as its performance is much better.

The bed can contain either sorbent material or limestone. The sorbent that has been used in the reactor can be used to capture SO₂ in the CaO-bed, before it is removed as solid waste. However it is not known whether there will be a regular supply of used sorbent and in which condition this sorbent material will be. Therefore it is chosen to use limestone instead. Limestone typically consists of 70-99 % CaCO₃. When limestone is calcinated CO₂ is omitted and CaO remains. The CaO reacts with SO₂ to CaSO₄. The molar volume of CaSO₄ however is much bigger than the molar volume of CaO. For limestones with a high content of CaO this can lead to pore plugging: pores are blocked by CaSO₄. This will be the case first at the outer surface of the particle, as the sulphation rate is the highest there. The innerside of the particle can't be converted then. This is the reason that only part of the CaO in limestone can be converted. The final conversion that can be reached, depends on the particle size and the porosity of the limestone. For sulphation of the limestone the temperature should be between 750 and 900 °C.

For this calculation it is assumed that the limestone used in the CaO-bed has a CaO content of 90 % after calcination and a maximum CaO conversion of 25 % is possible. When it is assumed that just as for the sorbent the CaO conversion in a fixed bed has reached 90 % of the maximal conversion before the SO₂ retention becomes lower than 70 %, the dimension of the bed can be estimated. A vessel of 60 l filled with 30 kg limestone is then sufficient for more than 100 hours. It is chosen to make two vessels to be able to work continuously during long experiments. Each vessel has a height of 0.40 m and a diameter of 0.45 m. The pressure drop over these vessels can be calculated with Erguns equation for the pressure drop over fixed beds:

$$\frac{\Delta p_b}{l_b} = 150 \cdot \frac{(1-\epsilon_b)^2}{\epsilon_b^3} \cdot \frac{\mu_g \cdot u_g}{d_p^2} + 1.75 \cdot \frac{(1-\epsilon_b)}{\epsilon_b^3} \cdot \frac{\rho_g \cdot u_g^2}{d_p} \quad 8.4$$

The superficial gas velocity in the bed will range from 0.2 to 0.46 m/s, the pressure drop over the bed from 600 to 1500 Pa. The particle diameter of the limestone shouldn't be chosen too small, because else the bed might become fluidized, which will reduce the effectiveness of the SO₂ retention.

8.4 Cooling of the gas flow and dust removal in a bag filter

After the CaO-bed the gas flow can be blown out to the environment. The gas flow is still hot and will contain fine dust particles which haven't been removed by the cyclone. It is possible that the CaO-bed will act as filter for the fine dust, on the other hand it is also possible that dust from the CaO-bed is carried along with the gas. If required the dust should be removed by a filter. As the most used filter, the bag filter, works at moderate temperatures, the gas flow must first be cooled down. Because it is not known yet whether these last two steps are necessary, no detailed work has been done on these last two steps. The calculations are only indications and the costs of the equipment are not included in the estimation of the investment costs.

To cool the gas flow a water cooler can be used. The maximum amount of heat that has to be removed when the gas is cooled down from 850 to 100 °C is 19 kW. The cooling water is heated from 15 to 30 °C, so 1100 l of cooling water per hour is needed. The logarithmic mean difference temperature is 308 °C. When a heat transfer coefficient of 15 W/(m².K) (Wijers, 1987) is assumed, the heat transfer area is 4.1 m².

In a bag filter the dust-laden gas is blown through cylindrical bags made of a thin filter cloth. The dust is captured on the bags. By shaking the bags or with an air pulse in the opposite direction the dust is periodically removed from the bags and collected in a box. The cloth can be made of various materials, but in this case a cloth should be chosen that is resistant to oxidizing environments and preferably also to sulphurous environments as not all the SO₂ will be removed in the CaO-bed. The needed cloth area depends on the choice of the cloth, the allowed pressure drop over the filter and the solids loading of the gas. The air permeability of a normal bag filter is 2 m³/(m².min). With a maximum gas flow of 1.4 m³/min the cloth area should be minimal 0.7 m².

Chapter Nine: Process control

The description of the process control in the pilot plant is divided into two parts. In the first part it will be explained for each section of the pilot plant, which parameters have to be controlled. The reasons for controlling these parameters is included in this part. The second part deals with the description of the control mechanisms which are necessary to manipulate the parameters mentioned in the first part. The different control mechanisms will be presented in a process control diagram. This chapter will be ended with an indication of the global procedures for the operation of the pilot plant.

9.1 Control strategies

The choice of parameters which have to be controlled will be discussed separately for each section of the pilot plant. For the supply, the reactor and the off-gas treatment sections a description of these parameters will be presented below.

1 Supply section

Controlled parameters for the supply of the different feed gases to the reactor:

Pressure

The pressure of the gases in the supply section has to be sufficiently high to overcome the pressure drop over the reactor and the off-gas treatment section.

Mass flows

The mass flows of the gases have to be controlled to get a good definition of the reactor conditions (superficial gas velocity and composition of the gas flow).

Temperature

The temperature of the gases has to be controlled because it is impossible to keep the reactor temperature constant with reactor heating only.

Controlled parameters for the supply of the solids (coal and sand) to the reactor with the conveying gas:

Pressure

Solids: The pressure in the solids feed hopper has to be sufficiently high to avoid that gas can flow into the hopper.

Gas: The pressure of the conveying gas has to be sufficiently high to overcome the pressure drop over the line to the reactor.

Flows

Solids: The flow of the solids has to be controlled. The coal particles have to be carefully feeded to the reactor to allow a save combustion with no sudden increases of temperature. A constant and well defined coal flow ensures a good comparison with simulation experiments regarding the sulphur capture. A constant sand flow allows well defined segregation

experiments in bed 2.

Gas: The gas flow for the pneumatic conveying system has to be sufficiently high to ensure that all solids flow into the reactor and that no settling in the line to the reactor will occur.

2 Reactor section

Temperature

The temperature in the reactor has to be controlled in order to obtain a well defined temperature that can be related to the sulphur capture at actual coal combustion conditions.

Pressure

The pressure in the reactor has to be (nearly) atmospheric so that simulation experiments can be compared with actual coal combustion at atmospheric pressure. A high pressure drop over the off-gas treatment section leads to a higher pressure in the reactor. In all cases the pressure may not become too high to avoid unrealistic reactor conditions compared with coal combustion.

3 Off-gas treatment (converter)

Temperature

The temperature of the gases in the converter has to be sufficiently high to allow a complete conversion of the combustible components.

Flows

The temperature of the gases in the converter is controlled by the flow of natural gas. The flows of natural gas and air have to be supplied to the converter in a certain ratio necessary for good combustion in the converter.

Pressure

The pressures of natural gas and air have to be sufficiently high to overcome the pressure drop over the lines to the converter.

9.2 Control mechanisms

Based on the discussion of the parameters which have to be controlled, control mechanisms have been set up. Using the same systematically approach the different solutions for the control mechanisms will be discussed for each section of the pilot plant.

1 Supply section

Control mechanisms for the supply of the different feed gases to the reactor:

Pressure

The pressure control for each of the feed gases is realized by a reducing valve. With this valve the pressure of the gas from its storage will be reduced to a pressure that is sufficiently high to overcome the pressure drop over the reactor and the off-gas treatment. Reducing the

pressure may be based on pressure indicators up- and downstream of the valve. The pressure may not be set too high since then the pressure drop over the mass flow controller of the gas become too high. The control valve in the mass flow controller will then become a reducing valve.

Mass flows

The mass flow control for each of the feed gases is realized by a combination of a mass flow measurement device and a control valve. Based on mass flow measurements the control valve can manipulate the gas flow so that a constant mass flow can be ensured. A set point given to the control element is used for this manipulation. As already discussed for the pressure control the upstream pressure of the mass flow controller may not become too high to avoid an excessive pressure drop over the control valve.

Temperature

The temperature control for the feed gases to each bed is realized by a temperature measurement at the outlet of the preheating section. Based on temperature measurements, the electrical input to the heating is varied so that a constant temperature of each gas flow can be ensured. A set point given to the control element is used for this variation. There are two different situations in relation with temperature control: experiments with simulation gases and actual coal combustion experiments. For the first type of experiments the set point will have the same temperature as the desired reactor temperature. The set point for the temperature of the gases for bed 1 will be substantially lower in case of coal combustion in bed 1. The colder feed gas flow to bed 1 will then be heated up to the desired reactor temperature by the heat produced by the combustion.

Control mechanisms for the supply of the solids (coal and sand) to the reactor with the conveying gas:

Pressure

Solids: The pressure in the solids feed hopper is controlled by a thin line which connects the hopper with the inlet of the pneumatic conveying line.

Gas: The pressure control for the conveying gas is realized by a reducing valve. The pressure of the gas from its storage will be reduced to a pressure which is sufficiently high to overcome the pressure drop over the line.

Flows

Solids: The solids flow control to the reactor is realized by the driver gear system of the screw conveyor system. In this system a screw has been installed for a certain range of solids flow. The number of revolutions of the screw is related to the speed of an electric motor. At the end of the screw, the solids will be blown into the reactor using a gas flow with a sufficiently high velocity.

Gas: The gas flow control for the pneumatic conveying system is realized by a flow controller. Since this gas flow is relative small compared to the fluidization gas flow into bed 1, it is sufficient to know the volumetric gas flow. This gas flow has to be high enough to ensure solids feeding to the reactor. Since the solids flows are very small, the gas flow control is not related to the solids flow control.

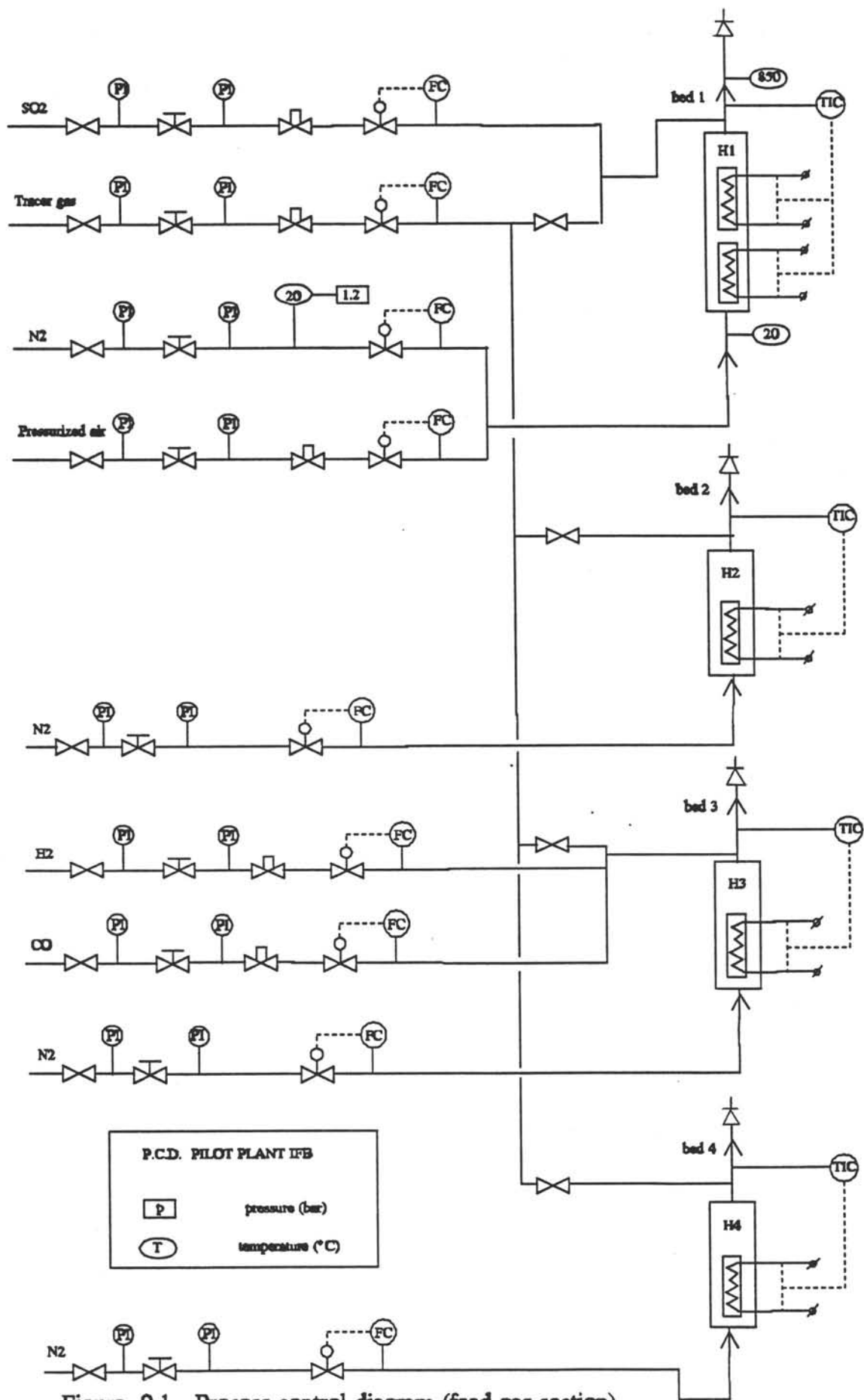


Figure 9.1 Process control diagram (feed gas section)

2 Reactor section

Temperature

The temperature control for the gases and the sorbent particles in the reactor is realized by temperature measurements, in or near the reactor wall. Based on these measurements the electrical input to the reactor heating elements can be varied so that a constant temperature in the reactor can be ensured. A set point given to the control elements is used for this variation.

During start-up, maximum heat will be supplied by the heating elements to heat up the reactor material and the sorbent particles.

For experiments with simulation gases the temperature of the reactor will be controlled as above. During coal combustion experiments the heating elements will be switched off.

Pressure

The pressure control of the reactor is realized by a control valve in the reactor outlet of the gas flows. Based on pressure measurements the control valves are adjusted so that a constant pressure in the reactor can be ensured.

3 Off-gas treatment (converter)

Temperature

The temperature control of the gases in the converter is realized by a temperature measurement at the outlet. Based on temperature measurements, the heat input to the gases in the converter will be varied so that a sufficiently high temperature is ensured. The variation of the heat input is realized by more or less combustion of natural gas. In this control mechanism the temperature measurement device sends a signal to its control element, this element changes the set point of the mass flow controller. With this new set point the mass flow controller manipulate the natural gas flow to the converter.

Flows

The flow control is realized by a combination of a mass flow measurement and a control valve. Both the natural gas flow and the air flow are manipulated by a mass flow controller. The air flow is controlled by a ratio controller based on measurements of both flows, so that both flows enter the converter in a preset ratio.

Pressure

The pressure control for the gases is realized by a reducing valve. The pressure of the gas from its storage will be reduced to such a pressure which is sufficiently high to overcome the pressure drop over the line to the converter.

The flowsheet of the pilot plant has been extended with the process control mechanisms as shown in figures 9.1 (feed gas section) and 9.2 (reactor section). In figure 9.3 a list of symbols and equipment is shown. In these process control diagrams valves are added as the result of safety measures. These safety measures will be discussed in the next chapter. In appendix 9 measurement methods and valves are discussed. In these discussions different possibilities are compared and the most suitable options are indicated.

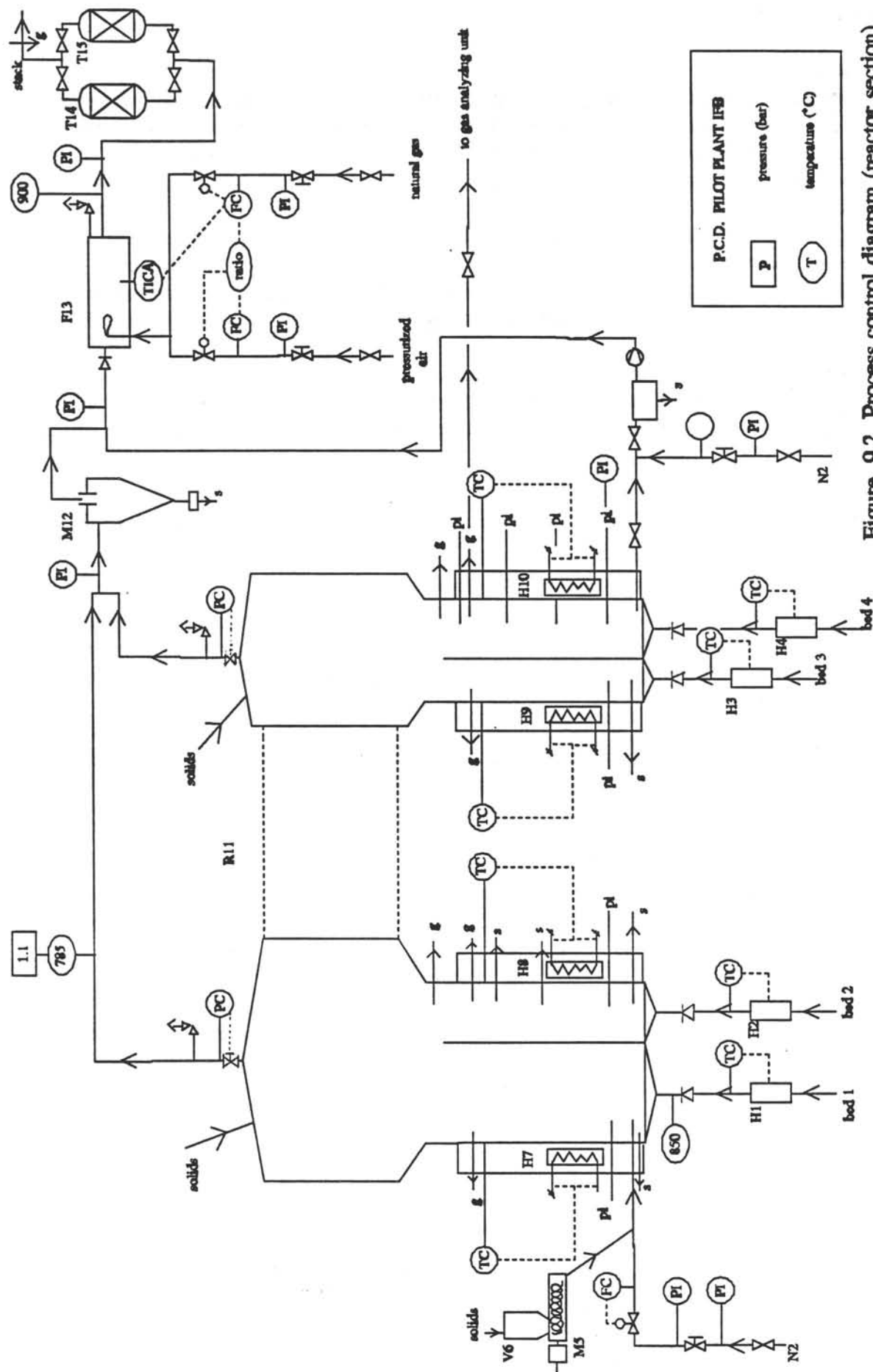


Figure 9.2 Process control diagram (reactor section)

9.3 Global procedures for the pilot plant operation

Experiments with the pilot plant will be carried out at a temperature of 850 °C. This means that first the reactor section has to be heated up. As the reactor and the bed material have high values for the heat capacity, this will take some time.

Before starting any experiment it should be checked whether sufficient amounts of the desired gases are available and whether the reactor is filled with sorbent and the CaO-bed with limestone. If necessary replace empty gas cylinders, sorbent and limestone.

Start-up

- Open the safety cylinder with nitrogen: open its main valve and adjust the pressure with the reducing valve.

- Open the main stop valve in the nitrogen supply line.

- Adjust the pressure in the supply line with the reducing valve.

- Adjust the four nitrogen flows with the mass flow controllers to the maximum values. These controllers may be provided with a soft start procedure which allows a slow increase of the mass flow to the preset value. This feature is especially useful for large changes in mass flow rates.

- Turn on the electrical heating elements of the gas preheating and of the reactor heating. The nitrogen flows and the reactor heating will heat up the reactor and the bed material.

- When the reactor is at the desired temperature, readjust the nitrogen flows to the values desired for the experiment by the mass flow controllers. The temperature is kept constant in the reactor by the temperature controller.

- Adjust the flows of natural gas and pressurized air to the converter and light the burner.

- Open the cylinders with the reactive gases needed for the experiment and reduce the pressure.

- Adjust the different flow rates by the mass flow controllers.

For experiments with coal combustion the start-up procedure is the same, only the fluidization gas flow to bed 1 will now be a mixture of N₂ and air. When the reactor is at the desired temperature, the coal combustion is started with a small amount of coal. The amount of coal is gradually increased and the temperature of the inlet gas flow is gradually decreased, while the temperature in the reactor is kept constant. The temperature of the air flow is limited by the minimum temperature needed for the ignition of the coal particles.

Shut down

The following shut-down procedure can be applied.

- Shut off the supply of the reactive gases so that only nitrogen flows to the reactor.

- Switch off the electrical heating elements.

- Shut off the supply of natural gas and air to the converter.

- Keep the beds fluidized with the cold nitrogen flows so that the beds are cooled down quickly.

- Shut off the nitrogen supply if the beds are sufficiently cooled down.







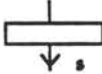



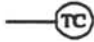



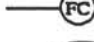

Symbols	
	valve
	relief valve
	control valve
	check valve
	magnetic valve
	safety valve
	storage of solids
	furn
	line
	control line
	temperature controller
	temperature indicator controller
	pressure indicator
	pressure controller
	flow controller
	ratio controller
Equipment	
H1	Electrical gas preheater, bed 1
H2	Electrical gas preheater, bed 2
H3	Electrical gas preheater, bed 3
H4	Electrical gas preheater, bed 4
M5	Screw conveyor system
V6	Solids feed hopper
H7	Electrical reactor heater, bed 1
H8	Electrical reactor heater, bed 2
H9	Electrical reactor heater, bed 3
H10	Electrical reactor heater, bed 4
R11	IFB reactor
M12	Cyclone
F13	Waste gas converter
T14	CaO packed bed
T15	CaO packed bed

Figure 9.3 List of symbols and equipment used in the process control diagram

Chapter Ten: Safety

In the description of the safety aspects of the pilot plant, a systematic approach will be used to analyse these aspects. Based on these considerations safety measures will be suggested. These measures can be used to fill in the safety report. This report will be judged by the safety committee of CPT whether safe operation of the pilot plant can be ensured. Only after the approval of the safety report by this committee, the construction of the pilot plant can be started.

10.1 Safety study

A safety study in which a systematical analysis of the safety aspects of the pilot plant is performed, is a Hazard and operability study (Hazop). A Hazop is a method for identifying hazards and problems which prevent safe and efficient operation of a plant. In this type of study, questions will be asked regarding all possible ways in which hazards or operating problems might arise. The results of a Hazop can be presented in a systematic way based on the guide words (none, more or less of, part of, more than, other than) together with the terms: deviation, possible causes, consequences and the action required. A Hazop is carried out by a team of specialists with an independent chairman who is an expert in the Hazop technique, not the plant.

The safety study which has been done for the pilot plant has been based on a Hazop. In this safety study only the main parts of the pilot plant have been considered. In appendix 10 the results of this study are presented.

10.2 Safety measures

Based on the results of the safety study from appendix 10, a number of safety measures will be presented. In appendix 11 an extensive presentation of the safety aspects of the gases will be given. In appendix 12 it is shown how these safety measures may be included in the safety report.

The following safety measures are suggested:

1 Protection system of the beds

When in coal combustion experiments as a consequence of emergency cases the gases are blown out through the relief valve, the reactor may become overheated. When bed 1 is defluidized, the sorbent and ash particles may clot together. To prevent this undesired effect the beds must be fluidized with nitrogen. The electrical heating must be switched off so that the nitrogen will cool down the beds. If the pressure in the fluidization gas supply lines becomes below a certain value, the safety cylinder with nitrogen must be opened automatically so that the nitrogen flow to the beds is continued.

2 Pressure safety system

The reactor and the converter are each provided with a pressure safety system. This system consists of an electrical and a mechanical pressure safety device. Two different electrical devices are possible: (1) the use of pressure transducers in relation with the process computer,

in which the pressure safety action can be programmed or (2) the use of contact manometers which can be preset to the maximum pressure and be connected to the control box. The electrical devices ensure that the electrical feed will be switched off when the pressure in the reactor or converter becomes too high. The magnetic valves in feed lines of the reactive gases are closed and the electrical heating is switched off. With the mechanical relief valve too high pressures can be lowered by blowing gases out off the pilot plant into the atmosphere outside the 'Proeffabriek'. In appendix 9 relief valves are discussed. A final choice for the relief valve depends on the construction of the reactor and converter. Calculations of strength of the equipment determine the maximum allowable pressure. The choice of seats for the valve will be limited by the high temperatures.

3 Temperature safety system

Temperature will be measured to prevent any overheating in the feed section and the reactor. These temperature measurements are independent of the measurements for controlling purposes. If the preset temperature is exceeded, all the electrical heating elements will be switched off.

A minimum temperature in the converter is required; in case the temperature has become below this minimum an alarm will be switched on.

4 Valves

Magnetic valves are included in the reactive feed gas lines. In emergency cases the electrical feed is disconnected by a signal produced by a process computer or the control box. The magnetic valves will prevent that reactive gases will flow into the pilot plant. The nitrogen feed gas lines do not contain a magnetic valve since nitrogen will be used to keep the bed fluidized after a dangerous situation has arisen.

Check valves are installed at the inlet of the reactor and of the converter to prevent travelling of a starting explosion back into the upstream section of the pilot plant (the reactor and the feed gas section). The check valves have to be equipped with seats which are resistant to high temperatures and suitable for low pressures.

5 Downstream blockage protection

Blockage of the downstream equipment can be detected by manometers up- and downstream the cyclone and the CaO-bed system. These manometers indicate the pressure drop over the equipment.

6 Noxious gas leakage detection system

The working place concentrations of CO, SO₂ and H₂S in the environment of the pilot plant will continuously be checked by a gas monitoring system. A monitoring system which is used for another pilot plant in the Proeffabriek, consists of two independent section branches equipped with electrochemical measuring heads for detection of relevant gaseous species. In this optional system one measuring head for detection of the sulphurous compounds is convenient since the head will be practically equally sensitive to both SO₂ and H₂S. In case of higher concentrations of a gas then a preset value, all reactive gas flows will be shut off by magnetic valves. As a warning for other people in the Proeffabriek, an alarm have to be switched on in case of too high concentrations.

7 Red button

A red button must be available to switch off the gas flows and the electrical feed.



Chapter Eleven: Cost estimation

The estimation of the costs of the new pilot plant will be divided into two parts, estimation of the investment costs and estimation of the operating costs.

11.1 Estimation of the investment costs

In this estimation are included the costs of all the materials and equipment and the costs of the labor for constructing the pilot plant.

The reactor, the cyclone, the conversion tube and the CaO-beds will all be made of the same material, Haynes HR-120. Based on the dimensions of this equipment, it is estimated that about 170 kg of this material is needed. The price will be about Hfl. 75,-/kg, so the investment for the material will be Dfl. 12,750.-.

All the connecting pipelines between the gas preheating elements, the reactor, the cyclone, the converter and the CaO-beds must also be made of a special material, resistant to oxidizing, reducing and sulphurous environments at high temperature. Costs are estimated to be about Dfl. 5,000.-.

For all the other pipelines and connecting equipment and the storage box for the solids samples stainless steel is chosen, costs are estimated at Dfl. 5,000.-.

The set-up from the heating elements to the CaO-beds should be well insulated. The insulation material is available in rolls of 0.622*7.32 m with a thickness of 26 mm and a density of 128 kg/m³. When it is assumed that 4 layers are used, approximately 8 rolls of Dfl. 239,- each are needed, making the total investment for the insulation Dfl. 1,900.-.

An estimation of the costs of the valves and instrumentation is given in table 11.1, of the costs of other equipment in table 11.2.

Table 11.1 Estimation of the costs of valves and instrumentation

description	price/item (Dfl.)	number of items	total (Dfl.)
mass flow controllers	2,000	11	22,000
safety valves	2,000	3	6,000
check valves	500	6	3,000
magnetic valves	500	5	2,500
reducing valves	400	14	3,600
ball valves	400	12	4,800
pressure indicators	1,500	7	10,500
manometers	300	13	3,900
pressure switches	1,000	3	3,000
thermocouples			4,000

Table 11.2: cost estimation of other equipment

description equipment	price (Dfl.)
solids feed system	8,000
reactor heating	3,600
gas preheating	4,000
control box	50,000
soft-ware for control	10,000
personal computer	5,000
fan for solids sampling	2,000

Only the cost of labor of the 'Centrale werkplaats' (CW), where the reactor and other equipment will be made is estimated here. The making of construction drawings and the building of the pilot plant is done by people of the Laboratory of CPT. The costs are not calculated through to the project. One hour of labor at the CW costs Dfl. 30.-. The time needed for the construction of the reactor, the cyclone and the CaO-beds is estimated to be two months, or 320 hours, so the total costs for labor will be Dfl. 9,600.-.

The total amount of investment costs are then about Dfl. 180,000.-.

11.2 Operating costs of the pilot plant

The main operating costs are the costs of the gases. In table 11.3 an estimation is given of the costs of the gases in an average experiment. The costs are calculated in Dfl. per hour experiment.

Table 11.3: costs of the gases

gas	price (Dfl./Nm ³)	total cost (Dfl./hour experiment)
N ₂	0.50	26.1
SO ₂	80	2.5
H ₂ *	4.80	1.3
CO*	80	21.2
natural gas	0.26	0.08

* Only H₂ or CO is used, not both at the same time

The costs of the sorbent are not included here, as there still is a storage of 500 kg. Coal is only used in a few experiments, so also the costs of the coal are not considered here. The costs of the limestone are about Dfl. 0.03 per hour experiment.

The costs for electricity are mainly determined by the reactor heating and the gas preheating. The electricity costs will be about Dfl. 4.- per hour experiment.

For an average experiment with regeneration with H_2 the operating costs will be Dfl. 34.-. When CO is used as regeneration gas, the operating costs will be about Dfl. 54.-.

Chapter Twelve: Conclusions

The Interconnected Fluidized Bed pilot plant has been designed for the regenerative desulphurization of simulation gases containing SO_2 with the sorbent SGC-500 (particle diameter: 2.5 - 3 mm). It is possible to burn small quantities of coal in the pilot plant. This pilot plant can also be used for the removal of H_2S from fuel gases by a sorbent of MnO on $\gamma\text{-Al}_2\text{O}_3$, although for this process the gas costs will be very high.

Very large amounts of nitrogen (maximum flow $67 \text{ Nm}^3/\text{h}$) are needed in the pilot plant, as it is used as the main fluidization gas. Therefore N_2 will be supplied from a large storage vessel. Air will be supplied by the local pressurized air system while all other gases (SO_2 , H_2 , CO) are supplied from gas cylinders. A wide range of gas flows and compositions are possible. The fluidization gas flows (nitrogen, air) will be heated up electrically by porous ceramic elements which contain electrical wires. These elements are directly placed in the gas flow lines. The sum of the maximum heat inputs to the four fluidization gas flows is 19 kW. During experiments small quantities of coal or sand (for segregation experiments) can be fed continuously to the reactor with a screw conveyor system. At the end of the screw the solids will be blown by a cold nitrogen flow (5% of the total gas flow to bed 1) into the reactor. There will be no problems with this feed system concerning the disturbance of the bed.

The choice of the dimensions of the reactor are based on model calculations and on the results from downscaling of the preliminary design of a 100 MW power plant. The choice for the four bed areas is based on a high ratio of the areas of bed 1 and 3 and on the minimum dimensions of bed 3. The chosen dimensions are for bed 1 $0.14 \times 0.14 \text{ m}$, bed 3 $0.06 \times 0.06 \text{ m}$, bed 2 and 4 $0.06 \times 0.14 \text{ m}$. A bed height of 0.3 m is chosen, with space to extend the height to maximum 0.6 m. The size of the orifices is variable from 10 to 40 mm. The orifice between bed 4 and 1 is just above the distributor, while the orifice between bed 2 and 3 will be at a height of 0.07 m. It is possible to dismantle the reactor so that the weir heights and the orifice diameter can be changed. The reactor and the downstream equipment will be constructed of an alloy which is resistant to oxidizing, reducing and sulphurous environments at high temperatures. The reactor will be provided with an electrical heating jacket for extra heat input (heat capacity 4 kW). The reactor and the downstream equipment will be insulated well so that excessive heat losses are prevented. Perforated plates with holes of 2 mm will be used as gas distributors to ensure uniformly fluidized beds. There are sampling points for both gas and solids in each of the four beds. A small settling chamber will be used in the solids sampling method. The choice for the analyzing equipment is not treated in this design. A diameter of 0.3 m and a height of 0.6 m of the freeboard allows that particles larger than $135 \mu\text{m}$ will return to the fluidized bed.

In the off-gas treatment both dust and hazardous and environmental harmful components are removed. In this section first dust will be removed with a cyclone to prevent accumulation of dust particles which may cause blockage of the gas flow. The efficiency of the cyclone is expressed by the particle size at which 50% of the particles are collected. This particle size ranges from 6.7 to $9.7 \mu\text{m}$. The combustible components (H_2S , S_2 , H_2 , CO) will be converted in a tube with a diameter of 0.2 m and with a length of 0.5 m. The conversion will be carried out at a temperature of 900°C which is reached by burning of natural gas. The only sulphur compound in the gas flow is now SO_2 and will be removed in a fixed bed containing CaO .

Limestone is used as bed material. Optional is the removal of fine dust with a bag filter. The gas flow should first be cooled with a water cooler. Detailed design of the bag filter and the water cooler hasn't been done yet.

The process control mechanisms must ensure a safe and stable operation. Pressure, temperature and mass flow controllers are included in the pilot plant design. The pressure and the temperature of the feed gases and of the gases in the reactor will be controlled. Mass flow controllers will be used for the feed gases. The safety measures consists of a pressure and a temperature safety system to keep the consequences of an explosion in the pilot plant limited. In emergency cases the magnetic valves in the lines with the reactive gases will be closed and the electrical heating elements will be switched off. Nitrogen will be used to keep the beds fluidized until they are sufficiently cooled down. A safety cylinder with nitrogen will be available. The safety report has to be completed after consulting the safety committee.

The investment costs of the pilot plant are estimated at Dfl. 180,000.-. These investment costs include most of the material and equipment, and the cost of the labor for constructing the pilot plant. The costs of the analyzing equipment, the water cooler and the bag filter are not included. The operating costs are Dfl. 34 per hour experiment.

List of symbols

Latin symbols

A	area	m^2
Ar	Archimedes number	-
B	width	m
c	corrosion factor	m
C	gas concentration	mol/m^3
Cd _{or}	orifice constant	-
C _d	discharge coefficient	-
C _p	specific heat	J/(mol.K), J/(kg.K)
d, D	diameter	m
D _{soxf}	diffusion coefficient of SO _x in the film around the particle	m^2/s
D _{soxs}	diffusion coefficient of SO _x in the shell of the particle	m^2/s
E	welding factor	-
f	friction factor	-
g	gravity constant = 9.81	m/s^2
ΔG	Gibbs free energy	kJ/mol
H	height	m
k	reaction rate constant	d.o.r.*
k _f	mass transfer coefficient in the film	m/s
k _p	shape factor of the particle	-
k _s	surface based reaction rate constant	$m^3/(m^2.s)$
K	equilibrium constant	d.o.r.*
L	length	m
l _j	jet length	m
mlf	maximal loading factor	-
M	mass	kg
M	molar mass	kg/mol
M	mixing index	-
n	number of rotor pockets	-
N _p	number of particles	-
N	number of revolutions	rev/s
N _{or}	number of orifices	-
Nu	Nusselt number	-
O	perimeter	m
ΔP	pressure drop	Pa
P	pressure	Pa
Pr	Prandl number	-
q	molar CaO surface concentration	mol/m^2
q _f	number of sulfided fast exchangeable manganese sites	mol/m_{sb}^3
q _s	number of sulfided slow exchangeable manganese sites	mol/m_{sb}^3
q _i	number of Langmuir adsorption sites occupied by component i	mol/m_{sb}^3
Q _f	number of fast exchangeable manganese sites	mol/m_{sb}^3
Q _s	number of slow exchangeable manganese sites	mol/m_{sb}^3
Q _L	number of Langmuir adsorption sites	mol/m_{sb}^3

Q	heat flow/heat input	W
r_i	reaction rate for reaction number i	$\text{mol}/(\text{m}_r^3 \cdot \text{s})$
r_j	net change in adsorption equilibrium for component j	$\text{mol}/(\text{m}_r^3 \cdot \text{s})$
r_c	unreacted core radius	m
r_0	particle radius	m
R	gas constant = 8.314	J/(mol.K)
Re	Reynolds number	-
Sc	Schmidt number	-
Sh	Sherwood number	-
t	time	s
t_d	thickness of the distributor plate	m
t_w	wall thickness	m
T	temperature	K, °C
THD	Transport Disengagement Height	m
u	superficial velocity	m/s
U	heat transfer coefficient	W/($\text{m}^2 \cdot \text{K}$)
V	volume	m^3
W_t	theoretical work	W
x	weight fraction	w %
z	velocity ratio	-
z	distance	m

* d.o.r.: depending on reaction

Greek symbols

α	CaO conversion in bed 1	-
α_1	surface fraction CaSO_4 - Ca in bed 3	-
α_2	surface fraction CaO - Ca in bed 3	-
α_3	surface fraction CaS - Ca in bed 3	-
α_f	help variable for diffusion of SO_x through film	s/m^3
α_L	heat transfer coefficient insulation-air	$\text{W}/(\text{m}^2.\text{K})$
α_s	help variable for diffusion of SO_x through shell	s/m^3
γ	specific heat ratio	-
Γ	pitch	m
δ	thickness of film layer around sorbent particle	m
ε	bed voidage	-
η	efficiency	-
λ	thermal conductivity	$\text{W}/(\text{m}^*\text{K})$
λ	pitch of the screw	m
μ	viscosity	$\text{Pa}\cdot\text{s}$
ρ	density	kg/m^3
σ_b	Stefan-Boltzmann constant	$\text{W}/(\text{m}^2.\text{K}^4)$
σ_t	yield strength of the material	Pa
τ	residence time	s
ϕ	mass flow	kg/s
ϕ_m	molar flow	mol/s
ϕ_v	volumetric flow	m^3/s
X	stoichiometric constant	$\text{mol CaO}/\text{mol SO}_3$

Indices

b	bulk	p	particle
c	cyclone	r	reactor
ch	settling chamber	ro	rotor
d	gas distributor	s	shell
env	environment	sb	sorbent
f	film	sc	screw
fb	freeboard	sh	shaft
g	gas	so	solids
i	component	st	steel
ins	insulation	u	outlet
j	flow	t	terminal
mf	minimal fluidization	0,i	inlet
or	orifice		



List of references

Babu S.P., Shah B., Talwalkar A., 'Fluidization correlations for coal gasification materials - minimum fluidization velocity and fluidized bed expansion ratio', AIChE symposium series 176, 74, 176-186, 1978

Benard C.J., 'Handbook of Fluid Flowmetering', The Trade and Technical Press Limited, Surrey, 1988

Bleek C.M. van den, Duisterwinkel A.E., Frens G., Gerritsen A.W., Hakvoort G., Korbee R., Lin W.G., Verheijen P.J.T., Wolff E.H.P., 'Regenerative desulphurization in fluidized bed combustion of coal' 8th progress report Commission of the European Communities contr. no. EN3F-0014-NL (GDF) / Management Office for Energy Research contr. no. 20.35-016-30, Delft, March 1990a

Bleek C.M. van den, Duisterwinkel A.E., Frens G., Gerritsen A.W., Hakvoort G., Korbee R., Lin W.G., Schouten J.C., Verheijen P.J.T., Wolff E.H.P., 'Regenerative desulphurization in fluidized bed combustion of coal' 9th progress report Commission of the European Communities contr. no. EN3F-0014-NL (GDF) / Management Office for Energy Research contr. no. 20.35-016-30, Delft, December 1990b

Bleek C.M. van den, Duisterwinkel A.E., Frens G., Gerritsen A.W., Hakvoort G., Korbee R., Lin W.G., Schouten J.C., Verheijen P.J.T., Wolff E.H.P., 'Regenerative desulphurization in fluidized bed combustion of coal' final report Commission of the European Communities contr. no. EN3F-0014-NL (GDF) / Management Office for Energy Research contr. no. 20.35-016-30, Delft, April 1991

Brain T.J.S., 'Mass flow measurement methods', Metron, 1 (1), 1-6, 1969

Crijns G., Liebrechts S., 'Steenkool wacht nieuwe toekomst', Chemisch Magazine, 11, 578-580, nov. 1992

Chemiekaarten, 'Gegevens voor Veilig Werken met Chemicaliën', achtste editie 1992/1993, edited by: NIA, VNCI and Samson H.D.Tjeenk Willink, Alphen aan den Rijn, 1992

Daubert T.E., Danner R.P., 'Physical and Thermodynamic Properties of Pure Chemicals, Data Compilation', Hemisphere Publishing Corporation, New York, 1989

Davidson J.F., Clift R., Harrison D., 'Fluidization', 2nd edition, 1985

Dekker J., Eyssen J., 'Regenerative Desulphurization in Interconnected Fluidized Bed Combustion of Coal', Internal report FVO nr. 3004, Delft University of Technology, 1992

Fox C., Molodtsot Y., Large J.F., 'Control mechanisms of fluidized solids circulation between adjacent vessels', AIChE J., 35 (12), 1933-1941, 1989

Geldart D., Baeyens J., 'The Design of Distributors for Gas-Fluidized Beds' Powder Technol.

42 (1), 67-78, 1985

Geldart D., 'Gas Fluidization Technology', John Wiley and Sons, Chichester, 1986

Graauw J. de, Bruinsma O.S.L., hand-outs of the course API-2, Delft, 1992

Hoffmann A.C., 'Modellen voor het voorspellen van het scheidingsvermogen van cyclonen', I² procestechnologie, 5 (11), 12-20, 1989

Hommel G., 'Handbuch der gefährlichen Güter Band 1', 4th ed. Springer-Verlag, Berlin, 1986

Hout J. van, Keep P. van, 'The design of an Interconnected Fluidized Bed Combustor with Regenerative Sulphur Retention', Internal report FVO nr. 2965, Delft University of Technology, 1992

Howard J.R., 'Fluidized Bed Technology, Principles and Applications', Adam Hilger, Bristol, 1989

Kennedy R.H., 'Selecting temperature sensors', in: 'Practical Process Instrumentation and Control, Volume II', 265-282, edited by: Matley J., The Staff of Chemical Engineering, McGraw-Hill Publications Co., New York, 1986

Kirk-Othmer Encyclopedia of Chemical Technology, 3rd edition, John Wiley and Sons, New York, 1983

Korbee R., Schouten J.C., Bleek C.M. van den, 'Modelling Interconnected Fluidized Bed Systems', AIChE Symp. Series, 281 (87), 1991

Kossen N.W., Krouwel P.G., 'Schaalvergroten', Delft University of Technology, 1984

Kunii D., Levenspiel O., 'Fluidization Engineering', 2nd edition Butterworth-Heinemann, Boston, 1991

Lin W.G., Valkenburg P.J.M., Bleek C.M. van den, 'Prediction of NO_x and SO_x emissions in FBC of coal using easy to determine coal and sorbent characteristics', Fuel Processing Technology, 24 (1-3), 399-405, 1990

Maas J.H., 'Gas-Solid Separations', in: Handbook of Separation Techniques for Chemical Engineers, Edited by: Schweitzer, P.A., McGraw-Hill, New York, 1979

Masson H.A., 'Design of a compact twinned FB system', Fluidization VI, Banff, Alberta, Canada, 383-392, 1989

Merry J.M.D., 'Penetration of a Horizontal Gas Jet into a Fluidized Bed', Trans. Inst. Chem. Eng., 49, 189-195, 1971

Merry J.M.D., 'Penetration of vertical Jets into Fluidized Beds', AIChE J., 21 (3), 507-510, 1975

Pearson G.H., 'Valve design', Mechanical Engineering Publications Ltd., London, 1978

Pell M., 'Handbook of Powder Technology, Volume 8: Gas Fluidization', Elsevier, Amsterdam, 1990

Perry R.H., Green D., 'Perry's Chemical Engineers' Handbook', 6, McGraw-Hill, 1984

Quershie A.E., Creasy D.E., 'Fluidised Bed Gas Distributors', Powder Technol., 22, 113-119, 1979

Rikken H., Berends E., 'Wervelbedverbranding van steenkool met regeneratieve zwavelvangst' internal report FVO no. 2766, Delft University of Technology, 1989

Sathiyamoorthy D., Rao C.S., 'The Choice of Distributor to Bed Pressure Drop Ratio in Gas Fluidised Beds', Powder Technol., 30 (2), 139-143, 1981

Schouten J.P., Bleek C.M. van den, 'The influence of oxygen-stoichiometry on desulfurization during FBC: a simple sure modelling approach', Chem. Eng. Sci., 43 (8), 2051-2060, 1988

Sie S.T., 'Possibilities and limitations of scale reduction in catalytic process R&D', Delft, 1992

Smith J.M., Stammers E., Janssen L.P.B.M., 'Fysische Transportverschijnselen I', Delftse Uitgevers Maatschappij, Delft, 1984

Wakker J.P., 'Development of a high temperature steam regenerative H₂S removal process based on alumina supported MnO and FeO', Ph.D. thesis, Delft University of Technology, 1992

Webci/Wubo, 'DACE-prijzenboekje', 16th edition, Leidschendam, nov. 1992

Wolff, E.H.P., 'Regenerative sulfur capture in fluidized bed combustion of coal: a fixed bed sorption study', Ph.D. thesis, Delft University of Technology, 1991

Woodcock C.R., Mason J.S., 'Bulk Solids Handling; an Introduction to the Practice and Technology', Blackie and Son Ltd., Glasgow, 1987

Wijers W.G., 'Werktuigen voor de procesindustrie: Warmtewisselaars', Eindhoven, 1987

Zenz F.A., Weil N.A., 'A Theoretical Empirical Approach of Particle Entrainment from Fluidised Beds', AIChE J., 4 (4), 472-479, 1958

Zenz F.A., Weil N.A., 'Fluidization and fluid-particle systems', Reinhold Publishing Corporation, New York, 1960



Appendix 1: Modelling of regenerative desulphurization in an Interconnected Fluidized Bed (SO₂ removal)

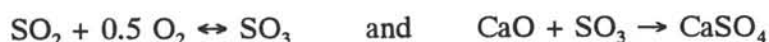
The modelling of the regenerative desulphurization in an Interconnected Fluidized Bed consists of two parts: the modelling of the sorbent sulphation in bed 1 for which the SURE2 model is used, and the modelling of the regeneration in bed 3. These two models are combined into an integral model for the desulphurization in an Interconnected Fluidized Bed.

Modelling of the sorbent sulphation (Sulphur RETention, SURE) in a fluidized bed.

This model is developed at the TU Delft and described by Wolff (1991), Schouten and Van den Bleek (1988) and Van den Bleek et.al. (1991). The combustion of coal is not considered here, while the inlet gas flow is a simulation gas containing SO₂ and O₂.

The following model assumptions are made:

- An ideally mixed gas flow model (ISTR) is applied.
- The solids are assumed to be ideally mixed; particles are spherical and of uniform size.
- Attrition, elutriation and freeboard phenomena are not taken into account.
- SO₃ is an important intermediate gaseous reactant in the sulphation reaction. The following reactions are assumed:



The SO₂ oxidation reaction is in equilibrium and the rate of formation is high.

- For the sorbent sulphation a shrinking unreacted core model is used.

In the shrinking unreacted core model the sulphation rate is determined by three steps:

- 1 Diffusion of the gaseous reactants (SO₂ and SO₃) from the gas bulk phase through a film layer to the outer surface of the particle.
- 2 Diffusion of the gaseous reactants through the shell to the reaction front.
- 3 Reaction of SO₃ with the CaO at the unreacted core surface. The CaO conversion rate is first order in the SO₃ concentration and in the total external reactive sorbent surface area.

The conversion equation of one particle is then given by:

$$\frac{dr_c}{dt} = - \frac{\frac{C_{\text{SO}_2,1} \cdot \chi}{C_{\text{CaO}}}}{\frac{1}{k_s \cdot K_{eq} \cdot \sqrt{C_{\text{O}_2,1}}} + r_c^2 \cdot (\alpha_f + \alpha_s)} \quad \text{A1.1}$$

with the initial condition that $r_c = r_0$ at $t = 0$ and:

$$\alpha_f = \frac{1}{D_{SO_2,f} + D_{SO_3,f} K_{eq} \sqrt{C_{O_2,1}}} \left[\frac{1}{r_0} - \frac{1}{r_0 + \delta} \right] \quad A1.2$$

$$\alpha_s = \frac{1}{D_{SO_2,s} + D_{SO_3,s} K_{eq} \sqrt{C_{O_2,1}}} \left[\frac{1}{r_c} - \frac{1}{r_0} \right] \quad A1.3$$

where the index 'f' stands for film and 's' for the shell of reacted sorbent through which the diffusion must take place. All symbols are defined in the list of symbols.

The film thickness, δ , is calculated with:

$$\delta = \frac{1}{\frac{k_f}{D_{soxf}} - \frac{1}{r_0}} \quad A1.4$$

The mass transport coefficient in the film, k_f , is calculated with:

$$k_f = [0.765 Re_p^{-0.82} + 0.365 Re_p^{-0.386}] Sc^{-0.667} \frac{u_1}{\epsilon_1} \quad A1.5$$

with:

$$Re_p = \frac{\rho_g u_1 d_p}{\mu_g} \quad \text{and} \quad Sc = \frac{\mu_g}{\rho_g D_{soxf}}$$

The molar balance for SO_2 in an ISTR is:

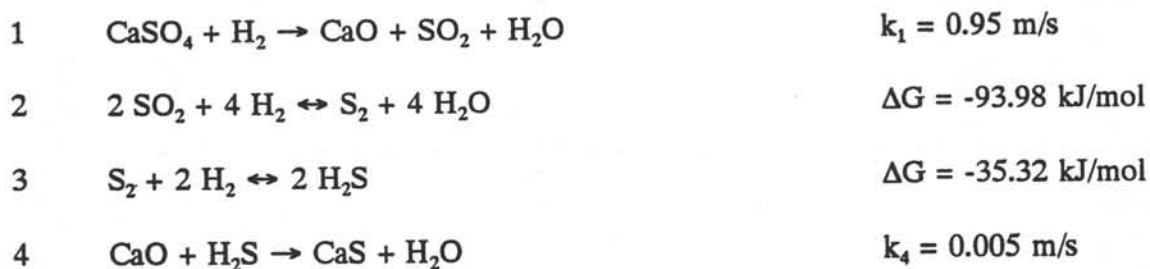
$$V_g \frac{dC_{SO_2,1}}{dt} = \phi_g (C_{SO_2,1}^0 - C_{SO_2,1}) - \frac{1}{(1 + K_{eq} \sqrt{C_{O_2,1}})} \cdot \frac{4 \pi \bar{r}_c^2 C_{SO_2,1} N_p V_r}{\left[\frac{1}{k_s K_{eq} \sqrt{C_{O_2,1}}} + \bar{r}_c^2 (\alpha_f + \alpha_s) \right]} = 0 \quad A1.6$$

The average CaO conversion in the reactor, α , is defined as:

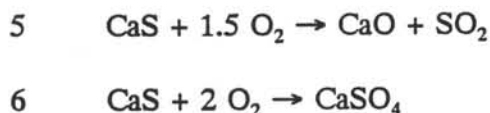
$$\bar{\alpha} = 1 - \left[\frac{r_c}{r_0} \right]^3 \quad A1.7$$

Modelling of the sorbent regeneration

The sorbent can be regenerated with H_2 or CO . In industrial applications also a mixture of these gases produced by substoichiometric combustion of coal can be used. For the modelling it is assumed that the sorbent is regenerated with H_2 . In this case the following reactions can take place:



Reaction 2 and 3 are assumed to be in equilibrium. The formation of CaS is undesirable because it decreases the available amount of active sorbent. The CaS formed in bed 3 will be oxidized in bed 1 to CaO and $CaSO_4$, according to the reactions:



It is assumed that 10% of the CaS reacts according to reaction 5, and 90% according to reaction 6.

The active surface of a sorbent particle, the Ca surface consists of CaO , CaS and $CaSO_4$. α_1 , α_2 and α_3 are defined as:

α_1 = surface occupied by $CaSO_4$ / total Ca surface

α_2 = surface occupied by CaO / total Ca surface

α_3 = surface occupied by CaS / total Ca surface

For the model the following assumptions are made:

- Both the gas and the solids are considered to be ideally mixed in the reactor.
- The rates of the gas-solid reactions are first order in the gas concentration and in the outer surface of the particle.

calculation outline SO₂ model

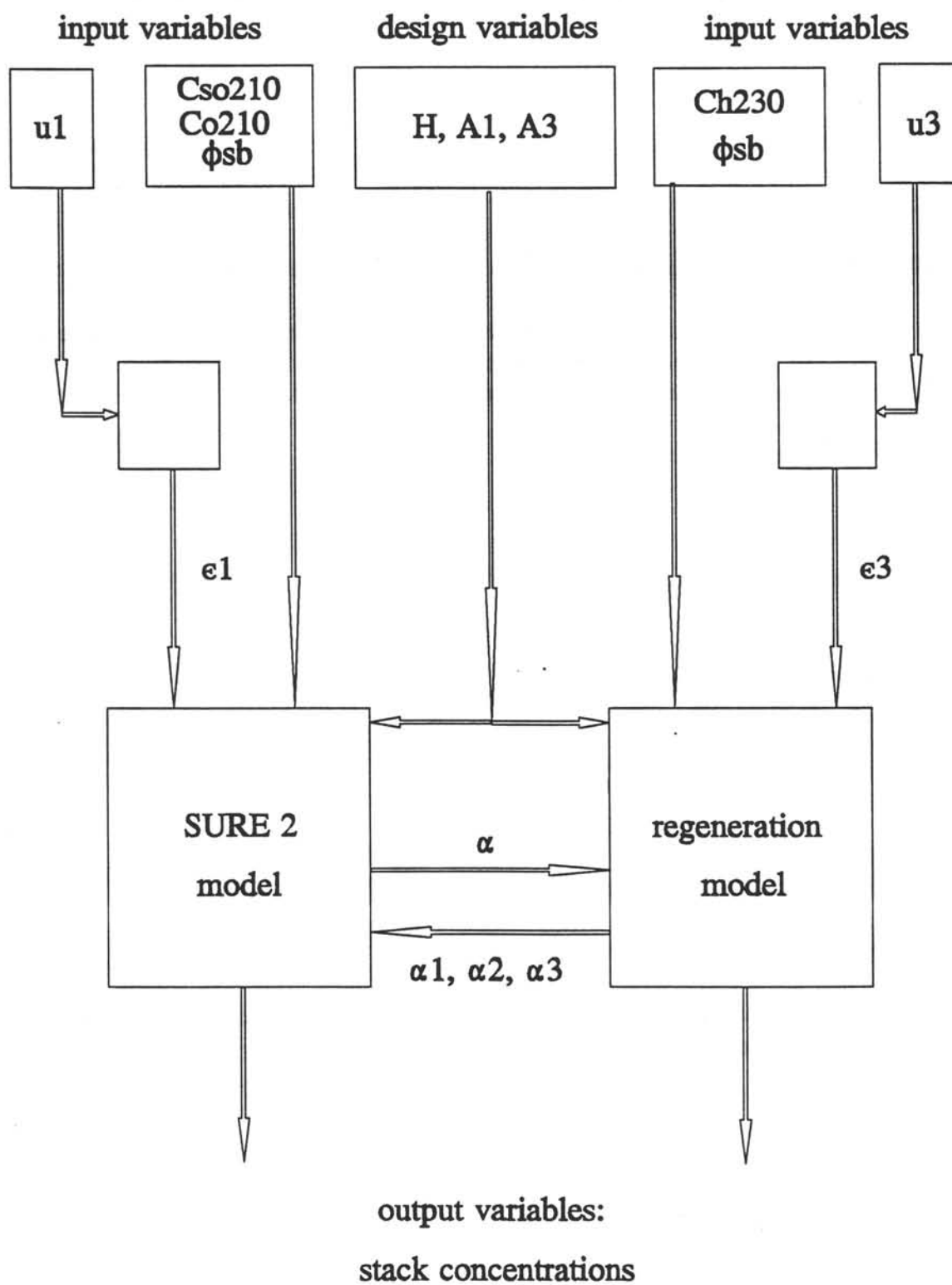


Figure A1.1: Calculation outline of the SO₂ model

The average α 's over the bed are then calculated with:

$$\overline{\alpha}_1 = \frac{\overline{\alpha} \cdot q}{q + k_1 \cdot C_{H2,3} \cdot \tau_3} \quad A1.8$$

$$\overline{\alpha}_2 = \frac{k_1 \cdot C_{H2,3} \cdot \overline{\alpha}_1}{k_4 \cdot C_{H2S,3} - k_1 \cdot C_{H2,3}} + \frac{1 - \overline{\alpha} - \frac{\overline{\alpha} \cdot k_1 \cdot C_{H2,3}}{k_4 \cdot C_{H2S,3} - k_1 \cdot C_{H2,3}}}{1 + k_4 \cdot C_{H2S,3} \cdot \frac{\tau_3}{q}} \quad A1.9$$

$$\overline{\alpha}_3 = 1 - \overline{\alpha}_1 - \overline{\alpha}_2 \quad A1.10$$

q is the molar Ca surface concentration and is calculated with:

$$q = \frac{d_{sb} \cdot \rho_{sb} \cdot x_{Ca}}{6 \cdot M_{Ca}} \quad A1.11$$

These equations are combined with the mass balances of H, S and O over the bed and the equilibrium equations of the reactions 2 and 3.

The models for the sulphation and the regeneration can be combined. The calculation outline of the model is shown in figure A1. A program for these calculations has been written in Mathcad 2.5. The α obtained by the sulphation model is put into the regeneration model, while α_1 , α_2 , α_3 , obtained by the regeneration model are put into the sulphation model. The calculations are repeated until constant values of α , α_1 , α_2 and α_3 are obtained.

The process input variables of this model are the superficial gas velocities in bed 1 and bed 3, u_1 and u_3 , the inlet gas concentrations in bed 1 of SO_2 and O_2 , $C_{so2,1}^0$ and $C_{o2,1}^0$, the inlet concentration of the regeneration gas, H_2 , $C_{H2,3}^0$ in bed 3, and the sorbent flow through the IFB, ϕ_{sb} . A list of the input variables and their range is given in table A1.

The design variables are the areas of bed 1 and bed 3, A_1 and A_3 , the bed height H , and the sorbent characteristics. As sorbent SGC-500 is used, its characteristics are shown in table A2. The output variables are the stack concentrations of all components. A list of the output variables and their range is shown in table A3. The parameters in the model are shown in table A4. Their value was calculated from literature data or estimated by fitting experimental data.

Table A1: List of the input variables for the SO₂ retention model and their range

variable	description	range	dimension
u_1	superficial velocity bed 1	1 - 2	m/s
u_3	superficial velocity bed 3	1 - 2	m/s
$C_{o2,1}^0$	inlet O ₂ concentration in bed 1	0 - 5	mol %
$C_{so2,1}^0$	inlet SO ₂ concentration in bed 1	300 - 1300	ppm
$C_{h2,3}^0$	inlet H ₂ concentration in bed 3	0 - 5	mol %
ϕ_{sb}	sorbent flow through the IFB	0.5 - 5	g/s

Table A2: Characteristics of the sorbent SGC-500

calcium content	weight %	8.91
pore volume	ml/g	0.40
porosity	m ³ /m ³	0.56
density	kg/m ³	1400
particle diameter	mm	2.5-3
minimum fluidization velocity at 850 °C	m/s	0.65

Table A3: List of the output variables for the SO₂ retention model and their range

variable	description	range	dimension
$C_{o2,1}$	outlet O ₂ concentration bed 1	0-5	mol %
$C_{so2,1}$	outlet SO ₂ concentration bed 1	50-800	ppm
$C_{so2,3}$	outlet SO ₂ concentration bed 3	0-1	mol %
$C_{s2,3}$	outlet S ₂ concentration bed 3	0-1	mol %
$C_{h2s,3}$	outlet H ₂ S concentration bed 3	0-1	mol %
$C_{h2,3}$	outlet H ₂ concentration bed 3	0-5	mol %
$C_{h2o,3}$	outlet H ₂ O concentration bed 3	0-5	mol %

Table A4: List of the parameters in the model and their value at 850 °C

parameter	description	value	dimension
$D_{SO_2,f}$	diffusion coefficient SO_2 in the film	$7.53.10^{-7}$	m^2/s
$D_{SO_2,s}$	diffusion coefficient SO_2 in the shell	$1.34.10^{-4}$	m^2/s
k_s	surface based sulphation rate constant	0.149	$m^3/(m^2.s)$
K_{eq}	equilibrium constant SO_2 oxidation	0.548	$(mol/m^3)^{-0.5}$
k_1	reaction rate constant $CaSO_4$ to CaO	0.95	m/s
k_4	reaction rate constant $CaSO_4$ to CaS	0.05	m/s
ΔG_2	Gibbs free energy of reaction 2	-93.98	kJ/mol
ΔG_3	Gibbs free energy of reaction 3	-35.32	kJ/mol

Appendix 2: Modelling of a regenerative H₂S removal process with alumina supported MnO.

In this appendix the modelling of the second process to be investigated in the pilot plant will be discussed. The H₂S process is developed for removing H₂S and COS at high temperatures (675-1075 K) from fuel gases produced by a coal gasifier. As acceptor MnO/ γ -Al₂O₃ is used. The sulphidated material is regenerated with steam at the same temperature and pressure. The possibilities of this process were investigated by Wakker (1992). He developed a kinetic model to describe his experimental results on sulphation and regeneration of this sorbent. His model was used as the basis for the model developed here.

The following model assumptions are made:

- The gas flow and the solids are considered to be ideally mixed in each bed.
- The reaction rates are first order in the gas concentrations of the reacting components and in the number of active sites on the sorbent.
- According to Wakker there are no diffusion limitations

The reactions that can take place during sulphation and regeneration are discussed in more detail now.

1 sulphation of the acceptor



In fact two reactions have to be considered: a reaction of fast exchangeable manganese sites and a reaction of slow exchangeable manganese sites with H₂S. The fast exchangeable sites are on the surface of the acceptor, while the slow exchangeable sites are situated below the surface and will diffuse out of the alumina support to the acceptor surface. The equilibrium constant, K_f is about 1 at 875 K. This means that it is possible to regenerate the acceptor with steam but also that any water in the feed will have a negative effect on the removal of H₂S. Also the removal will never be 100 % because of the equilibrium. The reaction rate constant for the forward reaction is k_f , the reaction rate of the forward reaction is r_1 and for the backward reaction r_2 . These are calculated with:

$$r_1 = k_f \cdot C_{\text{H}_2\text{S}} \cdot (Q_f - q_f) \cdot (1 - \epsilon) \quad \text{A2.1}$$

$$r_2 = \frac{k_f}{K_f} \cdot C_{\text{H}_2\text{O}} \cdot q_f \cdot (1 - \epsilon) \quad \text{A2.2}$$

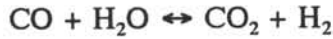
The equilibrium constant for the slow oxygen-sulfur exchange is K_s , the reaction rate constant for the forward reaction is k_s . K_s is equal to K_f , while k_f is much larger than k_s . The reaction rate of the forward reaction is r_3 , the reaction rate of the backward reaction is r_4 . They are calculated with:



$$r_3 = k_s \cdot q_f \cdot (Q_s - q_s) \cdot (1 - \epsilon)^2 \quad A2.3$$

$$r_4 = \frac{k_s}{K_s} \cdot q_s \cdot (Q_f - q_f) \cdot (1 - \epsilon)^2 \quad A2.4$$

2 water gas shift reaction



As CO reacts with H₂O, it improves the removal of H₂S. The high CO concentration in the fuel gases of the Shell coal gasification process will have a positive effect on the removal of H₂S. H₂ and CO₂ will have a negative effect. The dependency of the H₂S removal on the CO and H₂O concentration were both determined by Wakker (1992). K_{wgs} is the equilibrium constant of the water gas shift reaction, while k_{wgs} is the reaction rate constant of the forward reaction. r_5 is the reaction rate of the forward reaction, while r_6 is the reaction rate of the backward reaction. They are calculated with:

$$r_5 = k_{\text{wgs}} \cdot C_{\text{H}_2\text{O}} \cdot C_{\text{CO}} \quad A2.5$$

$$r_6 = \frac{k_{\text{wgs}}}{K_{\text{wgs}}} \cdot C_{\text{CO}_2} \cdot C_{\text{H}_2} \quad A2.6$$

3 formation of COS

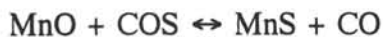


Although this reaction has a low equilibrium constant, the COS formation can be considerable when the CO concentration is high. K_{COS} is the equilibrium constant of this reaction, while k_{COS} is the reaction rate constant for the forward reaction. r_7 is the reaction rate of the forward reaction and r_8 is the reaction rate of the backward reaction. They are calculated with:

$$r_7 = k_{\text{COS}} \cdot C_{\text{H}_2\text{S}} \cdot C_{\text{CO}} \quad A2.7$$

$$r_8 = \frac{k_{\text{COS}}}{K_{\text{COS}}} \cdot C_{\text{H}_2} \cdot C_{\text{COS}} \quad A2.8$$

4 reaction of COS with the acceptor



The reaction of COS with the acceptor is faster than the reaction of H₂S with the acceptor.

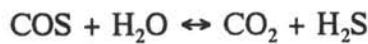


When the amount of COS formed is considerable, this reaction will be important. $K_{f,COS}$ is the equilibrium constant of this reaction, while $k_{f,COS}$ is the reaction rate constant of the forward reaction. The reaction rate of the forward reaction is r_9 , of the backward reaction r_{10} . They are calculated with:

$$r_9 = k_{f,COS} \cdot C_{COS} \cdot (Q_f - q_p) \cdot (1 - \epsilon) \quad A2.9$$

$$r_{10} = \frac{k_{f,COS}}{K_{f,COS}} \cdot C_{CO2} \cdot q_f \cdot (1 - \epsilon) \quad A2.10$$

The reaction of COS with H_2O :



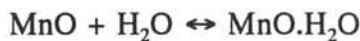
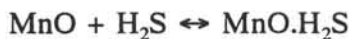
is very fast, but will play a minor role because of the low concentrations of COS and H_2O in bed 1. Wakker left this reaction out of his model. Incorporation of this reaction in the model has very little influence on the calculations, unless the COS concentration is high. K_{COSr} is the equilibrium constant of this reaction, while k_{COSr} is the reaction rate constant of the forward reaction. The reaction rate of the forward reaction is r_{11} while the reaction rate of the backward reaction is r_{12} . They are calculated with:

$$r_{11} = k_{COSr} \cdot C_{COS} \cdot C_{H2O} \quad A2.11$$

$$r_{12} = \frac{k_{COSr}}{K_{COSr}} \cdot C_{CO2} \cdot C_{H2S} \quad A2.12$$

5 Langmuir adsorption

Competitive Langmuir adsorption of CO , H_2S and H_2O on the surface manganese sites will occur. The influence of CO_2 and H_2 is neglected.



The equilibrium constants are K_{CO} , K_{H2S} and K_{H2O} respectively. Q_L is the total number of available Langmuir sites, while q_{CO} , q_{H2S} , q_{H2O} represent the number of Langmuir adsorption sites occupied by CO , H_2S and H_2O respectively. If equilibrium is assumed, q_{CO} , q_{H2S} and q_{H2O} can be calculated with:

$$q_{CO} = \frac{K_{CO} \cdot C_{CO}}{1 + K_{CO} \cdot C_{CO} + K_{H_2S} \cdot C_{H_2S} + K_{H_2O} \cdot C_{H_2O}} \cdot Q_L \quad A2.13$$

$$q_{H_2S} = \frac{K_{H_2S} \cdot C_{H_2S}}{1 + K_{CO} \cdot C_{CO} + K_{H_2S} \cdot C_{H_2S} + K_{H_2O} \cdot C_{H_2O}} \cdot Q_L \quad A2.14$$

$$q_{H_2O} = \frac{K_{H_2O} \cdot C_{H_2O}}{1 + K_{CO} \cdot C_{CO} + K_{H_2S} \cdot C_{H_2S} + K_{H_2O} \cdot C_{H_2O}} \cdot Q_L \quad A2.15$$

The net changes in the adsorption equilibria are calculated from the differences in q_{CO} , q_{H_2S} and q_{H_2O} between the beds. For example for bed 1:

$$r_{CO,1} = \frac{\phi_{sb}}{\rho_{sb}} \cdot (q_{CO,1} - q_{CO,4}) \quad A2.16$$

$$r_{H_2S,1} = \frac{\phi_{sb}}{\rho_{sb}} \cdot (q_{H_2S,1} - q_{H_2S,4}) \quad A2.17$$

$$r_{H_2O,1} = \frac{\phi_{sb}}{\rho_{sb}} \cdot (q_{H_2O,1} - q_{H_2O,4}) \quad A2.18$$

We can now set up the mass balances for each component (IN - OUT = CONVERSION) , assuming that all beds are ideally mixed for the gas and the solids.

Mass balance H_2S :

$$\phi v_g \cdot (C_{H_2S}^0 - C_{H_2S}) = (r_1 - r_2 + (r_7 - r_8 + r_{12} - r_{11}) \cdot \epsilon) \cdot V_r + r_{H_2S} \quad A2.19$$

Mass balance H_2O :

$$\phi v_g \cdot (C_{H_2O}^0 - C_{H_2O}) = (r_2 - r_1 + (r_5 - r_6 + r_{11} - r_{12}) \cdot \epsilon) \cdot V_r + r_{H_2O} \quad A2.20$$

Mass balance CO:

$$\phi v_g \cdot (C_{CO}^0 - C_{CO}) = (r_5 - r_6 + r_7 - r_8) \cdot \epsilon \cdot V_r + r_{CO} \quad A2.21$$

Mass balance CO_2 :

$$\phi v_g \cdot (C_{CO_2}^0 - C_{CO_2}) = (r_{10} - r_9 + (r_{12} - r_{11} + r_6 - r_5) \cdot \epsilon) \cdot V_r \quad A2.22$$

calculation outline H₂S model

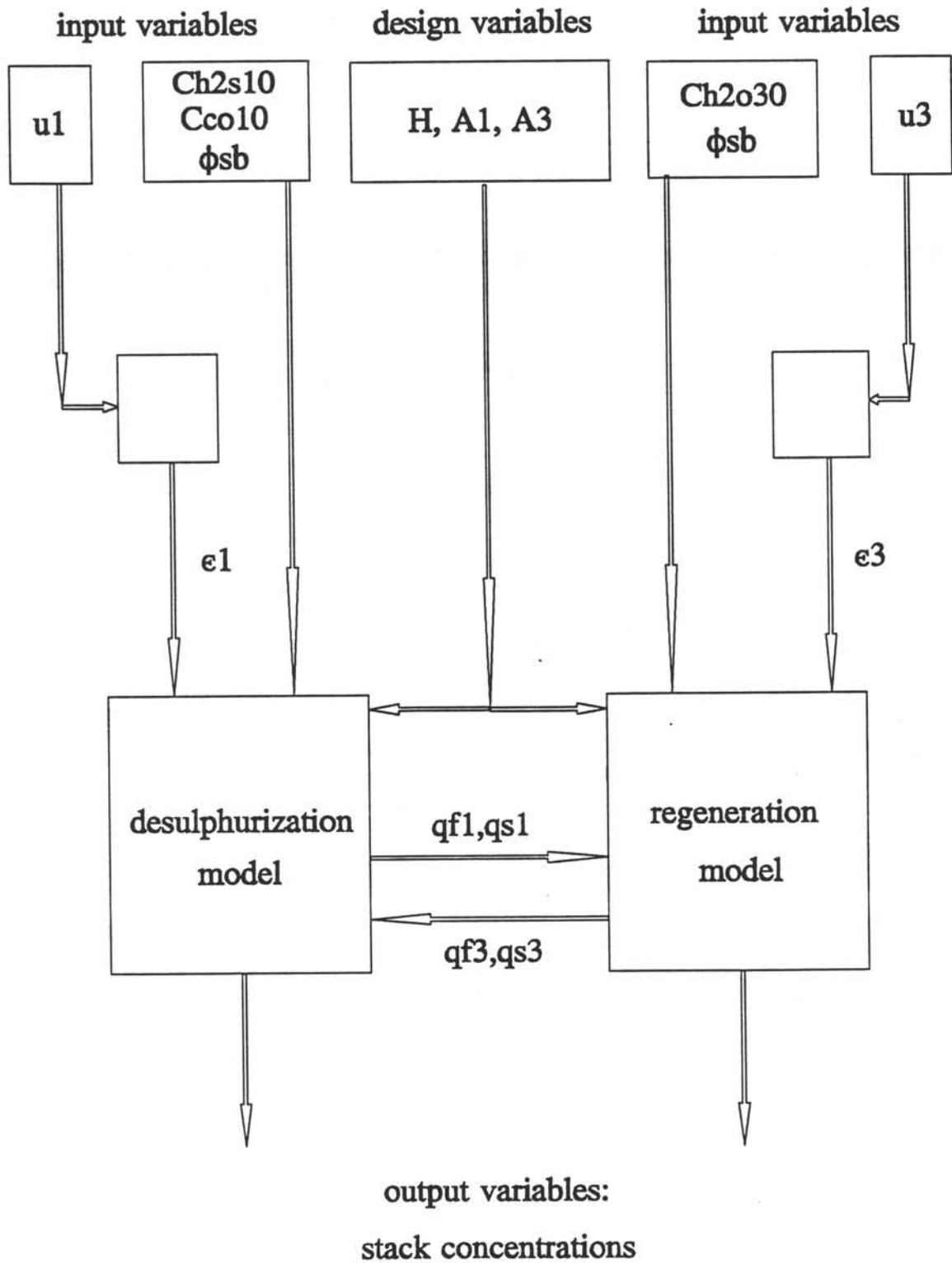


Figure A2.1: Calculation outline of the H₂S model

Mass balance H₂:

$$\phi v_g \cdot (C_{H_2}^0 - C_{H_2}) = (r_6 - r_5 + r_8 - r_7) \cdot \epsilon \cdot V_r \quad A2.23$$

Mass balance COS:

$$\phi v_g \cdot (C_{COS}^0 - C_{COS}) = (r_9 - r_{10} + (r_{11} - r_{12} + r_8 - r_7) \cdot \epsilon) \cdot V_r \quad A2.24$$

Mass balance fast exchangeable manganese sites:

$$\frac{\phi_{sb}}{\rho_{sb}} \cdot (q_{f,in} - q_{f,out}) = (r_1 - r_2 + r_4 - r_3 + r_9 - r_{10}) \cdot V_r \quad A2.25$$

Mass balance slow exchangeable manganese sites:

$$\frac{\phi_{sb}}{\rho_{sb}} \cdot (q_{s,in} - q_{s,out}) = (r_3 - r_4) \cdot V_r \quad A2.26$$

These mass balances should be set up for all the four beds separately. However it is assumed that in bed 2 and bed 4 no reactions will occur as these beds are fluidized with pure nitrogen. Only Langmuir desorption of CO, H₂S and H₂O will occur, and simplified mass balances for these components are used. For the model a program has been written in MathCad 2.5. The calculation outline of the model is shown in figure A2.1. The input variables are the superficial gas velocities in each bed, the inlet concentrations of each component in each bed and the sorbent flow through the IFB. The output variables are the outlet concentrations of each component in each bed. The design variables are the areas of each bed, the height of the IFB and the characteristics of the sorbent. The characteristics of the sorbent used by Wakker are shown in table A2.1. The values of the different parameters used by Wakker in the kinetic model are given in table A2.2. The equilibrium constants were calculated with thermodynamic data or found in the literature. The parameters k_f , k_s , k_{wgs} , k_{COS} , $k_{f,COS}$, Q_f , Q_s , Q_L and K_{CO} were estimated by fitting experimental data.

Table A2.1: Characteristics of a sorbent of MnO on Al₂O₃

manganese content	weight %	7.1-8.25
surface area	m ² /g	180-200
average pore diameter	nm	4-5
particle diameter	mm	0.25-0.42
minimum fluidization velocity	m/s	0.03



Table A2.2: Description and values of the parameters in the kinetic model for the removal of H₂S.

parameter	description	value	dimension
K_f	equilibrium constant sulfur exchange	1	-
k_f	reaction rate constant fast sulfur exchange	0.4	$m_g^3/(mol.s)$
k_s	reaction rate constant slow sulfur exchange	7.10^{-7}	$m_r^3/(mol.s)$
K_{wgs}	equilibrium constant water gas shift reaction	2.54	-
k_{wgs}	reaction rate constant water gas shift reaction	0.4	$m_g^3/(mol.s)$
K_{COS}	equilibrium constant COS formation	0.054	-
k_{COS}	reaction rate constant COS formation	0.4	$m_g^3/(mol.s)$
$K_{f,COS}$	equilibrium constant COS exchange	6	-
$k_{f,COS}$	reaction rate constant COS exchange	0.4	$m_g^3/(mol.s)$
K_{COSr}	equilibrium constant reaction COS with H ₂ O	10^{18}	-
k_{COSr}	reaction rate constant reaction COS with H ₂ O	10^4	$m_g^3/(mol.s)$
K_{H_2S}	equilibrium constant Langmuir adsorption H ₂ S	1.36	m_g^3/mol
K_{H_2O}	equilibrium constant Langmuir adsorption H ₂ O	12.36	m_g^3/mol
K_{CO}	equilibrium constant Langmuir adsorption CO	10	m_g^3/mol
Q_f	number of fast exchangeable manganese sites	676	mol/m_s^3
Q_s	number of slow exchangeable manganese sites	469	mol/m_s^3
Q_L	number of Langmuir adsorption sites	290	mol/m_s^3



Appendix 3: Equations for calculating the terminal and the minimal fluidization velocities and the bed voidage.

In this appendix some equations are given for calculating fluidization properties of particles and the bed voidage. Numerous, most empirical, equations are available (see for example Geldart (1986)). The equations which were used in this report are given here.

The terminal fluidization velocity of a particle is the gas velocity at which the particle is dragged along with the gas. Howard (1989) gives the following equations for different ranges of Re_t :

$$Re_t < 0.4 \quad u_t = \frac{d_p^2 \cdot (\rho_p - \rho_g) \cdot g}{18 \cdot \mu_g} \quad A3.1$$

$$0.4 < Re_t < 500 \quad u_t = \left[\frac{4}{225} \cdot \frac{(\rho_p - \rho_g)^2 \cdot g^2}{\rho_g \cdot \mu_g} \right]^{1/3} \cdot d_p \quad A3.2$$

$$500 < Re_t < 200000 \quad u_t = \left[\frac{3.1 \cdot g \cdot (\rho_p - \rho_g) \cdot d_p}{\rho_g} \right]^{0.5} \quad A3.3$$

The terminal Reynolds number Re_t is equal to:

$$Re_t = \frac{\rho_g \cdot u_t \cdot d_p}{\mu_g} \quad A3.4$$

The minimum bed voidage, ϵ_{mf} and the minimum fluidization velocity, u_{mf} should be determined experimentally. When this is not possible the following equations can be used:

$$\epsilon_{mf} = 0.513 \cdot \left[\frac{u_t^2}{g \cdot \mu_g \cdot (\rho_p - \rho_g)} \right]^{-0.017} \quad A3.5$$

For the calculation of u_{mf} first the Archimedes number Ar is calculated:

$$Ar = \frac{d_p^3 \cdot \rho_g \cdot (\rho_p - \rho_g) \cdot g}{\mu_g^2} \quad A3.6$$

u_{mf} is then calculated with an equation given by Goroshko:

$$u_{mf} = \frac{\mu_g}{d_p \cdot \rho_g} \cdot \frac{Ar}{\left[150 \cdot \left[\frac{1 - e_{mf}}{e_{mf}^3} \right] + \left[1.75 \cdot \frac{Ar}{e_{mf}^3} \right]^{0.5} \right]} \quad A3.7$$

The bed expansion H/H_{mf} is calculated with a equation given by Babu (1978):

$$\frac{H}{H_{mf}} = 1 + \frac{14.314 \cdot (u - u_{mf})^{0.738} \cdot d_p^{1.006} \cdot \rho_p^{0.376}}{u_{mf}^{0.937} \cdot \rho_g^{0.126}} \quad A3.8$$

The bed voidage is calculated with the bed expansion:

$$\epsilon = 1 - (1 - \epsilon_{mf}) \cdot \frac{H_{mf}}{H} \quad A3.9$$

Appendix 4: Segregation of ash and sorbent

The anorganic components in the coal will remain after the coal has been burned. These anorganic residus are partly removed as fly ash, small particles which are carried along with the gases and are collected in the cyclone. Bigger ash particles will stay in the bed. To avoid accumulation of ash in the system, the ash will have to be separated from the sorbent particles and removed. When the ash particles differ in size and density they can be separated from the sorbent particles by segregation. Bed 2 is used for this purpose. When the particles are bigger and heavier than the sorbent particles, the ash will sink, and can be removed at the bottom of the bed. For experiments without coal combustion in the pilot plant the ash can be simulated with sand particles.

A measure for the effectivity of the segregation is given by the mixing index M . When the bed is completely mixed, the ash fraction in the toplayer is the same as in the rest of the bed. The mixing index is 1 in this case. If there is no ash in the toplayer at all, the segregation is complete and the mixing index is 0. The mixing index is a function of the fluidization velocity in bed 2 and of the fluidization properties of the ash and the sorbent. The mixing index is defined as:

$$M = \frac{1}{1 + e^{-z}} = \frac{x}{\bar{x}} \quad A4.1$$

In this equation z is the velocity ratio defined by:

$$z = \frac{u_2 - u_{TO}}{u_2 - u_{mf, sb}} \cdot e^{\frac{u_2}{u_{TO}}} \quad A4.2$$

u_{TO} is the takeover velocity, which is defined as the velocity at which the mixing index is 0.5. It is given by:

$$\frac{u_{TO}}{u_{mf, sb}} = \left[\frac{u_{mf, ash}}{u_{mf, sb}} \right]^{1.2} + 0.9 \cdot \left[\frac{\rho_{ash}}{\rho_{sb}} - 1 \right]^{1.1} \cdot \left[\frac{d_{ash}}{d_{sb}} \right]^{0.7} + 2.2 \cdot \sqrt{\bar{x}} \cdot \left[1 - e^{-\frac{H}{D}} \right]^{1.4} \quad A4.3$$

\bar{x} is the weight fraction ash in the toplayer, while x is the average weight fraction ash in bed 2 and is calculated as:

$$\bar{x} = \frac{\phi_{ash}}{\phi_{ash} + \phi_{sb}} \quad A4.4$$

The height of the ash layer is calculated with:

$$H_{ash} = H \cdot \left[1 - \left[1 + \frac{1 - e_{mf, sb}}{1 - e_{mf, ash}} \cdot \left[\frac{\frac{\bar{x}}{1 - \bar{x}} - \frac{x}{1 - x}}{\frac{x}{1 - x} + \frac{\rho_{ash}}{\rho_{sb}}} \right]^{-1} \right] \right] \quad A4.5$$



Appendix 5: Modelling of the solids flow and the gas leaks through the orifices

The Interconnected Fluidized Bed (IFB) consists of four beds, which are connected in such a way that the sorbent particles are circulating through the system. When bed 1 and 3 are lean beds, and bed 2 and 4 dense beds, the sorbent can be transported from bed 1 to bed 2 and from bed 3 to bed 4 over a separating weir, and from bed 2 to bed 3 and from bed 4 to bed 1 through an orifice in the wall. For the proper operation of bed 1, desulphurization of a gas flow, and bed 3, the regeneration of the sorbent, it is important to control the flow rate of the sorbent through the IFB.

In the control of the circulation rate of the solids three phenomena are important (Fox et al., 1989):

- the vertical resisting force to the flow in each bed due to the friction of particles with the walls
- the horizontal resisting force due to the contraction of the flow of the gas-solids mixture in the orifice
- the gas flow through the orifice, which is an undesired effect and therefore called gas leak

In a fluidized bed the friction of particles with the wall will be negligible, so the sorbent flow from a dense fluidized bed to a lean fluidized bed through an orifice depends only on the resisting force of the orifice. In the pilot plant this is the case for the sorbent flow from bed 2 to bed 3, because both beds are fluidized. For this case a model was developed by Korbee et al. (1991).

The driving force is the pressure drop over the orifice. When the heights of the two beds and the pressure above the beds are equal, the pressure drop over the orifice ΔP_{o23} can be calculated with:

$$\Delta P_{o23} = g \cdot (H - H_{o23}) \cdot (\rho_{p,2} \cdot (1 - \epsilon_2) - \rho_{p,3} \cdot (1 - \epsilon_3)) \quad A5.1$$

with H = height of the bed
 H_{o23} = the height of the orifice in the separating wall between bed 2 and bed 3.

For the sorbent flow through the orifice from bed 2 to bed 3 the following equation is derived:

$$\phi_{sb} = C_d \cdot A_{o23} \cdot \left[1 - \frac{k_p \cdot d_p}{d_{o23}} \right]^2 \cdot \sqrt{2 \cdot \rho_{p,2} \cdot (1 - \epsilon_2) \cdot \Delta P_{o23}} \quad A5.2$$

with A_{o23} = area of the orifice
 d_{o23} = diameter of the orifice
 k_p = shape factor of the particles
 C_d = discharge coefficient

k_p is taken to be 3.6 and C_d is taken to be 0.5.

Jones and Davidson divide the gas leak through the orifice into two contributions: an amount of gas having the particle velocity and a surplus amount having a slip velocity relative to the particles. They derived the following expression for the total gas flow through the orifice:

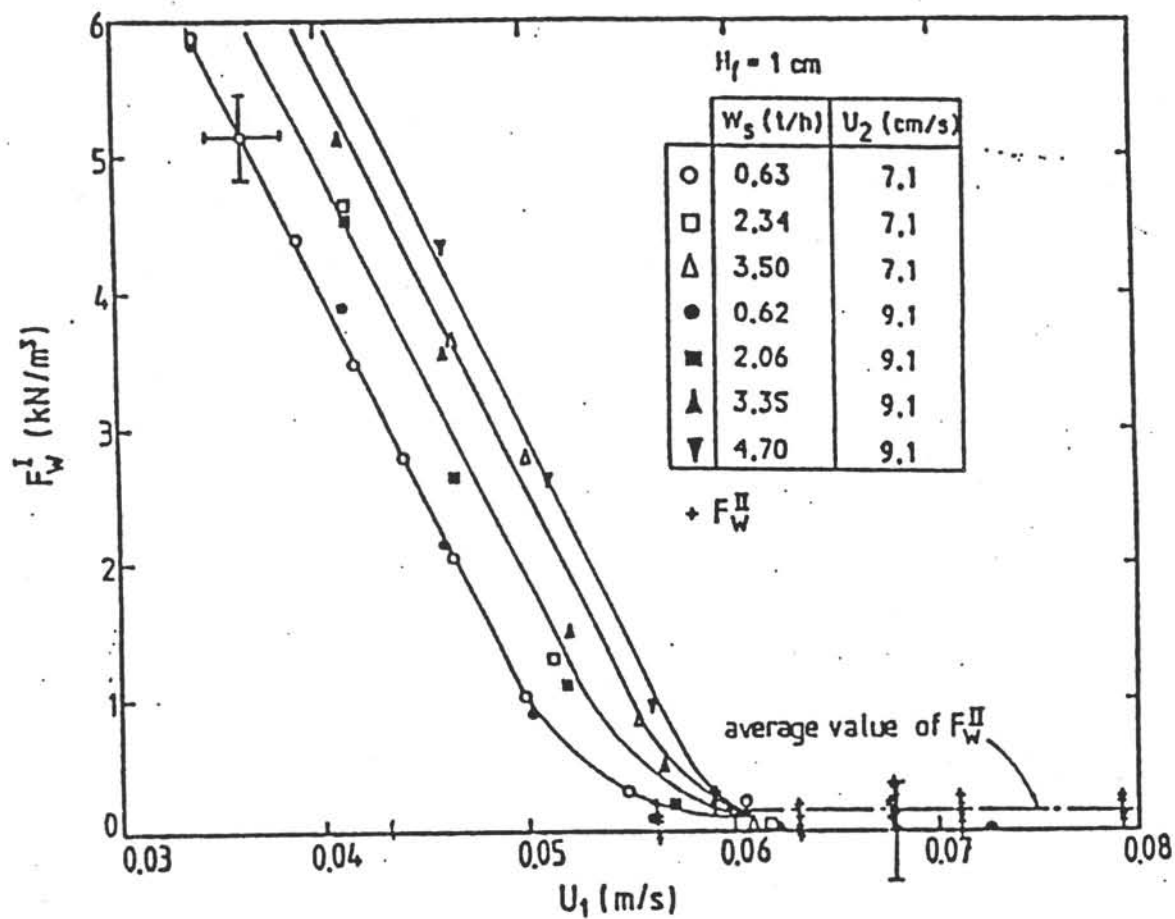


Figure A5.1: Influence of the superficial gas velocity on the vertical resisting forces in a defluidized bed at different solids flows (Fox, 1989)

$$\phi v_{23} = \frac{\phi_{sb}}{\rho_{sb}} \left[\frac{\epsilon_2}{1 - \epsilon_2} \right] + \frac{\pi \cdot u_{mf} d_{o23} \Delta P_{o23}}{2 \cdot \rho_{sb} \cdot (1 - \epsilon_{mf}) \cdot g} \quad A5.3$$

It is difficult however to control the solids flow through the IFB with this orifice. It is seen that the sorbent flow can be adjusted by varying the superficial velocities in bed 2 and bed 3 or varying the orifice diameter. Varying the orifice diameter in a plant at 850 °C is very difficult. The superficial velocity in bed 2 is used to control the segregation, while the possibilities of adjusting the sorbent flow by varying the superficial velocity in bed 3 are limited. The orifice diameter between bed 2 and bed 3 should not be chosen too small to prevent the sorbent flow is limited by this orifice. The orifice diameter should not be too big neither to prevent excessive gas leaks.

As said before the vertical resisting forces are not important in fluidized beds. When the bed however is defluidized, they are important. As seen in figure A5.1 (Fox, 1989) the vertical resisting force in a defluidized bed decreases with increasing superficial velocity in the bed, so the solids flow will increase with increasing superficial velocity. Fox (1989) concluded that control of the sorbent flow can be done by varying the superficial velocity in a defluidized bed. In the pilot plant bed 4 will be operated in this way.

The following model is used for predicting the gas leak at a certain solids flow when the bed is at minimum fluidization conditions. At minimum fluidization conditions the solids flow is assumed to be maximal. When the superficial velocity is decreased at this point the vertical resisting forces increase. When the superficial velocity is increased, the pressure drop over the orifice and thus the solids flow through the orifice decreases (this is the region where the model derived for the orifice between bed 2 and bed 3 becomes valid). It is assumed that both in the bed and in the orifice the voidage is equal to the minimum bed voidage. The absolute particle velocity through the orifice can then be calculated from the sorbent flow:

$$u_{abs} = \frac{\phi_{sb}}{\rho_{sb} \cdot (1 - \epsilon_{mf}) \cdot A_{o41}} \quad A5.4$$

with A_{o41} = surface of the orifice in the wall between bed 4 and bed 1

The downward particle velocity in bed 4 is also calculated from the sorbent flow:

$$u_s = \frac{\phi_{sb}}{\rho_{sb} \cdot (1 - \epsilon_{mf}) \cdot A_4} \quad A5.5$$

The absolute gas velocity in the bed is then:

$$u_{gas} = \frac{u_{mf}}{\epsilon_{mf}} - u_s \quad A5.6$$

The pressure drop ΔP_{o41} over the orifice is calculated with:

$$\Delta P_{o41} = g \cdot (H - H_{o41}) \cdot (\rho_{p,4} \cdot (1 - \epsilon_4) - \rho_{p,1} \cdot (1 - \epsilon_1)) \quad A5.7$$

With the equation of Ergun the horizontal slip velocity of the gas in the orifice u_{hor} is

calculated:

$$\Delta P_{o41} = A_4^{0.5} \cdot \left[150 \cdot \left[\frac{1}{\epsilon_{mf}} - 1 \right]^2 \cdot \frac{\mu_g}{d_{sb}^2} \cdot u_{hor} + 1.75 \cdot \left[\frac{1}{\epsilon_{mf}} - 1 \right] \cdot \frac{\rho_g}{d_{sb}} \cdot u_{hor}^2 \right] \quad A5.8$$

The gas leak ϕv_{41} through the orifice is calculated with:

$$\phi v_{41} = A_{o41} \cdot \epsilon_{mf} (u_{hor} + u_{abs}) \quad A5.9$$

Finally the superficial velocity u_4 for bed 4 can be calculated:

$$u_4 = u_{gas} \cdot \epsilon_{mf} + \frac{\phi_{g41}}{A_4} \quad A5.10$$

Appendix 6: Estimation of the capacity of the reactor heater

In this appendix the heating of the reactor at the start-up and the needed capacity of the reactor heater are discussed. It is assumed that at the start-up the reactor is heated with a nitrogen flow with a temperature of 850 °C and with a reactor heater with capacity Q_H . The temperature rise of the reactor material and the bed material are calculated. The following equations were used.

The heat balance for the reactor material (Haynes HR-120) is described with:

$$M_{st} \cdot C_{p,st} \cdot \frac{dT_{st}}{dt} = U_{st} \cdot A_{st,i} \cdot \left(\frac{T_{g,i} + T_{g,o}}{2} - T_{st} \right) - \frac{\lambda_{st}}{l_{st}} \cdot A_{st,o} \cdot (T_{st} - T_{fb}) - Q_L - Q_R + Q_H \quad A6.1$$

The left hand term is the accumulation of heat in the reactor material, while the first right hand term is the convective heat transfer from the gas and the particles to the reactor wall and the second term is the heat loss to the freeboard. Q_L is the heat loss through the insulation, Q_R the radiative heat transfer from the particles to the reactor wall and Q_H the heat input from the reactor heater.

The heat balance over the bed material (sorbent) is:

$$M_{bed} \cdot C_{p,bed} \cdot \frac{dT_{bed}}{dt} = U_{bed} \cdot A_{bed} \cdot \left(\frac{T_{g,i} + T_{g,o}}{2} - T_{bed} \right) - Q_R \quad A6.2$$

The left hand term is the accumulation of heat in the bed material, the right hand term is the convective heat transfer from the gas to the bed material.

The heat balance over the nitrogen flow is:

$$\phi v_{n2} \cdot C_{p,n2} \cdot (T_{g,i} - T_{g,o}) = U_{st} \cdot A_{st,i} \cdot \left(\frac{T_{g,i} + T_{g,o}}{2} - T_{st} \right) + U_{bed} \cdot A_{bed} \cdot \left(\frac{T_{g,i} + T_{g,o}}{2} - T_{bed} \right) \quad A6.3$$

The left hand term is the cooling of the nitrogen flow, while the right hand terms are the convective heat transfer from the gas to the reactor material and to the bed material.

Q_L is the heat loss through the insulation to the environment and is calculated with:

$$Q_L = \frac{1}{\frac{d_{ins}}{\lambda_{ins}} + \frac{1}{\alpha_L}} \cdot A_{st,o} \cdot (T_{st} - T_{env}) \quad A6.4$$

α_L is the film heat transfer coefficient for the heat transfer from the outside of the insulation layer to the surroundings by natural convection and radiation and was estimated from Perry (1984). Q_R is the radiative heat transfer from the bed material to the reactor material and is calculated with:

$$Q_R = A_R \cdot \epsilon_{bed} \cdot \sigma_b \cdot [T_{bed}^4 - T_{st}^4] \quad A6.5$$

The convective heat transfer coefficients are calculated with the following equations, which were taken from Pell (1990). The heat transfer coefficient U_{st} is for the convective heat transfer from the gas and the particles to the reactor walls and is calculated with:

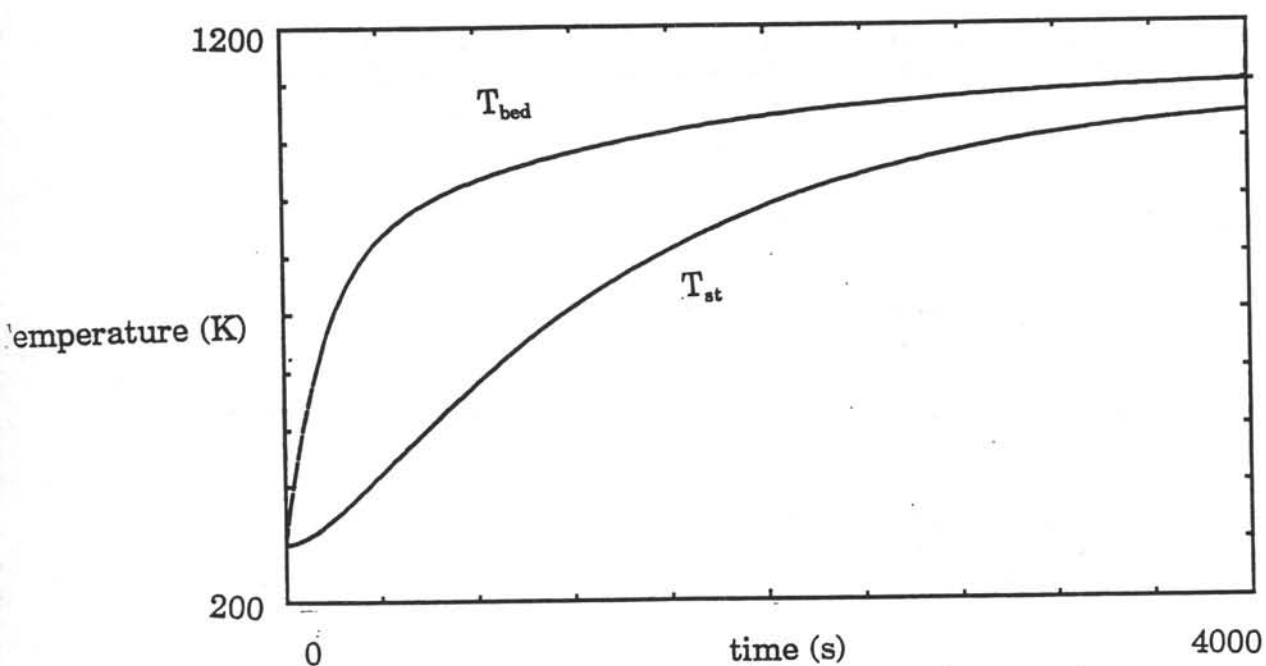


Figure A6.1: Heating of the bed material and the reactor material without a reactor heater.

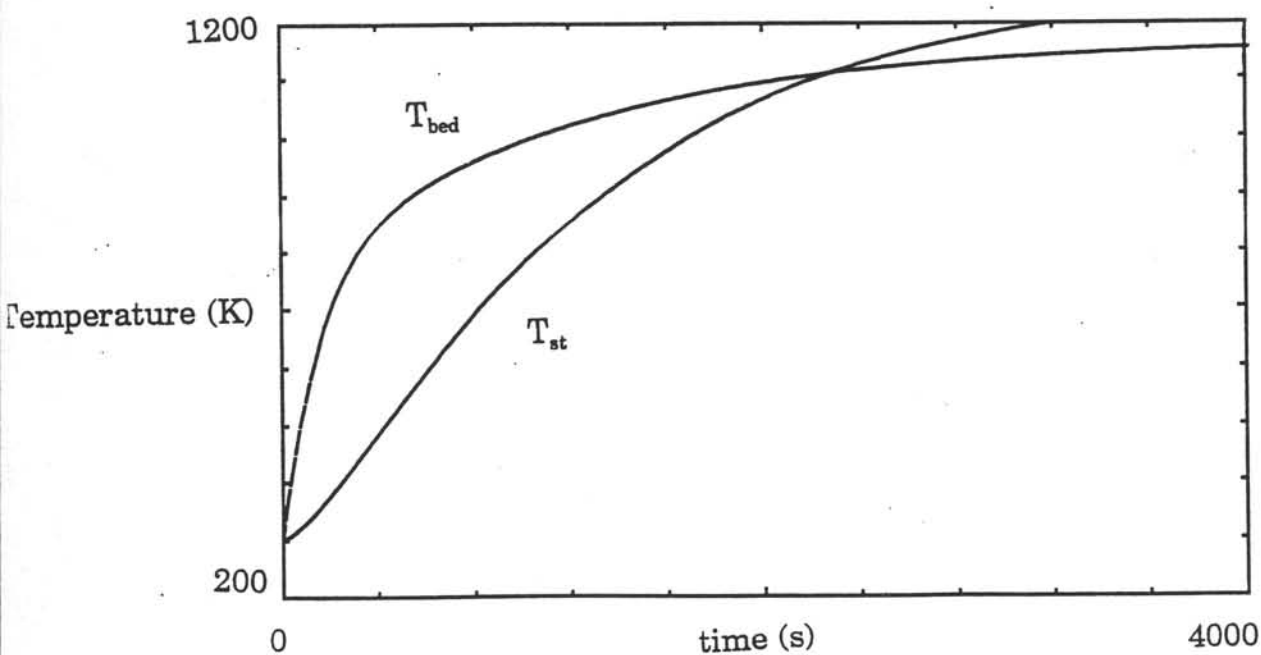


Figure A6.2: Heating of the bed material and the reactor material with a reactor heater with a capacity of 4 kW

$$U_{st} = \frac{900 \cdot \lambda_{N2} \cdot (1 - \epsilon_{bed})}{d_h} \cdot \left[\frac{\phi v_{N2} \cdot d_h \cdot \rho_s}{\rho_{N2} \cdot \mu_{N2}} \right] \cdot \left[\frac{\mu_{N2}^2}{d_p^3 \cdot \rho_s^2 \cdot g} \right]^{0.326} \cdot Pr^{0.3} \quad A6.6$$

The heat transfer coefficient U_{bed} is calculated with a Nu equation:

$$Nu_{bed} = 2.0 + 1.3 \cdot Pr^{0.15} + 0.66 \cdot Pr^{0.31} \cdot Re_p^{0.5} \quad A6.7$$

with:

$$Nu_{bed} = \frac{U_{bed} \cdot d_p}{\lambda_{N2}} \quad Pr = \frac{\mu_{N2} \cdot C_{p,N2}}{\lambda_{N2}} \quad Re_p = \frac{\rho_{N2} \cdot u_{N2} \cdot d_p}{\mu_{N2}} \quad A6.8$$

Remarks:

- The heat conduction to the freeboard can only be estimated. It is assumed that the temperature of the freeboard is 0.9 times the reactor temperature. The freeboard itself is also well insulated and is heated by the nitrogen flow and by heat conduction from the reactor.
- Average values have been taken for the specific heats and the thermal conductivities.
- For the properties of nitrogen the values at 1123 K have been taken.

In Table A6.1 the parameters in the equations and their values are given.

The differential equations A6.1 and A6.2 were integrated with a simulation program, PSI/c. In figure A6.1 the simulation is shown when there is no additional reactor heating, in figure A6.2 when there is a additional heating with an input of 4 kW. We see from picture A6.2 the reactor will be at the desired temperature within half a hour. As this is an acceptable time it is concluded that a reactor heater with a capacity of 4 kW is sufficient.



Table A6.1: parameters in reactor heating equations and their values

parameter	description	value	dimension
U_{st}	heat transfer coefficient gas-steel	19.4	W/(m ² .K)
U_{bed}	heat transfer coefficient gas-bed	178	W/(m ² .K)
$A_{st,i}$	inner reactor steel area	0.98	m ²
$A_{st,o}$	outer reactor steel area	0.5	m ²
A_{bed}	bed area	4.7	m ²
λ_{ins}	thermal conductivity insulation	0.20	W/(m.K)
λ_{st}	thermal conductivity steel	17	W/(m.K)
M_{st}	mass of steel	36	kg
M_{bed}	mass of bed	11	kg
$C_{p,st}$	specific heat of steel	600	J/(kg.K)
$C_{p,bed}$	specific heat of sorbent	964	J/(kg.K)
$C_{p,n2}$	specific heat of nitrogen	1142	J/(kg.K)
Φ_{n2}	mass flow of nitrogen	0.0194	kg/s
d_{ins}	insulation thickness	0.075	m
l_{st}	distance reactor-freeboard	0.3	m
μ_{n2}	viscosity nitrogen	$4.6 \cdot 10^{-5}$	Pa.s
λ_{n2}	thermal conductivity nitrogen	$7.17 \cdot 10^{-2}$	W/(m.K)
ρ_{n2}	density nitrogen	0.3	kg/m ³
d_p	particle diameter	$2.5 \cdot 10^{-3}$	m
d_h	hydraulic diameter steel plate	0.17	m
$A_{st,a}$	cross-sectional area steel	0.0048	m ²
$T_{g,i}$	inlet gas temperature	1123	K
$T_{g,o}$	outlet gas temperature	calculated	K
T_{st}	steel temperature	calculated	K
T_{bed}	bed temperature	calculated	K
T_{fb}	freeboard temperature	$0.9 \cdot T_{st}$	K
T_{env}	environment temperature	298	K
ρ_b	Stefan-Boltzmann constant	$5.8 \cdot 10^{-8}$	W/(m ² .K ⁴)
α_L	heat transfer coefficient insulation-air	10.4	W/(m ² .K)

Appendix 7: Design procedure for the gas distributor

This procedure starts with a suggestion for a minimum distributor to bed pressure drop ratio $\Delta P_d/\Delta P_{bed}$ which may be used in the actual design procedure of the distributor. The basis of this design is formed by the choice of the ratio u/u_{or} (u is the superficial gas velocity and u_{or} is the gas velocity through the orifices) which defines the open area in the perforated plate. With the value for this ratio the distributor to bed pressure drop ratio $\Delta P_d/\Delta P_{bed}$ and the number of orifices can be estimated. For the final design of the distributor the distribution of the holes over the plate area will be calculated. For the maximum gas velocity the penetration jet length will be calculated to check possible channeling of the gas through the bed.

1 Estimation of the minimum pressure drop over the distributor ΔP_d

Sathiyamoorthy and Rao (1981) suggested a procedure to estimate the minimum pressure drop over the distributor ΔP_d . The first step is to estimate the terminal velocity of the particle u_t with equation A3.2 (appendix 3). The minimum fluidization velocity $u_{mf} = 0.65$ m/s. The superficial gas velocity at which all orifices become operative in an uniformly fluidized bed, u_M is estimated with:

$$u_M = u_{mf} \left(2.65 + 1.24 \cdot 10^1 \log \left(\frac{u_t}{u_{mf}} \right) \right) = 2.84 \text{ m/s} \quad A7.1$$

It is now possible to calculate the minimum distributor to bed pressure drop ratio $\Delta P_d/\Delta P_{bed}$ using the equation:

$$\frac{\Delta P_d}{\Delta P_{bed}} = 2.7 * \left(\frac{u_{mf}}{u_M - u_{mf}} \right)^{2.32} = 0.16 \quad A7.2$$

Calculation of the distributor to bed pressure drop ratio $\Delta P_d/\Delta P_{bed}$

To calculate the distributor to bed pressure drop ratio $\Delta P_d/\Delta P_{bed}$ a choice have to be made for the value for the ratio u/u_{or} which defines the open area in the distributor plate. A value of about 2% for this ratio is commonly found. The maximum value is 10%.

For both the minimum and the maximum superficial gas velocity the distributor to bed pressure drop ratio $\Delta P_d/\Delta P_{bed}$ will be calculated. If the boundaries of the range for this ratio are not satisfying, another choice will be made for the ratio u/u_{or} . The ratio $\Delta P_d/\Delta P_{bed}$ may be limited by the value of about 0.5. Higher values mean excessive pressure drops over the distributor.

The bed pressure drop ΔP_{bed} can be calculated for both superficial velocities with:

$$\Delta P_{bed} = (1 - \epsilon_{bed}) (\rho_p - \rho_g) \cdot H_{bed} \cdot g \quad A7.3$$

where ϵ_{bed} is the bed voidage

H_{bed} is the bed height = 0.5 m

The pressure drop over the distributor ΔP_d for both cases can be determined by:

$$\Delta P_d = \frac{u_{or}^2 \cdot \rho_g}{2 \cdot C d_{or}^2} \quad A7.4$$

where $C d_{or}$ is the orifice constant which may be estimated using a relation of Qureshi and Creasy (1979) in which the value for $C d_{or}$ depends on the orifice diameter d_{or} and the plate thickness t_d :

$$C d_{or} = 0.82 \cdot \left(\frac{t_d}{d_{or}} \right)^{0.13} \quad A7.5$$

This relation may only be used for $t_d/d_{or} > 0.09$.

Determination of the number of orifices N_{or}^*

The number of holes N_{or} per unit area of distributor can be determined using:

$$N_{or} = 4 \cdot \frac{u}{\pi \cdot d_{or}^2 \cdot u_{or}} \cdot \frac{4}{\pi} \quad A7.6$$

For a bed area A_{bed} , the actual number of holes N_{or}^* can then be determined by:

$$N_{or}^* = N_{or} \cdot A_{bed} \quad A7.7$$

Two different distributions of the orifices over the plate area will be calculated here. If the holes are a triangular pitch Γ , the number of holes per unit grid area is $2/(\sqrt{3} \cdot \Gamma^2)$ and for a square pitch $1/\Gamma^2$. It is now possible to derive a relation between Γ , bed area A_{bed} and N_{or}^* (Mell (1990)):

triangular pitch:

$$\Gamma = \left(\frac{2}{\sqrt{3}} \cdot \frac{A_{bed}}{N_{or}^*} \right)^{0.5} \quad A7.8$$

square pitch:

$$\Gamma = \left(\frac{A_{bed}}{N_{or}^*} \right)^{0.5} \quad A7.9$$

The pitch Γ is between the center of a hole and the center of the hole next to it. It does not make any difference which distribution of orifices will be chosen for the final design of the distributors.

To calculate the penetration jet length l_j , Merry (1975) suggested the following equation:

$$l_j = 5.2 d_{or} \left(\frac{\rho_g d_{or}}{\rho_p d_p} \right)^{0.3} \left(1.3 \left(\frac{u_{or}^2}{g d_{or}} \right)^{0.2} - 1 \right) \quad A7.10$$

Results of the gas distributor calculations

In table A7.1 the results of the gas distributor calculations are shown. The gas velocity through the orifice at maximum conditions is in all the four beds below the suggested maximum value for this velocity ($u_{or} = 80 - 90$ m/s). The designs for the gas distributors proposed in table A7.1 are all limited by this velocity.

For all four beds the minimum value for the ratio $\Delta P_d / \Delta P_{bed}$ is somewhat below the minimum value proposed at the beginning of the design procedure ($\Delta P_d / \Delta P_{bed} = 0.16$). Although the maximum values for $\Delta P_d / \Delta P_{bed}$ have been limited in the choice of the fraction open area, they are above the suggested maximum value for the distributor to bed pressure drop ratio ($\Delta P_d / \Delta P_{bed} = 0.5$).

The choices for u/u_{or} can be verified by taking a higher and a lower value for these ratios. A higher value for u/u_{or} means that $\Delta P_d / \Delta P_{bed}$ becomes higher. This means that the under limit of the range for $\Delta P_d / \Delta P_{bed}$ becomes more satisfactory but the upper limit becomes less satisfactory. A lower value for u/u_{or} means that $\Delta P_d / \Delta P_{bed}$ becomes lower.

The values for the jet length show that channeling caused by jet penetration will not occur in the IFB. Only the danger for attrition of the sorbent particles caused by a high jet velocity may limit this velocity into the fluidized bed.

The results of the gas distributor calculations for bed 2 in case the orifice diameter has been chosen smaller, are also shown in table A7.1. The intention to do these calculations is to check the influence of this diameter on the design calculations. From this table it can be seen that the pressure drop over the distributor will decrease for a distributor with the same open area but with more and smaller orifices. This conclusion may only be valid for certain ranges of orifice diameters since for substantial changes in this diameter, this conclusion is not expected at all. The value for the pressure drop over the distributor depends on what kind of relation has been used to describe the orifice constant Cd_{or} . The reason to do these calculations for bed 2 is that in this bed segregation experiments may be set up with sand particles with a smaller diameter than the sorbent particles. Only for substantial smaller particles problems with possible drainage through the orifices are expected. Thus only when very small sand particles are used for segregation experiments, the gas distributor with orifices of 1 mm may have to be chosen. The simulation of bottom ash with such small sand particles will become far from reality. A distributor with orifices of 2 mm will be used for segregation experiments under normal conditions.

Table A7.1: The results of the gas distributor calculations for each of the four beds

Bed	#1 and #3	#2 ($d_{or}=1$ mm)	#2 ($d_{or}=2$ mm)	#4
u/u_{or} :	0.023	0.014	0.014	0.012
N_{or} (#/m ²)	7322	17826	4457	3820
N_{or}^* (#)	144 and 27	150	38	33
Minimum				
u (m/s)	1	0.65	0.65	0.65
ΔP_{bed} (Pa)	2960.4	4210.6	4210.6	4210.6
ΔP_d (Pa)	352.2	335.4	401.6	490.5
$\Delta P_d/\Delta P_{bed}$	0.12	0.080	0.095	0.13
u_{or} (m/s)	43.5	46.4	46.4	54.2
Maximum:				
u (m/s)	2	1.2	1.2	1
ΔP_{bed} (Pa)	1964.2	2648.7	1964.2	2960.4
ΔP_d (Pa)	1408.6	1143.0	1368.7	1293.7
$\Delta P_d/\Delta P_{bed}$	0.72	0.43	0.52	0.44
u_{or} (m/s)	87.0	85.7	85.7	83.3
l_j (m)	0.012	0.012	0.012	0.012
triangle: Γ (m)	0.0125	0.0080	0.0160	0.0170
square: Γ (m)	0.0117	0.0075	0.0149	0.0160



Appendix 8: Solids feed systems

In this appendix two solids feed mechanisms: the rotary valve and the screw conveyor will be compared. Calculations have been set up to estimate the dimensions of these mechanisms. Based on these calculations a suggestion will be made for the most suitable solids feed system.

Rotary valve

In figure A8.1 a schematic drawing of the solids feed system using a rotary valve, is presented. With a air lock gases are prevented to leak into the hopper bed. The solids fall into the pneumatic conveying line and are fed to the reactor. Woodcock (1987) suggested a simple design procedure for the dimensions of the rotary valve. The number of revolutions N can be determined by the equation:

$$N = \frac{\phi_{so}}{\rho_b \cdot n \cdot V} \quad \text{A8.1}$$

where ϕ_{so} is the solid mass flow (kg/s)

ρ_b is the bulk density (kg/m³)

n is the number of rotor pockets

V is the volume of one rotor pocket (m³)

This equation has been based on the assumption that the rotor has such a small speed that the rotor pockets will fill completely with solids with a bulk density ρ_b . The total volume of the rotor $n \cdot V$ can be estimated using the equation:

$$n \cdot V = \frac{1}{4} \cdot \pi \cdot (D_{ro}^2 - D_{sh}^2) \cdot L_{ro} \quad \text{A8.2}$$

where D_{ro} is the diameter of the rotor (m)

D_{sh} is the diameter of the shaft of the rotor (m)

L_{ro} is the length of the rotor (m)

In equation A8.2 it is assumed that the walls of the rotor pockets have a neglectable volume. Only the shaft has been taken into account as its volume cannot be filled up by solid particles. In table A8.1 the characteristics of the solids are presented. These characteristics have been used for the rotor calculations. In these calculations the number of revolutions will be determined for the different mass flows from table A8.1.

Table A8.1: Characteristics of the solids

solid:	coal	sand
ρ_b (kg/m ³)	840	1500
range ϕ_{so} (g/s)	0.04-0.4	0.01-0.1

Two rotor configurations are presented in table A8.2. The results of the calculations for these two configurations are presented in table A8.3.

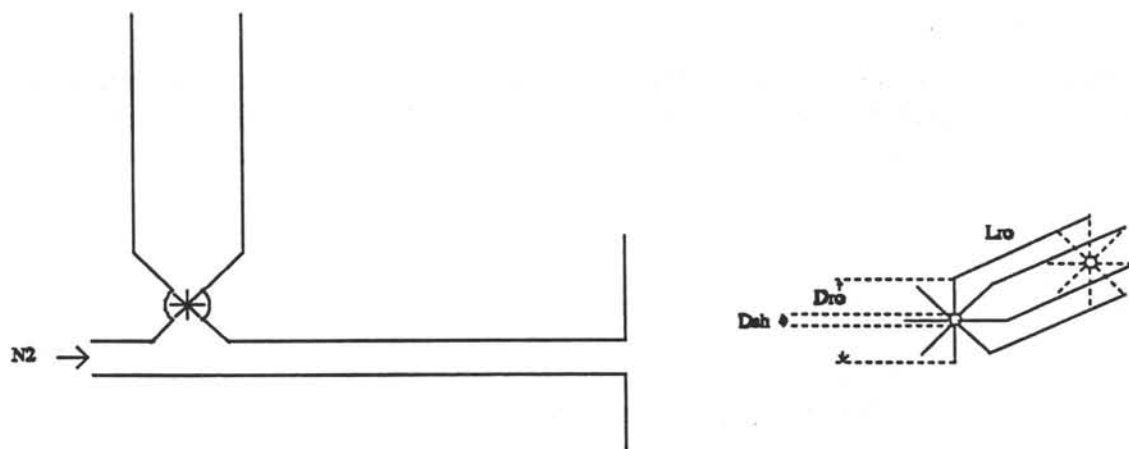


Figure A8.1 Schematic drawing of a rotary valve

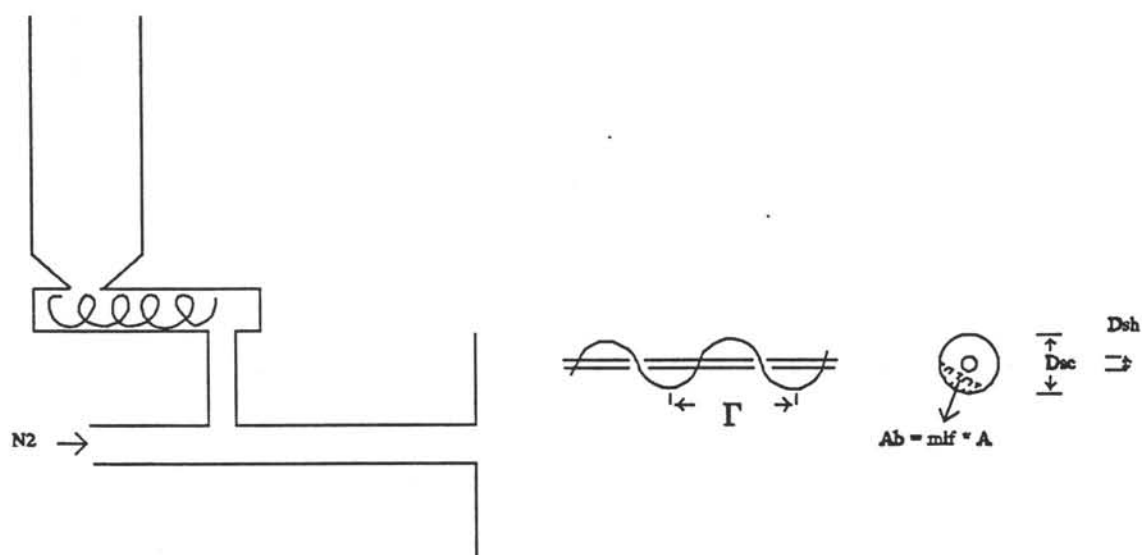


Figure A8.2 Schematic drawing of a screw conveyor

Table A8.2: Characteristics of the rotor

rotor configuration	1	2
D_{ro} (m)	0.03	0.018
D_{sh} (m)	0.004	0.003
L_{ro} (m)	0.015	0.01
$n \cdot V$ (m ³)	$1.04 \cdot 10^{-5}$	$2.5 \cdot 10^{-6}$

Table A8.3: Results of the rotor calculations

		rotor 1	rotor 2
	ϕ_{so} (g/s)	N (rev/s)	N (rev/s)
coal	0.04	0.0046	0.0193
	0.4	0.0457	0.1925
sand	0.01	0.0006	0.0027
	0.1	0.0064	0.0270

Screw conveyor

In figure A8.2 a schematic drawing of the solids feed system using a screw conveyor, is presented. The solids fall into the pneumatic conveying line and are fed to the reactor. Woodcock (1987) suggested a design procedure for the dimensions of the screw. The number of revolutions N are determined by the equation:

$$N = \frac{\phi_{so}}{\rho_b \cdot 0.25 \cdot \pi \cdot (D_{sc}^2 - D_{sh}^2) \cdot mlf \cdot \Gamma} \quad A8.3$$

where mlf is the maximal loading factor

Γ is the pitch (m)

D_{sc} is the diameter of the screw (m)

D_{sh} is the diameter of the shaft (m)

In this equation the flow area of the screw A_{sc} is expressed by $0.25 \cdot \pi \cdot (D_{sc}^2 - D_{sh}^2)$. The bulk area A_b can then be expressed by $A_{sc} \cdot mlf$. The value for mlf has been chosen as low as possible to avoid unnecessary attrition. A minimum value for mlf is 0.15 (Woodcock, 1987), and this value has been used in the screw conveyor calculations.

In these calculations the number of revolutions will be determined for the different mass flows and solids characteristics from table A8.1.

Two screw conveyor configurations are presented in table A8.4. The results of the calculations for these two configurations are presented in table A8.5.

Table A8.4: Characteristics of the screw

screw configuration	D_{sc} (m)	D_{sh} (m)	Γ (m)	A_{sc} (m)
1	0.025	0.004	0.025	$4.8 \cdot 10^{-4}$
2	0.015	0.003	0.015	$1.7 \cdot 10^{-4}$

Table A8.5: Results of the screw calculations

		screw 1	screw 2
	ϕ_{so} (g/s)	N (rev/s)	N (rev/s)
coal	0.04	0.0266	0.1248
	0.4	0.2655	1.2475
sand	0.01	0.0037	0.0175
	0.1	0.0372	0.1746

Comparison of the two solids feed system

The results of the rotor calculations, presented in table A8.3 show that the rotor will have very small dimensions and a rather low rotor speed because of the very small feed flows to the reactor. As can be seen from table A8.5, more reasonable values for the dimensions and the screw speed have been found. Based on the values for the dimensions, the screw conveyor may be used for solids feed flow control. Based on the results from table A8.5 it has been chosen for screw 2. This screw configuration gives reasonable values for the number of revolutions so that its speed can be controlled rather easily.

Constructors of screw conveyors supply complete units i.e. the screw together with the hopper and the driving gear system. A constructor who supply precision screw conveyor units is Gericke Solids Handling b.v. from Hoevelaken. In these units the screw can easily be replaced so that for each mass flow range the most suitable screw can be used to obtain as accurate as possible flow control. The driving gear system consists of an electric motor so that accurate speed control of the screw can be ensured.

Appendix 9: Measurement methods, valves and pipe sizing

Measurement methods and controllers for the manipulation of mass flow, temperature and pressure will be discussed first. A short description and discussion will be given of valves like the check valves, the reducing valves and the manual valves. This appendix will end with the estimation of the different pipe sizes.

Measurement methods and controllers

Mass flow

The mass flow controller consists of a mass flow measurement device and a control valve. There are basically three methods of mass flow measurement according to Benard (1988) and Brain (1969):

- By measuring the volumetric flow and making corrections for density, pressure and temperature compressibility etc., i.e. by using compensation techniques.
- By true mass flow measurement
- By inferential mass flow measurement (other than compensation techniques)

Compensation mass flow measurement techniques.

The mass flow can be calculated using the values for the volumetric flow and density. Volumetric flowmeters can be used for a wide range of flows. A disadvantage is that corrections have to be made for density. The combination of the density and volumetric flow measurements causes a difficult controlling mechanism. This type of mass flow measurement is normally used for flows larger than the flows which are expected in the IFB.

Direct true mass flow measurement.

In this type of flowmeter mass is experienced as an acceleration force. A calibrated string is used to measure the torque produced by the acceleration force. A disadvantage is that it is difficult to find a string which is linear over a wide range of deflection. Further these mass flowmeters are designed for one typical range and condition, and are not easily reconstructed for different purposes by changing one or two parts of the flowmeter.

Inferential mass flow measurement.

An example of this type of flowmeter is an thermal mass flowmeter. In this type of flowmeter, a heating coil is mounted on a flowtube and a small amount of heat is added to the fluid flow. Temperature sensors are placed upstream and downstream of the heating coil. Thermal mass flowmeters are normally used for smaller flows. Recent developments in these flowmeters show that full scale ranges of 1000 Nl/min can be measured. All the maximum values for the mass flows are within these ranges. An advantage of this type is that it can be used for different purposes or ranges by an easy change of the flow sensor. These type of flow controllers are suitable for measuring and controlling the feed gas flows as well as for measuring the gas flows to the converter.

In figure A9.1 a schematic drawing of the thermal mass flowmeter is shown. The measured temperature difference is directly proportional to the mass flow. From this difference a signal is produced that will be used to drive the control valve. The control valve contains a plunger which moves the valve seat up and down, relative to the orifice through which the gas flows. In case the electrical feed is switched off the valve will come in closed position. Brooks

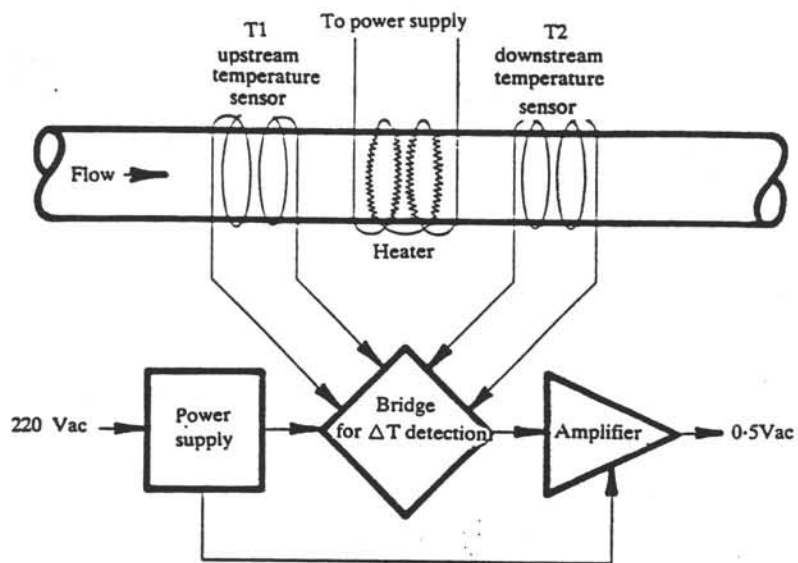


Figure A9.1 Schematic drawing of a thermal mass flowmeter

Instrument B.V. from Veenendaal can deliver thermal mass flow controllers for flow ranges up to 1000 NI/min (Trade name: Rosemount type of flow controllers).

Temperature

The most common sensors used for the measurement of temperature are thermocouples and resistance thermometers. Other possible sensors are based on mechanical or thermal radiation principles (like liquid-in-glass thermometers and pyrometers). These sensors are not suitable for the use in the pilot plant. Because of the high temperatures to be measured it has been chosen to use thermocouples. Kennedy (1986) has compared the different sensors and has presented typical ranges of temperature for thermocouples: -200 to 1700 °C and platinum resistance thermometers: -250 to 650 °C, so it has been chosen to use thermocouples. Thermocouples are usually provided with a protective well to prevent direct contact with the process environment and to increase the mechanical strength. The requirement for the protective well is that it is able to resist the different environments in the pilot plant: sulphurous, reducing or oxidizing.

Temperature sensors respond more slowly to temperature changes than pressure gauges or flowmeters respond to changes in those parameters. This is because the heat must be transferred through the protecting well to the sensor. This slowness can be compensated for by adding derivative action to the control scheme, which would cause the controller output signal to change at a rate proportional to the rate at which the temperature is changing.

Pressure

Pressure is sensed by a mechanical element, which offers the force a surface to act upon. Pressure-measuring devices may be divided into three groups: (1) those which are based on the measurement of the height of a liquid column, (2) those which are based on the measurement of the distortion of an elastic pressure chamber, and (3) electrical sensing devices. The choice of a sensor depends on the pressure range (this range should be around 1.5 times normal line operating pressure) accuracy and repeatability. For normal applications $\pm 1\%$ of full scale of range is sufficient (pressure indications purposes) but for precision measurements sensors with $\pm 0.1\%$ or even $\pm 0.01\%$ accuracy are available.

A pressure-indicating device frequently used is the C-string Bourbon-tube pressure gauge. In this sensor a tube in a -c- form will deform by the applied pressure.

For controlling purposes an electrical sensing device can be used. In this type of device commonly called strain gauge, the electrical resistance of a wire or other electrical conductor changes with the deformation of the conductor. Strain gauges are often attached to diaphragm elements. The distortion of a diaphragm is then transduced into usable electric signals. For pressure control this type of sensor is combined with an electrical control valve. Strain gauges can also be used as sensors to determine axial pressure profiles in the reactor.

Valves

Check valves (non-return valves)

These valves are used to prevent reversal of flow. The swing or hinged disc check valves are normally designed for use in horizontal lines, where the force of gravity on the disk is at

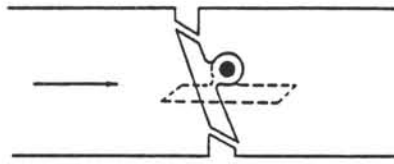


Figure A9.2 Schematic drawing of tilting-disk check valve

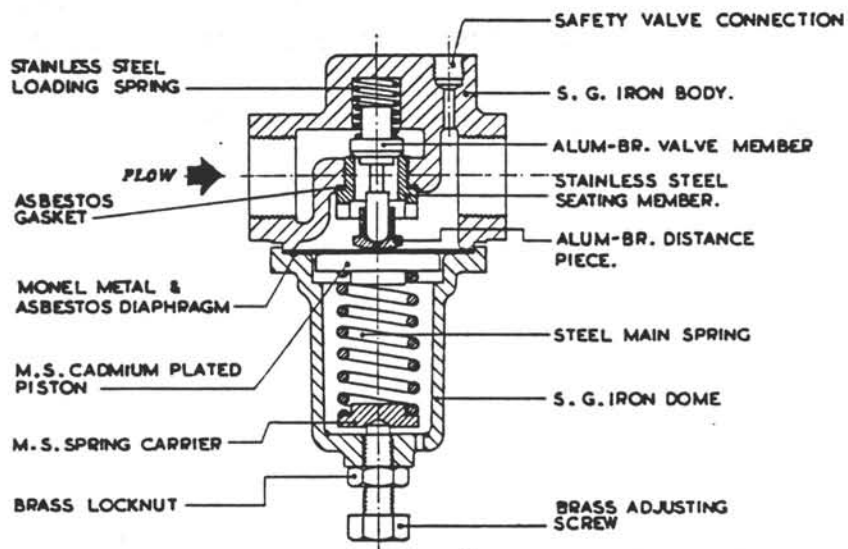


Figure A9.3 Reducing valve for the fluidization gases

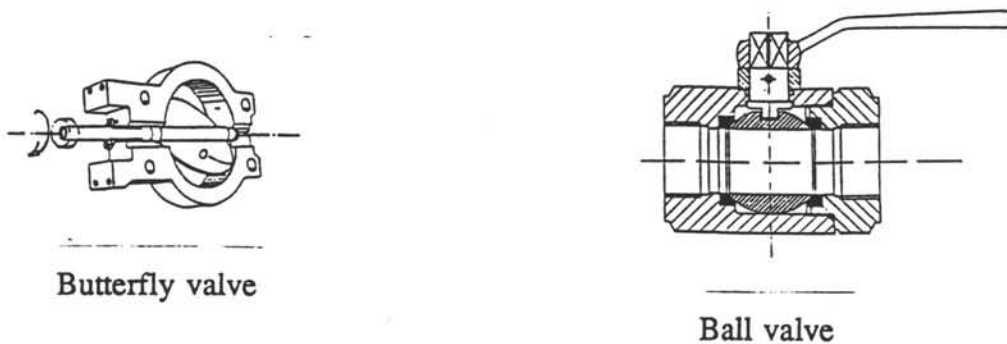


Figure A9.4 Butterfly valve and ball valve

maximum at the start of closing and at a minimum at the end of closing. Based on the same working principles are the tilting-disk check valves, see figure A9.2. These valves may be installed in a horizontal line or in lines in which the flow is vertically upward. Compared with swing check valves of the same size, pressure drop is less at low velocities but greater at high velocities. Closure at the instant of reversal of flow is most nearly attained in these valves. This type of check valve may be used in IFB for both horizontal and vertical upward flow. Another possible choice may be the lift check valve. This type of valve would cause some problems in case of using in the IFB especially when the fluid contains suspended solids. Because of the relative low pressures in the pilot plant, the seats for the valve will commonly be made of soft material which does not resist high temperatures. Special material for the seats is needed which is suitable for low pressures and high temperatures.

Reducing valves

To lower the pressure of the fluidization gas flows simple reducing valves are sufficient (Pearson (1978)). In such valves the main spring will be compressed by turning the adjusting screw, see figure A9.3. This action causes a pressing effect on a piston and a slight deflection on a diaphragm. The valve member will be lifted slightly off its sealing member and the valve causes a throttling effect to the gas flow.

Safety valves

The safety or relief valves may be classified into three basic types (Pearson (1978)): lever type, deadweight type and the direct spring-loaded type. The direct spring-loaded type is often used and seems to be a suitable valve which can be used in the pilot plant. To make the final choice for the relief valve, the pressure at which the valve will be opened has to be determined. This pressure depends on the construction of the reactor and converter. Calculations of strength of the equipment determine the maximum allowable pressure. The choice of seats for the valve will be limited by the high temperatures. Because of the relative low pressures in the pilot plant, the seats for the valve will commonly be made of soft material which does not resist high temperatures. Special material for the seats will be needed to withstand high temperatures.

Other valves

Butterfly valves are often used for the manual control of gas flows. A ball valve can be selected for shut-off purposes which should give a positive seal in the closed position and minimum resistance to the flow when open. In figure A9.4 the butterfly valve and the ball valve are shown.

Pipe sizing

The estimation of the different pipe sizes is based on (Smith (1984)):

$$\frac{\Delta P}{L} = 4 \cdot f \cdot \frac{\rho_g \cdot u^2}{2 \cdot D} \quad \text{A9.1}$$

The friction factor f in this equation is assumed to be equal to 0.0125. For cold gas flows it is assumed that: $P = 1.2$ bar and $T = 293$ K; for hot gas flows: $P = 1.1$ bar and $T = 1123$ K. The estimations are based on the following conditions: as few as possible different pipe sizes, reasonable values for the gas velocities in the pipe (maximum 30 m/s) and for the pressure

drop per meter (maximum 200 Pa/m). In table A9.1 the results of the pipe size estimations are presented for the maximum expected gas flows in the reactor.

Table A9.1: Estimation of the pipe sizes. The different pipes and symbols are explained in the text below this table.

pipe	ϕv (m ³ /s)	D (m)	u (m/s)	$\Delta P/L$ (Pa/m)
cold feed lines				
#1 N ₂	0.0093753	0.03	13	202
#2 N ₂	0.0024108	0.03	3.4	13
#3 N ₂	0.001722	0.03	2.4	6.8
#4 N ₂	0.002009	0.03	2.8	9.3
#1 SO ₂	0.0000122	0.005	0.62	6.1
#1 air	0.0093753	0.03	13	202
#3 H ₂	0.0000861	0.005	4.4	9.5
#3 CO	0.0000861	0.005	4.4	133
hot feed lines				
#1	0.0392	0.05	20	60
#2	0.01008	0.03	14	51
#3	0.0072	0.03	10	26
#4	0.0084	0.03	12	35
downstream lines				
#1 + #2	0.04941	0.05	25	95
#3 + #4	0.0156	0.05	7.9	9.5
#1+#2+#3+#4	0.06501	0.05	33	164

Explanation of table A9.1

In this table the diameter D, the gas velocity u and the pressure drop per meter $\Delta P/L$ are presented for different pipes in the pilot plant. These pipes are indicated in the first column by the number of the bed to or from which the gas flows. For the cold feed lines is indicated which gas flows through the pipe.

Three different pipe sizes are used: 0.005 m, 0.03 m and 0.05 m.

Appendix 10: Safety study

The safety study which is set up for the pilot plant has been based on a derived form of a Hazop. In this study the following main parts of the pilot plant will be considered:

- fluidization gas supply line (N_2 , air)
- reactive gas supply line (SO_2 , CO, H_2)
- reactor
- cyclone
- converter section
- CaO-bed system

Using the guide words of a normal Hazop for each part of the pilot plant, the hazards or operating problems which might occur, are identified.

Used abbreviations in this study:

- dev. deviation
p.c. possible cause
cons. consequence
act. action required

Fluidization gas supply line

This line includes the main stop valve, the reducing valve, the mass flow controller and the gas preheater. Nitrogen will be delivered at a pressure of 10 bar, air at 6-7 bar.

#1

- dev.: No nitrogen flow.
- p.c.: -Storage of N_2 is empty, the pressure in the nitrogen supply lines drops to zero.
-Blockage of the line.
- cons.: -The temperature in the heating elements may become too high with possible overheating of these elements.
-The gas flows to the reactor will consists of only reactive gases. Explosive mixtures can be formed with the oxygen from bed 1.
- act.: The supply of reactive gases must be closed immediately by the magnetic valves. A safety cylinder with nitrogen must be opened. The beds will remain fluidized and a slow shut down of the reactor can be achieved. The electrical heating elements must be switched off so that the beds will be cooled with the nitrogen from the cylinder.

Remarks: the safety cylinder with nitrogen must be opened before any experiment will be started. The valve after the reducing valve will be opened automatically when the pressure in the fluidization gas supply line will come below a certain value. The nitrogen flow line must be connected directly to the reactor.

#2

- dev.: No air flow in case of combustion experiments.
- p.c.: -Problems with the compressor, the pressure in the air supply line drops to zero.
-Blockage of the line.
- cons.: -Bed 1 will defluidized. Interruption of coal combustion means possible clotting of the particles (sorbent and coal (ash)) and overheating of bed 1.

-The temperature in the heating elements for bed 1 may become too high with possible overheating of these elements.

act.: The coal combustion must be stopped. The coal feed must be shut off and bed 1 will be fluidized with nitrogen from storage. The reactive gases to bed 3 (H_2 or CO) will be shut off, so that all beds will be fluidized with nitrogen.

#3

dev.: More air or nitrogen flow.

p.c.: Problems with the mass flow controller.

cons.: More heat input to the larger flow. In case the maximum heat input of the heating elements is exceeded, the gas flow cannot be heated up to the desired temperature. The temperature in the reactor will become lower; the heating elements of the reactor may supply the extra amount of heat.

act.: Shut down of the installation and check the mass flow controllers.

#4

dev.: Less nitrogen flow.

p.c.: Storage of N_2 nearly empty.

cons.: -The temperature in the heating elements may become too high with possible overheating of these elements.

-The gas flows to the reactor will then consists of nearly only reactive gases. Explosive mixtures can be formed with the oxygen from bed 1.

act.: Shut down of the installation.

#5

dev.: Higher pressure in the feed section.

p.c.: (partial) Blockage of a line or of the gas distributor. Reducing valve has been opened too far.

cons.: -Too small flows to the reactor.

act.: Shut down the installation and remove the blockage.

#6

dev.: Lower pressure in the feed section.

p.c.: Storage of N_2 is nearly empty.

conc.: As for #4.

act.: As for #1.

#7

dev.: Higher temperature.

p.c.: Problems with the heating elements.

cons.: The temperature may become too high with possible overheating of these elements.

act.: Shut down the installation and check the heating elements and the thermocouples.

#8

dev.: Lower temperature.

p.c.: Problems with the heating elements.

cons.: Temperature in the reactor will become lower.

act.: As for #7.

Reactive gas supply line

This line includes the standard fittings of a gas cylinder (the main stop valve and the reducing valve) and the mass flow controller. The reactive gases (SO_2 , CO , H_2) will be delivered at a maximum pressure of 200 bar.

#9

dev.: No flow.

p.c.: -The cylinder is empty: the pressure in the supply line drops to zero.
-Blockage of the line.

cons.: No reactive gas will flow into the reactor; the capture or regeneration will be disturbed.

act.: The flows of the other reactive gases must be stopped by automatically closing of the magnetic valves in the lines. Check the cylinder and remove the blockage.

#10

dev.: More flow.

p.c.: Problems with the mass flow controller.

cons.: Too high concentrations of reactive gases.

act.: The operator may take action to lower the flow, else shut down the installation.

#11

dev.: Less flow.

p.c.: -Cylinder is (nearly) empty.
-Blockage of the line.

cons.: As for #9.

act.: As for #9.

#12

dev.: Higher pressure.

p.c.: Partial blockage of the line.

cons.: -Too small flows to the reactor.
- SO_2 may remain as a liquid.

act.: Shut down the installation and remove the blockage.

#13

dev.: Lower pressure.

p.c.: Cylinder is (nearly) empty.

cons.: As for #9.

act.: As for #9.

Reactor

#14

dev.: Higher pressure.

p.c.: -Pressure rise due to starting of an explosion.
-Downstream blockage of the gas flow.

cons.: Pressure rise; possible damage of the equipment.

act.: The pressure will be lowered by opening a relief valve: the gas will be blown into the

atmosphere through the roof outside the Proeffabriek. A pressure controller which is connected with the control box, shuts off all the flows with reactive gases by closing the magnetic valves in these lines. The electrical heating will be switched off. The fluidization gases will be lowered so that minimum fluidization conditions will be maintained until the bed has been cooled down. The nitrogen (or air) will leave the reactor passing the relief valves.

Check valves at the inlet of the beds prevent that hot gases or a starting explosion can travel back into the feed section.

#15

dev.: Lower pressure.

p.c.: Blockage of the distributor (a higher pressure drop over the distributor means a lower pressure in the reactor).

cons.: The pressure drop over the downstream end may become too high and the gas flow to the reactor will stop.

act.: Shut down the installation and check the distributor.

#16

dev.: Higher temperature.

p.c.: -Problems with the heating elements.

-Starting of an explosion.

-Blockage of the air flow to the reactor in case of coal combustion.

cons.: Temperature rise; possible damage of the equipment.

act.: Problems with the heating elements or blockage problems: shut down the installation and check the elements and remove the blockage. Starting of an explosion: as for #14.

#17

dev.: Lower temperature.

p.c.: -Problems with the heating elements.

-Cold nitrogen flow is too high (the maximum input of the elements will be exceeded).

conc.: Decrease of temperature.

act.: Lower the nitrogen flows, else shut down the installation and check the heating elements.

Cyclone

#18

dev.: Higher pressure.

p.c.: Blockage of the cyclone: clotting of dust on the wall of the cyclone.

cons.: Pressure rise in the upstream section.

act.: Manometers up- and downstream of the cyclone indicate the pressure drop. The operator may take action based on the pressure indications.

Converter

#19

dev.: Higher pressure.

p.c.: Pressure rise due to starting of an explosion.
cons.: Pressure rise in the converter.
act.: Natural gas and air flows will be closed. Pressure will be lowered by opening a relief valve: the gas will be blown into the atmosphere outside the Proeffabriek. A pressure controller which is connected with the control box, shuts off all the flows with reactive gases by closing the magnetic valves in these lines.
Check valves at the inlet of the converter prevent that a starting explosion can travel into the upstream section.

#20

dev.: Higher temperature.
p.c.: -Starting of an explosion.
-Too high natural gas flow is burnt.
conc.: Temperature rise in the converter.
act.: Lower the natural gas flows, else shut down the installation and check the supply system for natural gas. Starting of an explosion: as for #19.

#21

dev.: Lower temperature.
p.c.: -The flame has been blown out by the inlet gas flow or by a disturbance in the natural gas supply.
-The inlet temperature of the gases is too low and the temperature control mechanism does not work.
cons.: The combustible components in the gas flow will not be converted completely.
act.: An alarm must be switched on so that the operator may immediately take action (burner should be lighted again).

CaO-bed system

#22

dev.: Higher pressure.
p.c.: Blockage of the CaO-bed
cons.: Pressure rise in the upstream section.
act.: Manometers up- and downstream of the CaO-bed system indicate the pressure drop.
The operator may take action based on the pressure indications.

#23

dev.: SO₂-capture fails
p.c.: Maximum conversion of limestone particles is reached.
cons.: SO₂ will be blown into the atmosphere.
act.: From time to time SO₂-concentration in the gas flow at the outlet will be checked.
Based on the results of these analyzing tests the operator may take action by switching the CaO-beds.

Appendix 11: Safety aspects of the gases

The safety aspects of the gases which will be used or formed in the pilot plant, will be discussed. These gases are: CO, H₂, SO₂, H₂S, S₂, COS, CO₂, O₂, N₂ and H₂O. For each gas attention will be paid to toxicity, physiological effect, first aid and fire prevention. Data regarding safety has been obtained from Chemiekaarten (1992), Hommel (1986) and Kirk Orthmer (1983). This information can be used in the safety report.

* Carbon monoxide, CO, will be used as a feed gas in bed 3. Carbon monoxide is a colourless, odourless, flammable and toxic gas. Its danger is the combination of the toxicity and the odourlessness, and it can thus not be detected by smell.

It burns readily in air or oxygen. Mixtures of carbon monoxide and air are flammable over a wide range of compositions at atmospheric pressure. The flammability limits of carbon monoxide-air mixtures change with pressure and temperature. As pressure increases, the lower limit increases and the upper limit decreases, as temperature increases an opposite effect of change of the limits will occur.

The gas can be absorbed into the human body by inhalation. The toxicity of carbon monoxide is a result of its reaction with the hemoglobin of blood which leads to blood deviations. In cases of severe poisoning disturbances with breathing, dizziness, weakness, mental confusion, loss of consciousness, and death may occur. In table A11.1 a survey is given in which these physiological effects are related with the concentration of carbon monoxide.

Table A11.1: Relation between the concentration of carbon monoxide and the physiological effects

Concentration of CO (ppm)	Physiological effects
0 - 200	slight headache
200 - 400	after 5-6 h exposure: headache, nausea, vertigo
400 - 700	after 4-5 h exposure: severe headache, weakness, muscular incoordination, vomiting, collapse
700 - 1100	weakness, vomiting, collapse
> 1600	after 1 h exposure: possible death

The poisoned patient must be removed to fresh air, kept warm and administered pure oxygen. Artificial respiration is necessary whenever breathing is inadequate. A physician must be called in all cases of suspected carbon monoxide poisoning.

Prevention of carbon monoxide poisoning is best accomplished by providing good ventilation where contamination is a problem.

* Hydrogen, H₂, will be used as a feed gas in bed 3. Hydrogen is a colourless and odourless gas. The gas is lighter than air and forms with oxygen or air the so called oxyhydrogen. It is not considered toxic but it can cause suffocation by the exclusion of air.

Hydrogen burns with a nearly invisible flame. The detonation and flammability limits for hydrogen-air mixtures are much wider than those of hydrocarbon-air mixtures: 4.0 - 75.0 vol% respectively 18.3 - 59.0 vol%.

For high concentrations of hydrogen in air, for example in a bad ventilated room, lack of oxygen may occur with possible loss of consciousness. To prevent high concentrations, ventilation must always be at the highest point. First aid may consist of fresh air, rest and if necessary insufflation may be applied.

* Sulphur dioxide, SO_2 , will be used as a feed gas in bed 3. Sulphur dioxide is a colourless gas with a characteristic pungent, choking odour. The gas is heavier than air. The solution of the gas in water is a moderate strong acid.

The gas can be absorbed into the human body by inhalation. The gas has caustic effects on eyes, skin and respiratory organs. Inhalation may cause pulmonary oedema, in severe cases it may be fatal. In case of fast evaporation the liquid may cause freezing.

In table A11.2 a survey is given in which these physiological effects are related with the concentration of sulphur dioxide.

Table A11.2: Relation between the concentration of sulphur dioxide and the physiological effects

Concentration of S_2O_2 (ppm)	Physiological effects
3 - 5	detectable odour
8 - 12	throat irritation
10	maximum concentration for prolonged exposure
> 20	eye irritation
50 - 100	maximum concentration for 30 min exposure
400 - 500	concentration that is dangerous for even short exposure

First aid may consist of fresh air and rest. In case of freezing, take no cloths off but spray with water over the contaminated skin and call a physician.

Symptoms of pulmonary oedema may usually just show up after a few hours and will be intensified by physical effort. Rest and admission in a hospital is then necessary.

Cylinders must be equipped with special fittings.

* Hydrogen sulfide, H_2S will be formed during regeneration with hydrogen in bed 3. Hydrogen sulfide is a colourless with a characteristic rotten-egg odour. The gas is heavier than air and is spreading just above the ground with possible ignition from a distance. During oxidation in a flame, hydrogen sulfide will be converted to sulphur dioxide (main product) and sulphur trioxide (by-product).

Hydrogen sulfide can be absorbed into the human body by inhalation and has an extremely high acute toxicity. It is fast-acting and the exposed patient may become unconscious quickly, with no opportunity to escape the contaminated space.

In table A11.3 a survey is given in which these physiological effects are related with the concentration of hydrogen sulfide.

Table A11.3: Relation between the concentration of hydrogen sulfide and the physiological effects

Concentration of H ₂ S (ppm)	Physiological effects
1	irritation of the eyes and respiratory system
30 -100	deceptively sweet smell
90	inflammation of the eyes for brief exposure
> 100	deadens of the sence of smell
> 180	unconsciousness, respiratory paralysis and death

As can be seen from this table, its odour is an unreliable indicator of dangerous concentrations. Therefore protective measures involving prompt detection and adequate ventilation have to be taken. Continuous monitoring is recommended to signal an evacuation alarm if the workplace concentration exceeds 50 ppm and a warning alert if it is present at 10-50 ppm.

First aid may consists of fresh air and rest. In case of severe poisoning a physician have to be called.

* Sulphur vapour will be formed during regeneration in bed 3. The molecular composition of sulphur vapour is a complex function of temperature and pressure. Mass spectrometric data for sulphur vapour indicate the presence of all possible S_n molecules from S₂ to S₈. In general, octatomic sulphur is the predominant molecular constituent of sulphur vapour at low temperatures, but the equilibrium shifts towards smaller molecular species with increasing temperature and decreasing pressure.

It reacts violently with oxygen. Another reactions are with iron and hydrogen. With the latter compound the toxic hydrogen sulfide is formed. When sulphur is burned in air, it forms predominately sulphur dioxide with small amounts of sulphur trioxide. Sulphur vapour can come into the human body by inhalation. Sulphur vapour has irritated effects on the respiratory organs.

The boiling point of sulphur in liquid state is 445 °C (1 atm). The temperature of the off-gases from the reactor has to be high enough to prevent condensation of sulphur vapour before it is converted in the converter section.

* Carbonyl sulfide, COS, will be formed during regeneration with carbon monoxide in bed 3. Carbonyl sulfide is a colourless and odourless gas. Carbonyl sulfide burns with a blue flame to carbonoxide and sulphur oxide. It reacts only slowly with water to form carbon dioxide and hydrogen sulfide. The mechanism of the toxic action appears to involve breakdown to hydrogen sulfide. It acts on the central nervous system with death resulting mainly from respiratory paralysis.

* Carbon dioxide, CO_2 is formed during combustion of compounds containing carbon and it will be formed during regeneration with carbon monoxide. Carbon dioxide is a colourless gas with a faintly pungent odour and acid taste. Although carbon dioxide is a constituent of exhaled air, high concentrations are hazardous. Up to 0.5 vol% carbon dioxide in air is not considered harmful but it concentrates in low spots because it is heavier than air. 5 vol% carbon dioxide in air causes a threefold increase in breathing rate and prolonged exposure to concentrations higher than 5 vol% may cause unconsciousness and death. Ventilation sufficient to prevent accumulation of dangerous percentages of carbon dioxide must be provided where carbon dioxide gas has been released.

* Other gases like nitrogen, air and water vapour (formed during combustion or during regeneration with hydrogen) will not lead to dangerous situations. Only for high concentrations of nitrogen in air a shortage of oxygen may arise (a leakage of nitrogen in a bad ventilated room). Attention should be paid to already small increases of the amount of oxygen in the atmosphere since the combustibility of all compounds will strongly increase.

General preventions to overcome dangers with combustible gases like CO , H_2 , H_2S , S_2 and COS are:

to prevent fire: no free fire, no sparks and no smoking,

to prevent explosions: closed apparatus, well ventilated room, explosion safe electrical equipment and lighting.

In case of fire with CO , H_2 or H_2S and with no danger for the environment, let the fire burn out or extinguish it with powder or carbon dioxide.

A summary of the main safety aspects regarding toxicity and flammability is presented in table A11.4. The meaning of the different parameters in this table is as follows. The threshold limit value is a measure for the toxicity of the gas. This value is the maximum allowable concentration of the gas in air at the working place for exposure of 8 hours a day. Prolonged exposure of the operator to this concentration has no effect on his health. The autoignition temperature is the temperature at which ignition of the gas is possible without any source. The minimum ignition energy is a measure for the ease of ignition. A low value means an easy ignition. Explosion limits in air determine the range of mixtures of air with the gas within which ignition causes explosion.

Table A11.4: Some data regarding the safety in the IFB

	Dutch Threshold Limit Values	auto ignition temperature	minimum ignition energy	explosive mixture in air
CO	25 ppm (29 mg/m ³)	605 °C	0.1 mJ	11 - 75 vol%
H ₂	not determined	585 °C	0.01 mJ	4 - 76 vol%
SO ₂	2 ppm (5 mg/m ³)	-	-	-
H ₂ S	10 ppm (15 mg/m ³)	260 °C	0.07	4.3 - 46 vol%
S ₂	not determined	235 °C	not known	not known
CO ₂	5000 ppm (9000 mg/m ³)	-	-	-
COS	not determined	250 °C	not known	9.6 - 33.2

Appendix 12: Safety report

The safety report will be judged by the safety committee of CPT whether safe operation of the pilot plant can be ensured. Only after the approval of the safety report by this committee, the construction of the pilot plant can be started. In this appendix it will be explained how information from this final report can be used for the completion of the safety report.

The outline of a safety report is given below:

- 1 General information about the project
- 2 Explanation of the pilot plant set-up
- 3 Location of the pilot plant
- 4 Working at higher pressures or vacuum in equipment made of glass
- 5 Working at high pressure
- 6 The use of chemicals and gases
- 7 Continuous operation of equipment
- 8 Removal of the excess chemicals
- 9 Literature used for the safety study

An explanation of these subjects in relation with the pilot plant is as follows:

- 1 The general contents of the project will be described here.
- 2 In this part the pilot plant set-up will be described using the process flow diagram in which the control mechanisms have been added. Information about the pilot plant set-up can be extracted from chapter 4 and 9 in which the flowsheet and the control mechanisms have been described. This explanation has to be completed with the actual choices for the different parts of the pilot plant (based on data from suppliers of the equipment). To this description the safety measures have to be added. These safety measures can be extracted from chapter 10.
Information for this part which cannot be extracted from any chapter, deals with the description of the control box and the process computer system. In this description it can be referred to the standards which are used for these equipment in the Proeffabriek. The control box will be equipped with standard power connections and the FIX system can be used as the process computer system. Schematic drawings of electrical circuits have to be included.
- 3 A floor plan of the Proeffabriek has to be drawn. In this drawing the pilot plant, fire extinguisher equipment, first aid facilities, emergency buttons have been indicated.
- 4 + 5 No glass will be used for the construction of the pilot plant. Experiments will be carried out at (nearly) atmospheric conditions.
- 6 The safety aspects of the gases will be described as is done in appendix 11.
- 7 Detailed information about continuous operation of equipment is not available yet. Safety devices may be powered on continuously.
Explanation of these devices will be given here. Some information can be extracted from chapter 10.
- 8 In this part the removal of the gases and solids from the pilot plant will be indicated.
- 9 A list of the literature used to fill in the safety report including old examples of safety reports.

Appendix 13: Modifications to the designed pilot plant for the H₂S removal process

Also the H₂S removal process will be investigated in the pilot plant. There are two possibilities doing this.

The first is using about the same gas flows as for the SO₂ process. This is possible when a suitable sorbent size is chosen. The sorbent should have a mean average particle size of 1.5 mm. Using the same gas flows will involve higher gas costs as in bed 1 CO and H₂ must be used instead of N₂. It is possible to do experiments without CO and H₂, but according to Wakker (1992) these components have considerable influence on the sulphation of the sorbent.

The second possibility is using smaller gas flows and a sorbent with a smaller mean particle size. The costs of the gases can be reduced in this way.

In both cases the equipment must be modified. The same reactor can be used, only in the case of smaller gas flows the gas residence time and the H₂S retention will be much higher. Bed 2 isn't used for segregation in this process, so both bed 2 and 4 can be used for controlling the sorbent flow through the IFB. The orifice between bed 2 and 3 can now also be placed near the bottom of the bed. The solids feed system isn't needed for this process and can be removed. The same gas and solids sampling points can be used.

The CO and H₂ supply should now be connected to bed 1. New connections for H₂S to bed 1 and steam to bed 3 should be made. The steam is used for the regeneration. In case smaller gas flows are used some of the mass flow controllers might be replaced.

In case of smaller gas flows less and smaller particles will be carried along through the freeboard, but the performance of the cyclone will be lower. The off-gases now have a high concentration of CO and H₂ and can directly be flared, without adding extra heat by burning natural gas. The same CaO-beds can be used.

The costs for changing the pilot plant won't be high, the main costs will be the replacement of some mass flow controllers. Because of the large amounts of CO and H₂, the operating costs will be higher, even when smaller gas flows are used. Maybe even the cheapest solution would be building a small coal gasification plant for the production of fuel gases.

